

Estimating Behavioral Learning Equilibria in DSGE Models*

Cars Hommes¹, Kostas Mavromatis² and Tolga Ozden¹

¹Faculty of Economics and Business, University of Amsterdam and Tinbergen Institute.

²Research Department, De Nederlandsche Bank (DNB)

April 11, 2018

Abstract

We estimate DSGE models under a simple misspecification learning equilibrium that arises from expectational frictions. The representative agent does not know the true underlying mechanism of the economy, but acts as an econometrician and uses a simple univariate sample autocorrelation learning rule to form his expectations about the future state of the economy. Over time, she learns the best univariate rule and his expectations become self-fulfilling, giving rise to *Behavioral Learning Equilibria (BLE)*. Under fairly general conditions, we show that DSGE models can be estimated under a *BLE* using standard Bayesian estimation methods without using projection facilities. We apply our estimation approach to two models that are commonly used in the DSGE literature: the baseline 3-equation NKPC à la Woodford (2003), and the workhorse Smets-Wouters (2007) model. Our results show that the empirical fit and forecasting performance of both models under *BLE* improve compared to the Rational Expectations models, while we observe important differences in our parameter estimates and the propagation mechanism of the model.

JEL Classification: E37; E47; C63; D83; C11.

Keywords: Adaptive Learning; Bayesian Estimation of DSGE Models; Bounded Rationality; Monetary Policy.

*Corresponding Author: Tolga Ozden (E-mail: t.ozden@uva.nl), Roetersstraat 11, 1018WD, Amsterdam, The Netherlands.

1 Introduction

The Rational Expectations Hypothesis (REH), first introduced by [Muth \(1961\)](#), is the dominant paradigm in macroeconomics where the agents' subjective probability distributions coincide with the objective distributions of the model. This essentially corresponds to a joint determination of the beliefs and the state of the economy. Accordingly, the agents in the model know the actual economic structure and the corresponding law of motion. However, rational expectations (RE) models typically do not provide a description of the complex dynamic problems that the agents have to figure out in order to discover the systematic relations in the economy. Instead, they are implicitly assumed to solve and exploit the complicated problems in order to form their expectations about the future states. But in a dynamic system where the expectations play an important role in determining the current state of the economy, the assumption of *how* the expectations are formed also plays a crucial role. In particular, if the learning process has an impact on the formation of expectations, then the assumption of rational expectations becomes far too strict and provides an unconvincing model specification. Under the RE approach, the agents observe and take into account the structural exogenous shocks affecting the economy. This is often far too extreme since, generally, the only information available to the households and firms are the historical time series of the observable macroeconomic variables. Aside from these conceptual concerns, there are also empirical drawbacks to studying macroeconomic models under the rational expectations approach: There is mounting evidence showing the RE models commonly fail to capture the inertia of macroeconomic systems and the propagation mechanism of the exogenous shocks, see e.g. [Estrella & Fuhrer \(2002\)](#) and [Collard & Dellas \(2004\)](#). The concepts of inertia and shock propagation here relate to both the *inherent persistence* of the macroeconomic variables, as well as the *persistent reactions to exogenous shocks* that are largely observed in empirical studies. This shortcoming to capture the persistence leads to many counterfactual implications and a failure to generate hump-shaped responses to structural shocks in the endogenous variables.

In this study, we deviate from the rational expectations approach and consider the estimation of DSGE models under a simple expectation formation rule introduced by [Hommes & Zhu \(2014, 2016\)](#): A representative boundedly rational agent uses a parsimonious linear sample autocorrelation (SAC) forecasting rule in order to exploit the time series of the variables and form his expectations about the economy. The agent does not know the true economic relations, but forms his expectations based on *the unconditional mean and first-order autocorrelation of the observed data*, which corresponds to an AR(1) learning rule. Under fairly general conditions, the economic system settles on an equilibrium where the beliefs converge to constants as their limiting values and the simplest form of misspecification equilibrium arises, which we define as a *Behavioral Learning Equilibrium (BLE)*. Accordingly, the boundedly rational agent learns the

best univariate forecasting rule by updating his beliefs about the mean and persistence of the observed realizations (Hommes & Zhu, 2016), without ever knowing the underlying complex economic structure. Once the system converges, this simple linear forecasting rule becomes self-fulfilling in terms of averages and first-order autocorrelations of all endogenous variables, where the forecast errors are unbiased. Such an equilibrium corresponds to a fixed point of the system where the economic outcomes do not contradict the agents' beliefs that generated them in the first place; hence the agent has no reason to deviate from the forecasting rule.

As our main contribution in this paper, we show that in a complex system where the economic structure is hard to understand, coordination of expectations on a BLE is a better characterization of the economic system compared to a rational expectations equilibrium. In order to validate our claim, we use a numerical framework to approximate a BLE, and subsequently apply it to the Bayesian estimation of two commonly used DSGE models: The first one is the small-scale baseline 3-equation New Keynesian model along the lines of Woodford (2003), which allows us to investigate the impact of learning on the model fit in the absence of a large number of frictions. Next we turn to the estimation of the Smets-Wouters DSGE model (2007), which became a workhorse in macroeconomic policy-making and research over the last decade. This is essentially a more elaborate version of the small-scale model that is enriched by numerous nominal and real frictions such as price & wage indexations, capital adjustment costs and habit formation in consumption, which are frequently criticized for being ad-hoc since they are not based on any micro-foundations. Moreover, these frictions are usually accompanied by highly persistent structural shocks, where the source of the autocorrelation has a dubious interpretation but still plays an important role in driving the economic fluctuations at the business cycle level. Therefore, introducing the AR(1) learning rule into the model not only serves as a potential way to improve the model fit relative to the RE approach, but also provides a robustness check for the empirical validity of these structural frictions in the presence of bounded rationality. Similar to previous studies in the adaptive learning literature, the relaxation of full rationality in both the NKPC and SW models results in an improvement in the empirical fit. However, unlike the previous studies, we also observe important differences in our parameter estimates under RE and BLE: In both models, the introduction of learning results in fairly weak persistence in some of the exogenous shocks, while the friction parameters typically become smaller. Forecasting under the BLE approach generally leads to more accurate predictions, particularly over the short- and medium-horizons. While the impact of monetary policy turns out to be fairly similar under both specifications, we find that monetary policy might lead to multiple BLE over some parameter ranges.

A BLE falls under the general class of Stochastic Consistent Expectations Equilibrium (SCEE) introduced by Hommes & Sorger (1998), which further falls under the class of a Restricted Per-

ceptions Equilibrium (RPE), where agents misspecify the law of motion but form their beliefs optimally given the misspecification ([Sargent, 1991](#); [Evans & Honkapohja, 2012](#)). Accordingly, our paper contributes to the growing literature on adaptive learning in macroeconomics, where the agents are modeled as econometricians that observe the variables and update their beliefs over time: [Bullard & Duffy \(2001\)](#) and [Mitra et al. \(2017\)](#) study adaptive learning in the RBC model; [Evans & Honkapohja \(2012\)](#), [Bullard & Mitra \(2002\)](#), [Branch \(2004\)](#), [Orphanides & Williams \(2004\)](#), [Gaspar et al. \(2006\)](#), and [Milani \(2005, 2007\)](#) study learning and monetary policy in various New Keynesian settings. Other examples along similar lines include [Orphanides & Williams \(2004\)](#), [Williams \(2003\)](#), [Collard & Dellas \(2004\)](#), [Eusepi & Preston \(2011\)](#)¹. In other closely related studies, [Fuster et al. \(2010, 2012\)](#) consider the impact of Natural Expectations in various settings on asset prices and macroeconomic fluctuations, where agents forecast based on parsimonious statistical models. Similar to our approach, these papers focus on the one-step ahead forecasts of the agents that result from the infinite-horizon decision problems, typically defined as Euler Equation Learning. [Preston \(2003\)](#) considers Infinite Horizon Learning as an alternative, which results from replacing the infinite-horizon decision problem with that of a multi-period. A common feature of these papers is to study adaptive learning as a minimal departure from the rational expectations approach and focus on the conditions under which the learning process will converge to a REE ([Evans & Honkapohja, 2012](#)). Accordingly, they focus on how agents learn a REE if they do not initially find themselves in such an equilibrium and as a result, the estimation of these models usually involves a constant gain learning approach, which prevents the ALM from converging to rational expectations as a fixed point and instead to an ergodic distribution around it. Examples of such an approach can be found in [Lansing \(2009\)](#), where the NKPC is estimated under the Consistent Expectations Equilibrium along the lines of [Hommes & Sorger \(1998\)](#); [Milani \(2007\)](#), where a small-scale DSGE model is estimated with various frictions under constant gain learning; and [Slobodyan & Wouters \(2012a\)](#), where the SW (2007) is estimated with a simple AR(2) forecasting rule under time-varying beliefs. The approach in these papers corresponds to nesting the rational expectations law of motion in the agents' perceived law of motion as a limiting case. This typically introduces additional learning parameters into the system, which is considered a shortcoming of adaptive learning models ([Marcet & Nicolini, 2003](#)) since it requires arbitrary assumptions on these parameters via calibration or the assumption of prior distributions. Unlike these previous papers, an important feature of SAC-learning is it does not introduce any additional learning parameters into the system: All learning coefficients are completely pinned down by the moments of the endogenous system variables through natural consistency requirements, which is a methodological distinction of our approach from the adaptive learning literature. Another important methodological difference of our approach relates to projection facilities: A common

¹See [Woodford \(2013\)](#) for a more detailed account of the research in macroeconomics that deviates from the rational expectations approach.

problem in constant/decreasing gain models is that, the data may push the estimated beliefs into regions of instability, leading to explosive dynamics. Projection facilities are needed to avoid these outcomes and ensure convergence, which re-initializes the learning algorithm in these cases. SAC-learning is consistent with stable dynamics by construction, therefore we are able to estimate the models without imposing a projection facility.

We further deviate from previous studies in two important conceptual aspects: A system may indeed converge to a REE when the agent in the model is endowed with a correctly specified law of motion in such scenarios, where the transitional dynamics of the model generate additional persistence in the endogenous variables. But what happens when the perceived law of motion does not nest the REE under consideration? In this sense, we conceptually deviate from the adaptive learning literature by specifically considering a misspecification equilibrium that results from an underparametrized perceived law of motion where the convergence to a REE trivially becomes impossible, but convergence of the learning coefficients is still not ruled out. Moreover, our approach deviates from the aforementioned studies in terms of time-variation in beliefs: In a Behavioral Learning Equilibrium, the belief parameters are fixed at their limiting values, hence there is no time-variation in beliefs. Our results show that estimation under a BLE improves upon the RE approach, which allows us to disentangle the effects of misspecification from time-variation in beliefs, and shows its empirical importance in isolation.

The rest of the paper is organized as follows: Section 2 discusses the estimation of linearized DSGE models under the simple univariate AR(1) learning rule, and introduces a general numerical framework to approximate and estimate a BLE. Sections 3 & 4 subsequently apply the estimation method to the small-scale baseline NKPC and medium-scale Smets-Wouters models under BLE, and compare the results with the rational expectations approach. Section 5 considers two applications in forecasting and monetary policy implications with a focus on the SW model under BLE, and scrutinizes the differences with the RE approach. Section 6 provides robustness checks for the SW model by examining the model sensitivity across different subsamples and small changes in the model parameters, and finally Section 7 concludes.

2 BLE in Linearized DSGE Models

Consider a linearized DSGE model governed by the following law of motion:

$$\begin{cases} X_t = A_1 + B_1 X_{t-1} + C \mathbb{E}_t X_{t+1} + D \epsilon_t \\ \epsilon_t = A_2 + B_2 \epsilon_{t-1} + E \eta_t \end{cases} \quad (2.1)$$

where X_t denotes the vector of endogenous variables, ϵ_t is the vector of (autocorrelated) exogenous shocks, and η_t is the vector of i.i.d disturbances. Before formally defining a BLE, we first present law of motion under the minimum state variable REE. Accordingly, suppose the agent observes the exogenous shocks ϵ_t and has the following perceived law of motion:

$$X_t = \xi_1 + \xi_2 \epsilon_t + \xi_3 X_{t-1} + v_t \quad (2.2)$$

where $v_t \sim$ i.i.d error term with $\mathbb{E}_t v_{t+1} = 0$. The corresponding 1-step ahead expectations are given as $\mathbb{E}_t X_{t+1} = (\xi_1 + \xi_2 A_2 + \xi_3 \xi_1) + (\xi_2 B_2 + \xi_3 \xi_2) \epsilon_t + \xi_3^2 X_{t-1}$. Plugging this back into (2.1) and re-arranging yields the implied ALM:

$$X_t = A_1 + C(\xi_1 + \xi_2 A_2 + \xi_3 \xi_1) + (B_1 + C\xi_3^2)X_{t-1} + (C(\xi_2 B_2 + \xi_3 \xi_2) + D)\epsilon_t \quad (2.3)$$

A REE corresponds to the fixed point of²:

$$\begin{cases} \xi_1 = A_1 + C(\xi_1 + \xi_2 A_2 + \xi_3 \xi_1) \\ \xi_2 = C(\xi_2 B_2 + \xi_3 \xi_2) + D \\ \xi_3 = B_1 + C\xi_3^2 \end{cases} \quad (2.4)$$

Note that in the special case with $A_1 = A_2 = 0$, we have $\xi_1 = 0$.

Next we turn to the notion of a BLE, where we relax the assumption that the structural shocks ϵ_t are observed. Accordingly, we start by re-writing the law of motion (2.1) to obtain a more compact notation. One can augment X_t with ϵ_t to obtain the law of motion in one equation:

$$\begin{bmatrix} 1 & -D \\ 0 & 1 \end{bmatrix} \begin{bmatrix} X_t \\ \epsilon_t \end{bmatrix} = \begin{bmatrix} A_1 \\ A_2 \end{bmatrix} + \begin{bmatrix} B_1 & 0 \\ 0 & B_2 \end{bmatrix} \begin{bmatrix} X_{t-1} \\ \epsilon_{t-1} \end{bmatrix} + \begin{bmatrix} C & 0 \\ 0 & 0 \end{bmatrix} \begin{bmatrix} \mathbb{E}_t X_{t+1} \\ \mathbb{E}_t \epsilon_{t+1} \end{bmatrix} + \begin{bmatrix} 0 \\ E \end{bmatrix} \eta_t \quad (2.5)$$

Define³:

$$\begin{aligned} \begin{bmatrix} X_t \\ \epsilon_t \end{bmatrix} &= S_t, \quad \begin{bmatrix} 1 & -D \\ 0 & 1 \end{bmatrix} = \tilde{\gamma}, \quad \tilde{\gamma}^{-1} \begin{bmatrix} A_1 \\ A_2 \end{bmatrix} = \bar{\gamma}, \quad \tilde{\gamma}^{-1} \begin{bmatrix} B_1 & 0 \\ 0 & B_2 \end{bmatrix} = \gamma_1, \\ \tilde{\gamma}^{-1} \begin{bmatrix} C & 0 \\ 0 & 0 \end{bmatrix} &= \gamma_2, \quad \tilde{\gamma}^{-1} \begin{bmatrix} 0 \\ E \end{bmatrix} = \gamma_3, \end{aligned}$$

Then the law of motion can be written as:

²The model under REE is estimated using the routines available in Dynare, hence we do not explicitly compute this fixed point.

³We assume the invertibility conditions of the corresponding matrices are satisfied throughout the paper.

$$S_t = \bar{\gamma} + \gamma_1 S_{t-1} + \gamma_2 \mathbb{E}_t S_{t+1} + \gamma_3 \eta_t, \quad (2.6)$$

where we assume S_t is a vector of length K . Given (2.6), we solve the model by using our parsimonious learning rule. The representative agent observes the mean and first-order autocorrelation of the forward-looking variables at each period and forms his expectations based on these two statistics, using a univariate AR(1) forecasting rule for each endogenous variable. More formally, define the learning vector for the mean coefficients α_t , and the diagonal learning matrix for the first-order autocorrelation coefficients β_t . Further denote the corresponding learning parameters by $\alpha_{x,t}$ and $\beta_{x,t}$ for each endogenous variable x_t . For ease of notation and without loss of generality, we assume the first N variables in S_t constitute the vector of forward-looking variables, and we introduce zeros for the state variables and exogenous shocks. Accordingly, we have:

$$\begin{cases} \alpha_t = (\alpha_{1,t} \alpha_{2,t} \dots \alpha_{N,t}, \mathbf{0}_{\mathbf{1}, K-N})' \\ \beta_t = \text{diag}(\beta_{1,t} \beta_{2,t} \dots \beta_{N,t}, \mathbf{0}_{\mathbf{1}, K-N}), \end{cases}$$

where $\mathbf{0}_{\mathbf{1}, K-N}$ denotes a zero vector of length $K - N$. This implies the agent's *perceived law of motion (PLM)*, and the corresponding 1-step ahead forecasting rule are respectively given by⁴:

$$\begin{cases} S_t = \alpha_{t-1} + \beta_{t-1}(S_{t-1} - \alpha_{t-1}) + v_t \\ E_t S_{t+1} = \alpha_{t-1} + \beta_{t-1}^2(S_{t-1} - \alpha_{t-1}) \end{cases} \quad (2.7)$$

where v_t denotes the unbiased forecast errors of the agent, satisfying $\mathbb{E}_t v_{t+1} = 0$. Plugging in the forecasting rule into the law of motion in (2.6) yields the implied ALM of the system with learning:

$$S_t = \bar{\gamma} + \gamma_1 S_{t-1} + \gamma_2 (\alpha_{t-1} + \beta_{t-1}^2(S_{t-1} - \alpha_{t-1})) + \gamma_3 \eta_t. \quad (2.8)$$

We assume the agents use *sample autocorrelation learning* to update the parameters in α_t and β_t . Accordingly, each $\alpha_{x,t}$ and $\beta_{x,t}$ is updated every period using the sample average and first-order autocorrelation, as new information becomes available:

$$\alpha_{x,t} = \frac{1}{t} \sum_{k=1}^t x_k, \quad (2.9)$$

$$\beta_{x,t} = \frac{\sum_{k=1}^{t-1} (x_k - \alpha_t)(x_{k+1} - \alpha_t)}{\sum_{k=1}^t (x_k - \alpha_t)^2}. \quad (2.10)$$

Denoting by α^* and β^* the equilibrium mean vector and first-order autocorrelation matrix respectively, we formalize the notion of a BLE as follows, following [Hommes & Zhu \(2016\)](#).

⁴Note that, in a given period, we have the following timeline: The (unobserved) shocks are realized, the expectations are formed and the state is realized. Therefore current

Definition 2.1: A *BLE* $(\boldsymbol{\alpha}^*, \boldsymbol{\beta}^*)$ corresponds to a fixed point of (2.8), where two consistency requirements are satisfied:

C1) The vector of unconditional means in S_t , which we denote by \bar{S} , coincides with the means in the agent's perceived law of motion:

$$\boldsymbol{\alpha}^* = \bar{S} = \mathbb{E}[S_t] \quad (2.11)$$

C2) The diagonal matrix of unconditional first-order autocorrelations in S_t coincides with the agent's perceived first-order autocorrelations, which yields:

$$\boldsymbol{\beta}^* = \frac{\mathbb{E}[(S_t - \bar{S})(S_{t-1} - \bar{S})']}{\mathbb{E}[(S_t - \bar{S})(S_t - \bar{S})']}. \quad (2.12)$$

Accordingly, finding the equilibrium law of motion requires analytical expressions for the unconditional means and first-order autocorrelations in the above system. A straightforward computation shows that the unconditional mean is given by:

$$\mathbb{E}[S_t] = \bar{S} = \boldsymbol{\alpha}^* = [I - \gamma_1 - \gamma_2]^{-1} \bar{\gamma}. \quad (2.13)$$

In particular, both the small-scale NKPC, as well as the medium-scale SW models considered in this paper are characterized by $A_1 = A_2 = 0$, implying $\bar{\gamma} = (0, 0)^T$ and hence $\boldsymbol{\alpha}^* = \bar{S} = \mathbb{E}[S_t] = 0$. In this case the law of motion in (2.8) reduces to:

$$S_t = \gamma_1 S_{t-1} + \gamma_2 \boldsymbol{\beta}_{t-1}^2 S_{t-1} + \gamma_3 \eta_t \quad (2.14)$$

In order to simplify the exposure, we compute the first-order autocorrelation parameters using the expression in (2.14). Denoting by Γ_0 and Γ_1 the variance-covariance and first-order autocovariance matrices respectively, one can show that:

$$\begin{cases} \text{Vec}(\Gamma_0) = [I - M(\boldsymbol{\beta}^*) \otimes M(\boldsymbol{\beta}^*)]^{-1} (\gamma_3 \otimes \gamma_3) \text{Vec}(\Sigma_\eta) \\ \text{Vec}(\Gamma_1) = [I \otimes M(\boldsymbol{\beta}^*)] \text{Vec}(\Gamma_0) \end{cases} \quad (2.15)$$

where $M(\boldsymbol{\beta}^*) = \gamma_1 + \gamma_2 \boldsymbol{\beta}^{*2}$, and Σ_η is the variance-covariance matrix of i.i.d disturbances η_t . This implies $\forall j = \{1, \dots, N\}, \beta_j^* = \frac{\text{Vec}(\Gamma_1)_{N(j-1)+j}}{\text{Vec}(\Gamma_0)_{N(j-1)+j}} = G_j(\boldsymbol{\beta}^*, \theta)$, where θ represents the set of structural parameters in γ_1, γ_2 and γ_3 . The next proposition collects our results to fully characterize a *BLE*.

Proposition 2.1: Given the law of motion in (2.14), there exists at least one BLE satisfying $\boldsymbol{\alpha}^* = 0$ if all eigenvalues of $(\gamma_1 + \gamma_2 \boldsymbol{\beta}^2)$ for each $\beta_i \in (-1, 1)$ lie inside the unit circle. Every

BLE satisfies the following system of equations:

$$\left\{ \begin{array}{l} S_t = \gamma_1 S_{t-1} + \gamma_2 \boldsymbol{\beta}^{*2} S_{t-1} + \gamma_3 \eta_t \\ \boldsymbol{\beta}^* = \text{diag}(\beta_1^* \beta_2^* \dots \beta_N^*, \mathbf{0}_{1, N-K}) \\ \forall j = \{1, \dots, N\}, \beta_j^* = \frac{\text{Vec}(\Gamma_1)_{N(j-1)+j}}{\text{Vec}(\Gamma_0)_{N(j-1)+j}} = G_j(\boldsymbol{\beta}^*, \theta) \\ \text{Vec}(\Gamma_0(\beta_1^* \dots \beta_N^*)) = \text{Vec}(\Gamma_0) = [I - M(\boldsymbol{\beta}^*) \otimes M(\boldsymbol{\beta}^*)]^{-1} (\gamma_3 \otimes \gamma_3) \text{Vec}(\Sigma_\eta) \\ \text{Vec}(\Gamma_1(\beta_1^* \dots \beta_N^*)) = \text{Vec}(\Gamma_1) = [I \otimes M(\boldsymbol{\beta}^*)] \text{Vec}(\Gamma_0) \\ M(\boldsymbol{\beta}^*) = \gamma_1 + \gamma_2 \boldsymbol{\beta}^{*2} \end{array} \right. \quad (2.16)$$

Furthermore, the E-stability principle applies. Accordingly, a BLE $(\boldsymbol{\alpha}^* \boldsymbol{\beta}^*)$ is locally stable if all eigenvalues of $(I - (\gamma_1 + \gamma_2 \boldsymbol{\beta}^{*2}))(\gamma_1 + \gamma_2 - I)$ have negative real parts, and all eigenvalues of $DG_{\boldsymbol{\beta}}(\boldsymbol{\beta}^*)$ have real parts less than one, where $DG(\boldsymbol{\beta})$ denotes the Jacobian matrix of $G(\boldsymbol{\beta})$

given by $DG(\boldsymbol{\beta}) = \begin{bmatrix} \frac{\partial G_1(\boldsymbol{\beta})}{\partial \beta_1} & \dots & \frac{\partial G_1(\boldsymbol{\beta})}{\partial \beta_N} \\ \vdots & \ddots & \vdots \\ \frac{\partial G_N(\boldsymbol{\beta})}{\partial \beta_1} & \dots & \frac{\partial G_N(\boldsymbol{\beta})}{\partial \beta_N} \end{bmatrix}.$

Proof: See Appendix B.

It is important to emphasize the distinction between the law of motion in (2.14) with time-varying learning parameters, and the BLE in (2.16) with fixed beliefs: The former characterizes a nonlinear law of motion under learning of the parameters $\boldsymbol{\beta}_t$. In the latter, we obtain the asymptotic behaviour of (2.14), where the learning has been completed and the parameters in $\boldsymbol{\beta}_t$ converged to their constant limiting values $\boldsymbol{\beta}^*$. Hence (2.16) characterizes a linear law of motion (where each learning parameter β_j^* is given by a nonlinear function in terms of $\beta_1^*, \dots, \beta_N^*$ and θ). Furthermore, comparing the 1-step ahead expectations given by (2.2) and (2.7) reveals a key difference between the REE and BLE. In the former, the expectations are formed in terms of the contemporaneous shocks ϵ_t , while in the latter, the expectations are characterized only in terms of previous realizations of the state variables S_{t-1} . Thus replacing the REE assumption with BLE allows us to endogenously generate additional persistence in the system, while the contemporaneous links between the endogenous variables become weaker. Therefore estimating a model under a BLE allows us to abstract away from time-variation in beliefs and investigate the empirical importance of these changes in the cross-restrictions of the REE in isolation.

Given the system in (2.16), we cannot obtain an analytical expression for the limiting belief parameters in $\boldsymbol{\beta}^*$ in terms of the structural parameters θ . Therefore, a key problem in the estimation of a BLE is how to jointly determine $\boldsymbol{\beta}^*$ along with θ . In order to address this issue, we start with the question of how to approximate a BLE quickly and accurately for a given θ .

While one can always simulate the SAC-learning process in (2.8) to obtain the limiting values of β^* , the learning dynamics often converge slowly and it takes a large number of simulations to accurately pin down β^* . Instead, we use an iterative approach in order to determine β^* , which is formalized below in Algorithm I.

Algorithm I: Numerical Approximation of a BLE with Fixed Parameters

Denote by θ the set of structural parameters, and by $G(\beta^{(k)}, \theta) = \text{diag}(G_1(\beta^{(k)}, \theta), \dots, G_N(\beta^{(k)}, \theta))$ the first-order autocorrelation function for a given θ .

- Step (0): Initialize the vector of learning parameters at $\beta^{(0)} = (\beta_1^{(0)}, \dots, \beta_N^{(0)})$.
- Step (I): At step k , using the first-order autocorrelation function, update the vector of learning parameters as follows:

$$\forall j = \{1, \dots, N\}, \beta_j^{(k)} = G_j(\beta^{(k)}, \theta) \Rightarrow \beta^{(k)} = G(\beta^{(k-1)}), \quad (2.17)$$

where $G(\beta^{(k-1)})$ is known from step $k-1$.

- Step (II): Terminate if $\|\beta^{(k)} - \beta^{(k-1)}\|_p < c$ for a small scalar $c > 0$ and a suitable norm distance $\|\cdot\|_p$, otherwise repeat Step (I).
-
-

Proposition 2.2: If Algorithm I converges to a stationary law of motion for a given K , the resulting system corresponds to an *approximate BLE*.

Proof: This trivially follows from Definition 2.1, where the first consistency requirement is satisfied by construction since $\alpha_t = \alpha^* = 0$, and the second consistency requirement is approximately satisfied since we have $G(\beta^K) \approx \beta^K$ after convergence, implying $\beta^* \approx \beta^K$.

Throughout the remainder of this paper, we use the L^1 -Norm as our norm distance, i.e. $\|\beta^{(k)} - \beta^{(k-1)}\|_p = \sum_{j=1}^N |\beta_j^{(k)} - \beta_j^{(k-1)}|$. The choice of the iteration function $G(\cdot)$ plays an important role in our scheme, which reduces Algorithm I to a simple fixed-point iteration. One could also consider a Quasi-Newton iteration:

$$\beta^{(k)} = (I - DG(\beta^{(k-1)})^{-1})^{-1}(\beta^{(k-1)} - DG(\beta^{(k-1)})^{-1}G(\beta^{(k-1)})) \quad (2.18)$$

where $DG(\beta^{(k)})$ denotes the Jacobian of $G(\beta)$ at iteration k , which we approximate using $\frac{\partial G_i(\beta^{(k)})}{\partial \beta_j^{(k)}} \approx \frac{G_i(\beta^{(k)} + h e_j) - G_i(\beta^{(k)})}{h}, \forall i, j \in \{1 \dots N\}$, where e_j denotes a suitable unit vector. We characterize the convergence properties of (2.17) and (2.18) below.

Proposition 2.3: Assume a locally stable (E-stable) *BLE* ($\alpha^* \beta^*$) exists. If all eigenvalues of $DG_\beta(\beta^*)$ lie inside the unit circle, then there exists a closed neighbourhood $\hat{I} = [\underline{I} \ \bar{I}]$, s.t $G(\cdot)$ is a contraction on \hat{I} . Accordingly, $\forall \beta^{(0)} \in \hat{I}$, we have $\lim_{k \rightarrow \infty} G^k(\beta^{(0)}) = \beta^*$.

Proof: See Appendix C.

Corollary: Define $\rho(G) = \max\{|\lambda| : \lambda \in \mathbb{C} \text{ an eigenvalue of } G\}$, and $\xi(G) = \max\{\text{Re}(\lambda) : \lambda \in \mathbb{C} \text{ an eigenvalue of } G\}$. Then the local stability and local contraction conditions jointly reduce to $\rho(DG_{\beta}(\beta^*)) < 1$ and $\xi((I - (\gamma_1 + \gamma_2\beta^{*2}))(\gamma_1 + \gamma_2 - I)) < 0$. Assuming the latter condition (which relates to the stability of mean dynamics) is satisfied, it follows that:

- (i) E-stability is a necessary condition for (2.17) to be a local contraction. This implies (2.17) does not converge to a locally unstable BLE. Interestingly, this does not hold for the Quasi-Newton iteration in (2.18); see Appendix B for more details.
- (ii) E-stability is not a sufficient condition for (2.17) to be a local contraction. This means, in general, there may exist a locally stable BLE that is not a stable fixed point of the iteration in (2.17). Therefore we complement the fixed-point iteration in (2.17) with corresponding Monte Carlo simulations in the upcoming sections in order to check whether additional locally stable equilibria exist.

The stability of learning dynamics under (2.17) is also known as the *iterative E-stability principle* in the learning literature (Evans & Honkapohja, 2012). Therefore we adopt this notation to denote stability under (2.17). As the above corollary makes it clear, *iterative E-stability* is a stronger condition than *E-stability*. Therefore, using the fixed-point iteration (2.17) does not only allow us to eliminate locally unstable BLE, but it also serves as a potential equilibrium selection mechanism when multiple E-stable equilibria exist. In the next two subsections, we examine the performance and convergence properties of this iteration scheme and compare it with the Quasi-Newton iteration in (2.18) using two generic variants of the baseline NKPC model along the lines of Woodford (2003).

2.1 The Case of a Unique BLE

Consider the baseline 3-equation NKPC model given by:

$$\begin{cases} x_t = \mathbb{E}_t x_{t+1} - \frac{1}{\tau}(r_t - \mathbb{E}_t \pi_{t+1}) + u_{x,t} \\ \pi_t = \lambda \mathbb{E}_t \pi_{t+1} + \gamma x_t + u_{\pi,t} \end{cases} \quad (2.19)$$

where $u_{x,t}$ and $u_{\pi,t}$ are structural exogenous shocks assumed to follow AR(1) processes:

$$\begin{cases} u_{x,t} = \rho_x u_{x,t} + \epsilon_{x,t} \\ u_{\pi,t} = \rho_{\pi} u_{\pi,t} + \epsilon_{\pi,t} \end{cases} \quad (2.20)$$

where ρ_x, ρ_{π} are the first-order autocorrelation coefficients, and $\epsilon_{x,t}, \epsilon_{\pi,t}$ are two uncorrelated i.i.d noise terms with variances $\sigma_x^2, \sigma_{\pi}^2$. In this simple setup, τ is the inverse elasticity of intertemporal substitution in consumption of the representative household (HH), which can be interpreted as the risk aversion coefficient. γ is related to price stickiness and measures the

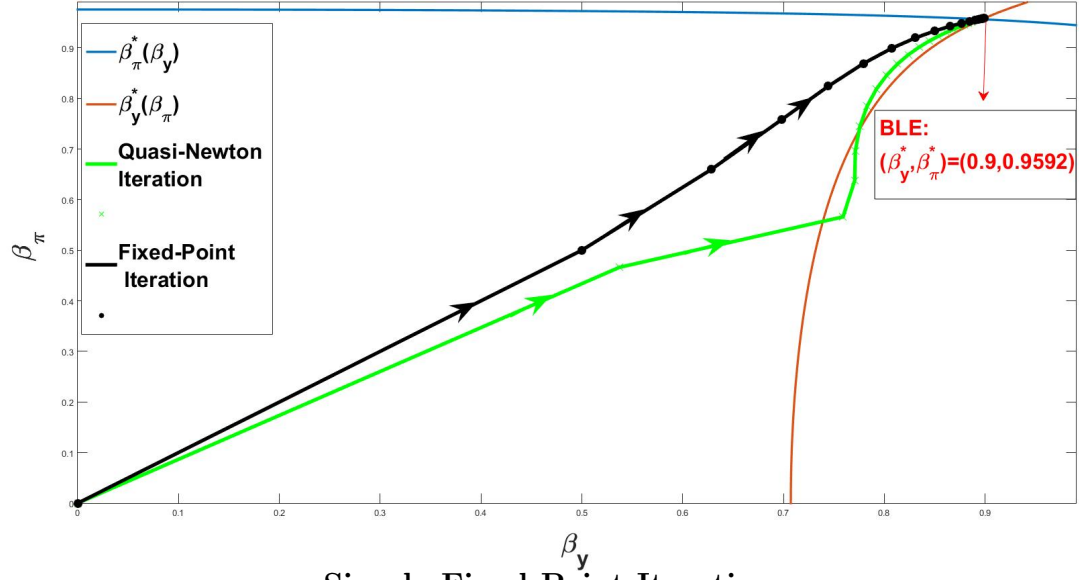
steepness of the Phillips curve, while λ is the discount factor of the representative HH. The model is supplemented with a standard Taylor-type policy rule, where the monetary policy is assumed to respond to inflation and output gap:

$$r_t = \phi_\pi \pi_t + \phi_y x_t \quad (2.21)$$

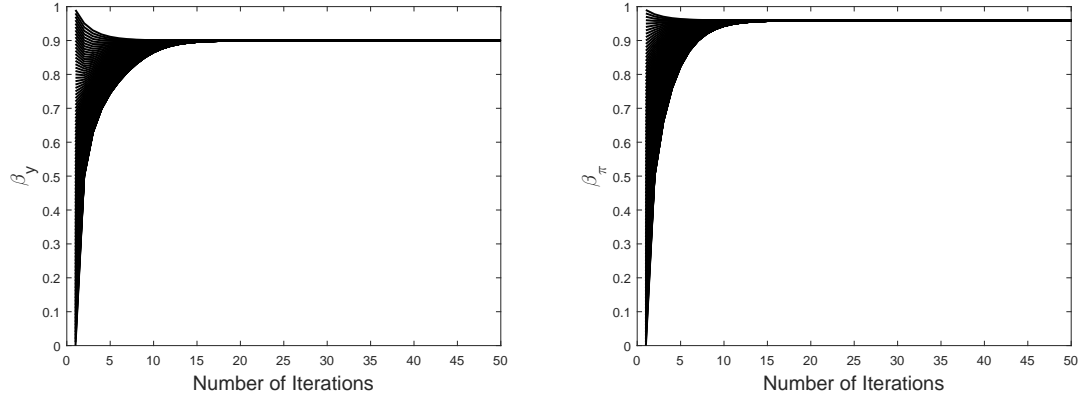
Since the model features two forward-looking variables, there are four corresponding learning parameters: the mean and first-order autocorrelation coefficients for inflation π_t and output gap x_t . [Hommes & Zhu \(2016\)](#) establish the uniqueness of the equilibrium under empirically plausible parameter values, and provide analytical expressions for $G_1(\beta)$ and $G_2(\beta)$. We apply the fixed-point and Quasi-Newton iterations in (2.17) and (2.18) using the same parameter values to examine their convergence properties. Accordingly, we set $\lambda = 0.99, \tau = 1, \gamma = 0.04, \frac{\sigma_x}{\sigma_\pi} = 0.5, \rho_y = \rho_\pi = 0.5, \phi_y = 0.5$ and $\phi_\pi = 1.5$. The top panel of Figure 1 shows the unique BLE $\beta^* = (\beta_y, \beta_\pi) = (0.9, 0.96)$, along with the convergence paths of the simple and Quasi-Newton iterations as specified in (2.17) and (2.18) when we initialize with $\beta^{(0)} = (0, 0)$. It is readily seen that both iteration schemes converge to the unique fixed point approximately at the same speed. In order to check the sensitivity of convergence to the initial values, the following two panels in the same figure show the convergence of the fixed-point and Quasi-Newton iterations with randomized initial values $\beta^{(0)} \in (0, 1)^2$. It is interesting to see that, for any given pair of initial values, the simple fixed-point iteration takes around 15 steps at most to converge, while this number is larger than 20 for the Quasi-Newton iteration. Nevertheless, both iteration types correctly identify the unique locally stable BLE of the system regardless of the initial values, which allows us to conclude that the open interval $(0, 1)$ is inside the equilibrium's basin of attraction β^* . As we noted before, since E-stability is not a sufficient condition for iterative E-stability, we complement the iterations with the corresponding Monte Carlo simulations of the system in (2.8). Figure 2 shows the resulting histograms of β_y and β_π for both learning parameters when we simulate the system with randomized initial values and errors η_t . It is clear that the system shows no sign of path dependence and multiplicity of equilibria, since the resulting distributions both have a single peak centered around the unique equilibrium values of β_y^* and β_π^* . In order to formalize this notion further, we provide the approximate distributions of β_y and β_π by smoothing the histograms and applying Hartigan's Dip Test of Unimodality⁵. The dip test clearly does not reject the null hypothesis of unimodality, providing no evidence of multiple BLE at the given parameter values. These results confirm that by using the simple fixed-point iteration with randomized initial values, along with the corresponding Monte Carlo simulations of the model, we can correctly identify the unique E-stable BLE. In the next section, we turn to the analysis of a system with multiple equilibria.

⁵This test is based on checking for multimodality by using the maximum difference between the empirical distribution, and the theoretical unimodal distribution function that minimizes the maximum difference. The null hypothesis of the test is unimodality, see [Hartigan & Hartigan \(1985\)](#) for more details.

Figure 1: Convergence of the fixed-point and Quasi-Newton iterations in (2.17) and (2.18) to the unique BLE: A Graphical Illustration. Top Panel: Convergence when we use the initial value $\beta^{(0)} = (0, 0)$. Bottom Panels: Convergence when we apply the algorithm 100 times with randomized initial values on $(0, 1)^2$ using the fixed-point and Quasi-Newton iterations.



Simple Fixed-Point Iteration:



Quasi-Newton Iteration:

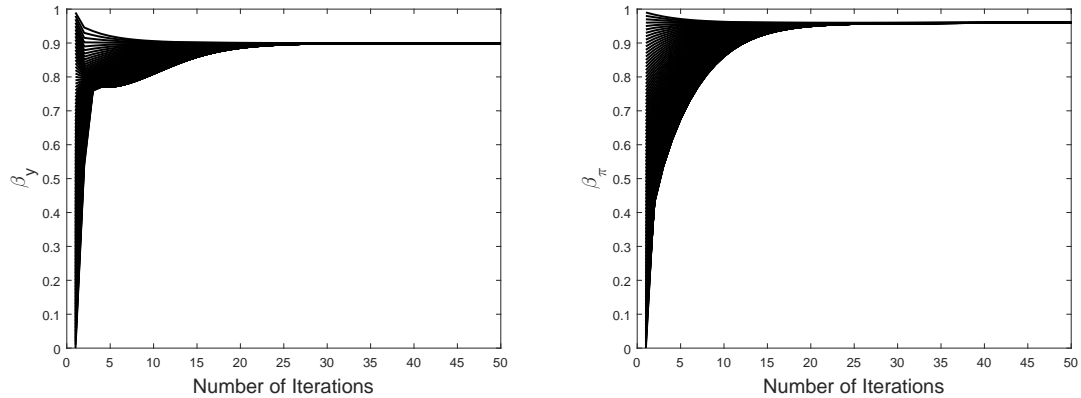
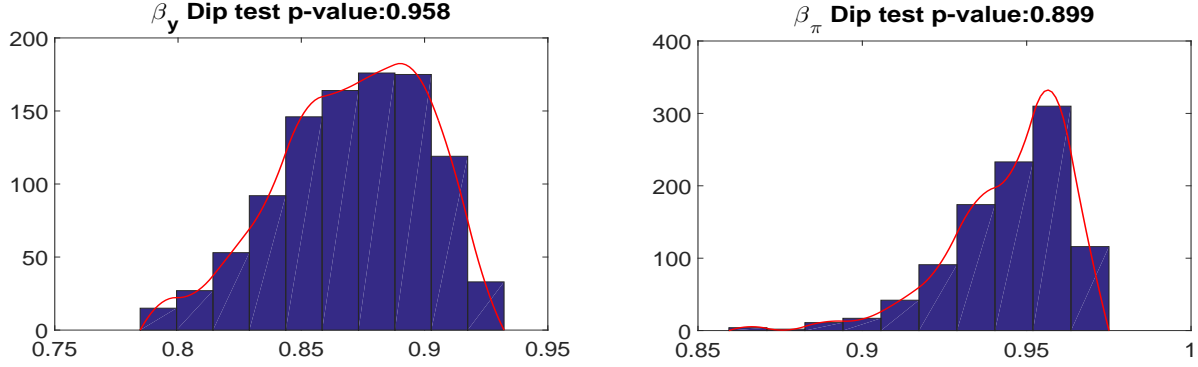


Figure 2: NKPC Model: Histograms of the long-run learning parameters β_y (Left) and β_π (Right) resulting from the Monte Carlo simulations, where the BLE is given by $\beta^* = (\beta_y, \beta_\pi) = (0.9, 0.96)$. The system given by (2.19), (2.20) and (2.21) is simulated 1000 times under BLE with randomized shocks and randomized initial values for the endogenous variables, using 20000 periods for each simulation. The red lines correspond to the smoothed histograms. The dip test yields a p-value of 0.96 and 0.9 for β_y and β_π respectively, providing no evidence of multiple equilibria.



2.2 The Case of Multiple BLE

In order to consider a simpler setup, in this section we abstract away from monetary policy and assume that output gap x_t follows an exogenous AR(1) process:

$$\begin{cases} \pi_t = \lambda \mathbb{E}_t \pi_{t+1} + \gamma x_t + u_t \\ x_t = a + \rho x_{t-1} + \epsilon_t \end{cases} \quad (2.22)$$

where u_t and ϵ_t denote white noise processes with variances σ_u and σ_ϵ respectively. In this setup, inflation π_t is the only forward-looking variable and there are only two learning parameters. Hommes & Zhu (2014) show that, under empirically plausible parameter values, the system features multiple equilibria, namely with $\delta = 0.99, \gamma = 0.075, a = 0.0004, \rho = 0.9, \sigma_\epsilon = 0.01, \sigma_u = 0.003162$. While the mean parameter is unique at $\alpha_\pi^* = 0.03$, there are three equilibria with respect to the persistence parameter β_π : two stable equilibria at $(\beta_1^*, \beta_3^*) = (0.3066, 0.9961)$ and one unstable equilibrium at $\beta_2^* = 0.7417$ ⁶, which are illustrated in the top panel of Figure 3. The middle panel of the same figure shows convergence of the fixed-point and Quasi-Newton iterations in (2.17) and (2.18) respectively with randomized initial values. In this case, depending on the initial state $\beta_\pi^{(0)}$ the iterations converge to different equilibria. Unlike the previous example, the Quasi-Newton iteration converges faster than the fixed-point iteration in general. However, an interesting result that immediately stands out is that, the Quasi-Newton itera-

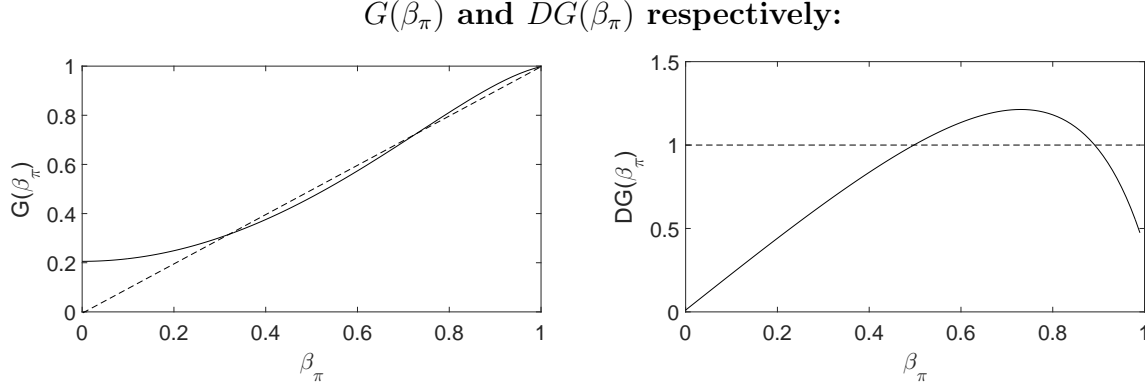
⁶Since there is only one forward-looking variable in this case, the mapping $G(\cdot)$ can be analytically computed and is given by $G(\beta_\pi) = \delta \beta_\pi^2 + \frac{\gamma^2 \rho (1 - \delta^2 \beta_\pi^4)}{\gamma^2 (\delta \beta_\pi^2 \rho + 1) + (1 - \rho^2)(1 - \delta \beta_\pi^2 \rho) \frac{\sigma_u^2}{\sigma_\epsilon^2}}$.

tion occasionally converges to the unstable equilibrium for initial values close to β_2^* , while the fixed-point iteration always converges to one of the stable equilibria. This confirms the results in Proposition 2.3. Notice that, for values close to β_2^* , the simple iteration (2.17) is not a contraction since $DG(\beta_\pi) > 1$. In these cases, the iteration is driven upwards or downwards depending on the initial value, until it reaches the basin of attraction for one of the stable BLE and becomes a local contraction again. This also explains why its convergence is slower in this case compared to the Quasi-Newton iteration, especially for starting values close to β_2^* . Convergence to unstable equilibria is an undesirable feature of the Quasi-Newton iteration in general, since these equilibria are not relevant from an empirical point of view⁷. Figure 3 shows the corresponding histogram resulting from 1000 Monte Carlo simulations of the system with randomized shocks and initial values: it is readily seen that the resulting histogram of β_π resembles a bimodal distribution with two peaks in the neighbourhoods of the two stable equilibria. The Dip test result confirms the presence of multiple equilibria, where unimodality is rejected with a p-value of 0.00.

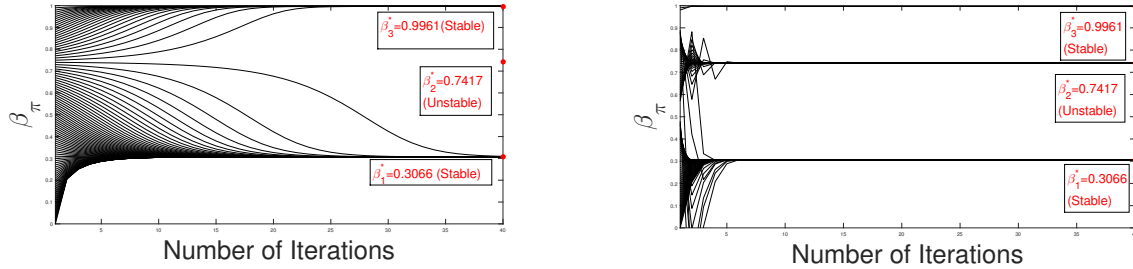
Our results indicate that, in the presence of multiple equilibria, we are able to correctly identify the multiplicity with both iterations in (2.17) and (2.18), as well as with the Monte Carlo simulations of the system. This is an important point before we move onto richer models since, in general, the expressions for β^* in (2.16) are complex enough that we do not know a priori whether the equilibrium at a given parameter set is unique or not. In such systems, the distributions resulting from the Monte Carlo simulations along with the iterations specified in (2.17) and (2.18) with randomized initial values can be used to examine the number of equilibria. It is important to note that, while iterative E-stability is stronger than E-stability in general, our analysis shows that they are equivalent in the two examples considered so far. Furthermore, we observe that the simple fixed-point iteration is more suitable to approximate BLE, since its convergence ensures the iterative E-stability of a given equilibrium, while the Quasi-Newton iteration may result in locally unstable equilibria. More importantly, while the Quasi-Newton approach may take a smaller number of steps to converge in case of multiple equilibria, this approach takes longer in general since the approximation of the Jacobian matrix is a computationally heavy step. Therefore, for the remainder of our paper, we use iterative E-stability as our equilibrium selection criterion and continue our analysis with the simple fixed-point iteration scheme (2.17) for the empirical validation of BLE.

⁷The Quasi-Newton iteration also occasionally leaves the unit circle along the convergence path, which we omit in our figure.

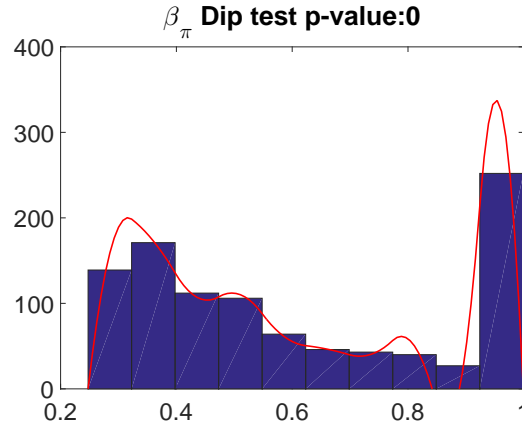
Figure 3: Top panel: The mappings $G(\beta_\pi)$ and $DG(\beta_\pi) = \frac{\partial G(\beta_\pi)}{\partial \beta_\pi}$ that illustrate the multiplicity of equilibria. Middle panel: Convergence of the iterations (2.17) and (2.18) with randomized initial values. We use a total of 100 iterations in both cases. Bottom panel: Histogram of the learning parameter β_π resulting from 1000 Monte Carlo simulations, along with the Dip Test result.



The simple iteration in (2.17), and Quasi-Newton iteration in (2.18) respectively:



Monte Carlo Simulations: $(\beta_\pi^1, \beta_\pi^2) = (0.3066, 0.9961)$.



2.3 Estimation of an Approximate BLE

The discussion so far is based on the assumption that the vector of model parameters θ is fixed at each iteration of the procedure. In this section, we provide a straightforward extension

of Algorithm I to accommodate the Bayesian estimation of an approximate BLE. In order to estimate the model, we supplement the law of motion in (2.16) with a set of measurement equations, which we characterize as follows:

$$y_t = \psi_0(\theta) + \psi_1(\theta)S_t + u_t \quad (2.23)$$

where y_t denotes a vector of observable variables, u_t is a vector of measurement errors, $\psi_0(\theta)$ and $\psi_1(\theta)$ are matrices of the deep parameters that relate the state variables S_t and the observable variables y_t . Together, (2.16) and (2.23) yield the state-space representation of the DSGE model of interest. Accordingly, we have a law of motion that is linear in the state variables S_t , but a subset of the parameters, namely β^* , are a non-linear function in terms of the deep parameters θ to be estimated. On the one hand, given the nonlinear function $\beta^* = G(\beta^*, \theta)$, we can only derive an approximation to the matrix β^* using an iterative method for given θ . On the other hand, whenever β^* is temporarily fixed at an arbitrary $\beta^{(k)}$ at any stage of the iteration, our model reduces to a backward-looking model that can be estimated using standard state-space methods. Building upon this idea, we consider the following iterative routine where we update the structural parameters θ and belief parameters β sequentially.

Algorithm II: Bayesian Estimation of an Approximate BLE

Denote by $Y_{1:T} = \{Y_1 \dots Y_T\}$ the matrix of the observable variables up to period T , and by $p(\theta)$ the prior distributions for the structural parameters θ that appear in matrices γ_1 , γ_2 and γ_3 . Consider the system characterized by (2.16) and (2.23):

$$\begin{cases} S_t = \gamma_1 S_{t-1} + \gamma_2 \beta^{*2} S_{t-1} + \gamma_3 \eta_t \\ \beta_j^* = G_j(\beta^*, \theta) \\ y_t = \psi_0(\theta) + \psi_1(\theta) S_t + u_t \end{cases} \quad (2.24)$$

- **Step (0)** Initialize a set of learning parameters $\beta^{(0)} = (\beta_1^{(0)}, \dots, \beta_N^{(0)})$. At the (temporarily) fixed $\beta^{(0)}$, the system (2.24) reduces to a standard state-space representation for the linearized DSGE model.
- **Step (I-a)** At each iteration k , one can obtain the likelihood function using the Kalman filter and the corresponding posterior distribution conditional on $\beta^{(k-1)}$ as follows⁸:

$$p(Y_{1:T}|\theta, \beta^{(k-1)}) = \sum_{t=1}^T p(y_t|Y_{1:T-1}, \theta, \beta^{(k-1)}); p(\theta|Y_{1:T}, \beta^{(k-1)}) = \frac{p(Y_{1:T}|\theta, \beta^{(k-1)})p(\theta)}{p(Y_{1:T}, \beta^{(k-1)})} \quad (2.25)$$

where $\beta^{(k-1)}$ is obtained from step $k-1$, and $p(Y_{1:T}, \beta^{(k-1)})$ denotes the marginal likelihood function. Denote by $\hat{\theta}^{(k)}$ the conditional posterior mode obtained from $\hat{\theta}^{(k)} = \text{argmax}_{\theta} p(\theta|Y_{1:T}, \beta^{(k-1)})$.

- **Step (I-b)** Using $\hat{\theta}^{(k)}$, update the matrix of learning parameters:

$$\beta_j^{(k)} = G_j(\beta^{(k-1)}, \hat{\theta}^{(k)}), \forall j = \{1 \dots N\}, \quad (2.26)$$

- **Step(II)** Proceed to Step (III) if $\|\beta^{(k)} - \beta^{(k-1)}\| < c$ and $\|\hat{\theta}^{(k)} - \hat{\theta}^{(k-1)}\| < c$ for some scalar $c > 0$, otherwise repeat Step (I).
 - **Step(III)** Use the Metropolis-Hastings algorithm to construct the posterior distribution *conditional on the approximated BLE*.
 - **Step(IV):** At the estimated posterior mode $\hat{\theta}^{(k)}$, apply Monte Carlo simulations and Algorithm I with randomized initial values to check for multiplicity of locally stable BLE.
-
-
-

⁸For a detailed textbook derivation of the likelihood function and the posterior distribution, see e.g. [Greenberg \(2012\)](#) or [Herbst & Schorfheide \(2015\)](#). In this paper, we make use of the routines available in Dynare to estimate the model at each step for a given set of fixed learning parameters.

Proposition 2.4: If algorithm II converges for a given $\beta^{(K)}$ and $\hat{\theta}^{(K)}$, the resulting law of motion is a *locally stable approximate BLE*. Furthermore, denote the converged set of learning coefficients and estimates as (β^*, θ^*) , with $\beta^* = G(\beta^*, \theta^*)$. If $\rho(DG(\beta^*, \theta^*)) < 1$, then there exists a closed neighbourhood $\hat{I} \in [\underline{I}, \bar{I}]$ such that $G(\cdot)$ is a contraction on \hat{I} . Accordingly, $\forall \beta^{(0)} \in \hat{I}$, we have $\lim_{k \rightarrow \infty} G^k(\beta^{(0)}, \theta^{(0)}) = (\beta^*, \theta^*)$.

Proof: See Appendix B.

Remark: Note that, $\forall \beta$ with $\beta_i \in (-1, 1)$ for each $i \in \{1..N\}$, we have $G(\beta) \in (-1, 1)^N$ since $G(\cdot)$ is the matrix of first-order autocorrelations by definition. This implies, $\forall \beta^{(0)}$ and β^* with $\beta_i^{(0)} \in (-1, 1)$ and $\beta_i^* \in (-1, 1)$ for each i , we have $G_i(\beta^{(k)}) \in (-1, 1), \forall i \in \{1..N\}$ and $\forall k \in \mathbb{N}$ and hence $\beta_i^{(k)} \in (-1, 1), \forall i \in \{1..N\}$ and $k \in \mathbb{N}$. Accordingly, as long as $\beta^{(0)} \in \hat{\beta}$, each $\beta_i, \forall i \in \{1, \dots, N\}$ remains inside the unit circle and within the stability region. Therefore, within our framework, the system is not arbitrarily pushed into a region with explosive dynamics and we do not need projection facilities for our estimation procedure for the BLE.

Our estimation routine as described above corresponds to a straightforward extension of Algorithm I, where we allow the structural (deep) parameters θ (and consequently the matrices γ_1, γ_2 and γ_3) to be re-estimated at each step of the fixed-point iteration in (2.17). Our approach is especially similar to the computation of initial beliefs in Slobodyan & Wouters (2012a), where the beliefs in β are treated as separate parameters and estimated along with θ . The main difference here is, we compute the beliefs consistent with the underlying BLE, such that the first-order autocorrelations in the PLM coincide with the ALM at the estimated posterior mode. In other words, the beliefs are actually consistent with the realizations. We opt for this estimation approach particularly due to its speed and ease of implementation, because the sequential updating mechanism allows us to approximate and estimate BLE at the posterior mode through a sequence of linear models. Since the beliefs in $\beta^{(k)}$ are updated at each step k based on the first-order autocorrelations of the state variables, the estimated parameters $\hat{\theta}^k$ tend to lead β^k towards the empirically relevant region. In turn, this allows the system to rapidly converge to the underlying BLE as we illustrate in the upcoming sections, where we subsequently estimate the baseline NKPC and the workhorse Smets & Wouters (2007) models.

3 Estimation of The Baseline NKPC Model

In this section, we apply Algorithm II to the small-scale NKPC-model given by (2.19) and (2.20). We augment the Taylor rule in (2.21) with an i.i.d shock to include the historical interest rate in our estimation, and generalize the equation with an interest rate smoothing parameter to allow the model to match the inertia of the historical interest rate:

$$r_t = \rho_r r_{t-1} + (1 - \rho_r)(\phi_\pi \pi_t + \phi_x x_t) + \epsilon_{r,t} \quad (3.1)$$

We estimate the small-scale system for the U.S economy over the period 1966:I-2016:IV. The U.S economy has experienced a large volatility reduction in most macroeconomic parameters in mid-80s, often referred to as the Great Moderation. Nevertheless we consider the entire sample period in this section: Inflation is highly persistent over the entire sample period, while its persistence is substantially reduced if we consider the post Great Moderation period. The highly persistent series allow us to illustrate the persistence amplification under the BLE estimation. Furthermore, empirical studies involving the U.S interest rate typically do not cover the post-2007 period due to concerns over the zero lower bound. Therefore, while we ignore the potential impact of the ZLB constraint in our main estimations, we show that the results are robust to different sample periods later on⁹. We use the following measurement equations for output gap, inflation and interest rate¹⁰:

$$\begin{cases} \log(x_t^{obs}) = \bar{\gamma} + x_t \\ \log(\pi_t^{obs}) = \bar{\pi} + \pi_t \\ \log(r_t^{obs}) = \bar{r} + r_t \end{cases} \quad (3.2)$$

where we use the HP-filtered output as our measure of output gap $x_t^{obs,11}$, while π_t^{obs} and r_t^{obs} denote the historical inflation and interest rate series respectively. $\bar{\gamma}, \bar{\pi}$ and \bar{r} correspond to the steady-state levels of output gap, inflation and interest rate. Note that, in this simple framework, the steady-state levels coincide with the sample means of the observable variables. The model is estimated using the same prior distributions under both the RE and BLE specifications, which guarantees that any differences that arise between the estimations is due to the difference in the expectation formation rule. The prior distributions are kept as close as possible to those commonly assumed in the literature, in particular Smets-Wouters (2007) and Herbst & Schorfheide (2015). The risk aversion coefficient τ is assigned a gamma distribution centered at 2 with a standard deviation of 0.5, covering values of approximately up to four. The parameter γ that relates real activity to inflation is assigned a Beta distribution with mean 0.3, covering both flat and steep cases for the Phillips curve¹². The policy response parameters for output gap and inflation are assigned beta distributions centered around 0.5 and 1.5, which are the typical values associated with the Taylor Rule in the literature. The autocorrelation coefficients have a Beta distribution centered at 0.5, and the standard deviations for the shock

⁹Furthermore, recent studies show that, if there are any biases at all on the estimated parameters related to ignoring the ZLB, these are limited to steady-state and monetary policy related parameters, while the rigidity and structural shock parameters remain unaffected. See Hirose & Sunakawa (2016) and Hirose & Inoue (2016) for more details.

¹⁰See Appendix A for more details on the observable variables.

¹¹In Appendix E, we consider alternative specifications of the output gap to see the sensitivity of our results to this specification.

¹²In particular, the nominal price stickiness ω relates to the slope of NKPC as $\gamma = \frac{(1-\lambda\omega)(1-\omega)}{\omega}$. Note that γ is decreasing in ω .

processes are assumed to follow an Inverted Gamma distribution with a mean of 0.1. The priors for the steady-state inflation rate, output growth and interest rate are taken directly from SW (2007) and have means of 0.625, 0.4 and 0.5 respectively. Finally, we fix the HH discount rate λ at 0.99 as is customary in empirical studies.

Table 1: Prior Distributions for the Structural Parameters of the Small-Scale NKPC Model.

| Parameter | Dist. | Mean | St. Dev |
|-------------|-----------|------|---------|
| τ | Gamma | 2 | 0.50 |
| γ | Beta | 0.3 | 0.15 |
| ρ_y | Beta | 0.50 | 0.20 |
| ρ_π | Beta | 0.50 | 0.20 |
| ρ_r | Beta | 0.50 | 0.20 |
| ϕ_y | Gamma | 0.50 | 0.25 |
| ϕ_π | Gamma | 1.5 | 0.25 |
| $\bar{\pi}$ | Gamma | 0.63 | 0.25 |
| \bar{y} | Normal | 0.40 | 0.25 |
| \bar{r} | Gamma | 0.50 | 0.25 |
| η_y | Inv Gamma | 0.10 | 2 |
| η_π | Inv Gamma | 0.10 | 2 |
| η_r | Inv Gamma | 0.10 | 2 |

Table 3 presents the posterior estimation results for the RE and learning models using these prior distributions.¹³ Before moving onto the estimation results, we first briefly discuss the convergence diagnostics of BLE: Initializing both β_y and β_π at fairly low values of 0.5 and using a convergence criterion $c = 10^{-5}$, the algorithm takes only 5 steps to converge to the BLE $(\beta_y^*, \beta_\pi^*) = (0.86, 0.79)$, which is fairly close to the true sample-autocorrelations of $(0.87, 0.88)$ over this period. The top panel of Figure 4 shows the norm distances between two consecutive sets of $\beta^{(k)}$ and $\theta^{(k)}$ at each step k , both of which rapidly converge towards 0. The largest eigenvalue of the Jacobian matrix $DG(\beta^{(k)}, \theta^{(k)})$ remains strictly inside the unit circle during the estimation, and stabilizes after the second step. The middle and bottom panels of Figure 4 show the corresponding MC simulations and the results of Algorithm I with randomized initial values. It is readily seen that the histograms for both β_y and β_π have a distribution centered around their estimated values of 0.86 and 0.79 with no sign of multiple equilibria. This is confirmed by the Dip Test results, which do not reject the null hypothesis of unimodality. A similar result also emerges from the bottom panel, where Algorithm I converges to the esti-

¹³Both models are estimated using Dynare (Adjemian et al., 2011), where the posterior distributions are constructed using the Metropolis-Hastings algorithm with 250000 draws, using the first 50000 as the burn-in sample. The step size for the scale parameter of the jumping distribution's covariance matrix is adjusted in both models to obtain a rejection rate of 70% in both models, which is in the commonly assumed appropriate range for the MH algorithm.

mated β^* for all initial values. These results indicate the unique locally stable equilibrium is also iteratively E-stable. It is also remarkable to note that, while the fixed-point iteration with fixed parameters takes up 100 iterations to fully converge, the estimation algorithm converges after only 5 steps. This relates to the additional flexibility resulting re-estimation of the structural parameters at each step: For a given set of belief parameters, the estimation results tend to yield first-order autocorrelations close to the true sample moments. Since the beliefs are updated based on these first-order autocorrelations in the next iterate, they quickly end up in the empirically relevant region, thus making the convergence faster.

Next we move onto the discussion of our estimation results. To start with the parameter estimates under the BLE and REE specifications, we observe several important differences¹⁴: Both persistence parameters for the inflation and output shocks, ρ_π and ρ_y , are substantially lower under BLE with 0.31 and 0.42 respectively, while they are 0.88 and 0.87 under REE respectively. This is a direct consequence of the difference in the expectation formation rule, which shows the persistence amplification property of a BLE. The backward-looking expectation rule endogenously generates additional inertia for the forward-looking variables, which in turn leads to much smaller persistence in the exogenous shocks to match the empirical autocorrelations of inflation and output gap. The low autocorrelation in u_π and u_y under BLE immediately imply higher estimated standard deviations for the i.i.d shocks of these AR(1) processes at 0.29 and 0.73, while these are 0.04 and 0.16 under REE¹⁵. Since interest-rate is not forward-looking, this result does not extend to the interest-rate smoothing ρ_r , which is estimated at 0.85 and 0.79, with similar levels of volatility at 0.29 and 0.3 under BLE and REE respectively. The steady-state parameters turn out fairly similar under both estimations, since they relate to sample means of the observable variance and are mostly independent of the expectation rule. The estimates of monetary policy parameters, ϕ_π and ϕ_y also turn out similar under both estimations, with 1.36 and 0.48 under BLE, and 1.39 and 0.46 under REE. Finally turning to the two structural parameters that determine the contemporaneous relation between the state variables, both the risk aversion coefficient τ and the slope of the NKPC γ turn out fairly different: These are estimated at 2.99 and 0.035 under BLE, while they are 4.27 and 0.007 under REE respectively. These differences arise due to altered cross-restrictions under learning: The additional inertia that we introduce under learning comes at the cost of a weaker contemporaneous relation between the state variables. While the state variables are only related to each other through τ and γ under BLE, they also indirectly affect each other through expectations

¹⁴As noted in the previous section, the first-order coefficients are computed based on the posterior mode values. Therefore, for completeness, the discussion and comparison of these results (both in this section and in the upcoming ones) is based on the posterior mode. It is worth noting that, given the small differences across the posterior means and modes, a similar discussion and conclusions easily extend to the posterior mean.

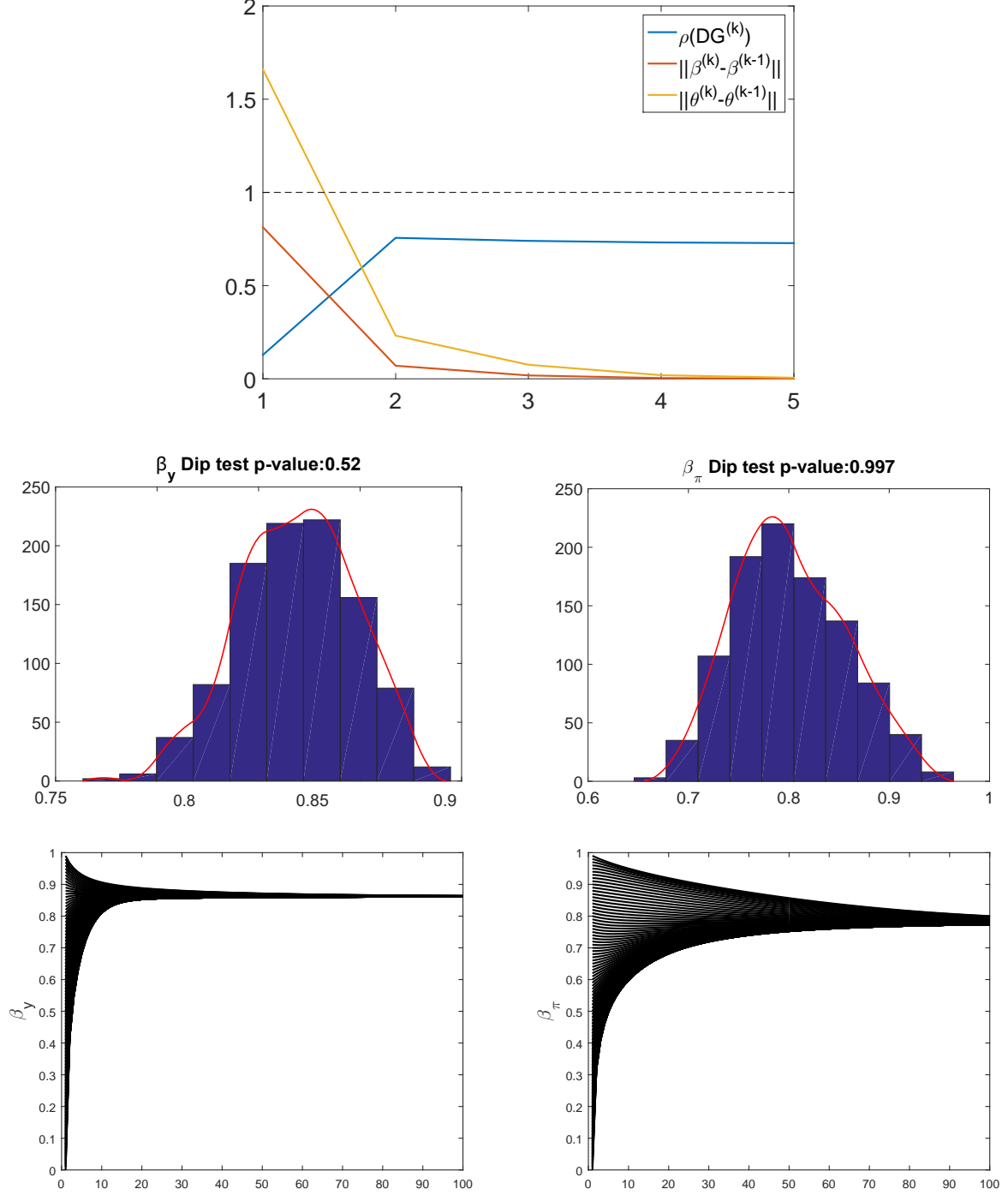
¹⁵Note that for an AR(1) process $x_t = \rho_x x_{t-1} + u_t$, $u_t \sim iid(0, \sigma_u)$, the unconditional variance is given by $var(x) = \frac{\sigma_u}{1-\rho_x^2}$. This implies, as ρ_x increases, $var(x)$ also increases.

under REE. As a result, the risk aversion coefficient turns out lower under learning, implying a larger direct impact from the ex-ante risk premium on output gap under BLE. Similarly, γ turns out higher under BLE, implying a stronger direct effect from output gap on inflation. The identity $\gamma = \frac{(1-\lambda\omega)(1-\omega)}{\omega}$ in turn implies the estimated nominal price stickiness ω is lower under BLE with around 0.83, while it is around 0.92 under REE. It is also interesting to note that confidence intervals for γ are almost mutually exclusive under these two specifications, with a lower bound of 0.012 under BLE and an upper bound of 0.017 under REE. Overall, our results suggest important differences in the estimated parameters and the propagation of shocks under BLE. These changes lead to a substantial improvement in the empirical fit, evident from the likelihood of -340 under BLE compared with -350 under REE. While small differences might arise in the parameter estimates when we use different measures of output gap, the overall results are robust across all specifications we consider, which is investigated in more detail in Appendix E. In the next section, we extend our framework to the workhorse [Smets & Wouters](#) (SW) model.

Table 2: Posterior Results under REE and BLE over the estimation period 1966:I-2016:IV. Lapl. refers to the Laplace likelihood approximation based on the posterior mode, while MHM refers to the Modified Harmonic Mean likelihood based on the posterior distribution.

| | BLE | | | | REE | | | |
|-------------|---------|-------|-------|------|---------|------|-------|-------|
| Laplace | -340.75 | | | | -350.84 | | | |
| MHM | -340.77 | | | | -350.89 | | | |
| Parameter | Mode | Mean | 5 % | 95 % | Mode | Mean | 5 % | 95 % |
| η_y | 0.73 | 0.74 | 0.68 | 0.8 | 0.16 | 0.17 | 0.13 | 0.22 |
| η_π | 0.29 | 0.3 | 0.27 | 0.32 | 0.04 | 0.04 | 0.03 | 0.05 |
| η_r | 0.29 | 0.3 | 0.27 | 0.32 | 0.3 | 0.3 | 0.28 | 0.33 |
| \bar{y} | 0.18 | 0.23 | 0.001 | 0.43 | 0.24 | 0.28 | 0.001 | 0.51 |
| $\bar{\pi}$ | 0.81 | 0.81 | 0.68 | 0.93 | 0.65 | 0.65 | 0.44 | 0.86 |
| \bar{r} | 1.19 | 1.18 | 0.91 | 1.46 | 1.06 | 1.07 | 0.73 | 1.41 |
| γ | 0.035 | 0.037 | 0.012 | 0.06 | 0.007 | 0.01 | 0.002 | 0.017 |
| τ | 2.99 | 3.13 | 2.32 | 3.95 | 4.27 | 4.35 | 3.35 | 5.37 |
| ϕ_π | 1.36 | 1.39 | 1.1 | 1.68 | 1.39 | 1.43 | 1.18 | 1.67 |
| ϕ_y | 0.48 | 0.52 | 0.31 | 0.72 | 0.46 | 0.49 | 0.33 | 0.65 |
| ρ_y | 0.42 | 0.42 | 0.32 | 0.52 | 0.87 | 0.86 | 0.82 | 0.91 |
| ρ_π | 0.31 | 0.33 | 0.22 | 0.43 | 0.88 | 0.87 | 0.83 | 0.91 |
| ρ_r | 0.85 | 0.86 | 0.82 | 0.91 | 0.79 | 0.8 | 0.76 | 0.84 |

Figure 4: Top Panel: Convergence of the norm distance for the learning coefficients, estimated parameters and the largest eigenvalue of the system. We use a critical value of $c = 10^{-5}$ as our stopping criterion. Middle Panel: Histograms of the long-run learning parameters based on 1000 Monte Carlo simulations (each with 20000 periods), where the BLE is given by $(\beta_y^*, \beta_\pi^*) = (0.86, 0.79)$. We use randomized shocks and randomized initial values, along with the unimodality tests. Bottom Panel: Algorithm I at the estimated posterior mode with randomized initial values.



4 Estimation of the Smets-Wouters Model

Building upon [Christiano et al. \(2005\)](#) and [Smets & Wouters \(2003\)](#), the SW (2007) model consists of 13 equations linearized around the steady-state growth path, supplemented with seven exogenous structural shocks. We deviate from the benchmark model by slightly restricting the parameter space of the model, where we assume all shocks follow an AR(1) process¹⁶. Further, we assume away the real wage and inflation indexation parameters, which are commonly criticised for being ad-hoc. In this section we briefly outline the resulting linearized model economy that is used in our estimation. To start with the demand side of the economy, the aggregate resource constraint is given by:

$$\begin{cases} y_t = c_y c_t + i_y i_t + z_y z_t + \epsilon_t^g \\ \epsilon_t^g = \rho_g \epsilon_{t-1}^g + \eta_t^g \end{cases} \quad (4.1)$$

where y_t, c_t, i_t and z_t are the output, consumption, investment and capital utilization rate respectively, while c_y, i_y and z_y are the steady-state shares in output of the respective variables. The second equation in (4.1) defines the exogenous spending shock ϵ_t^g where η_t^g is an i.i.d-normal disturbance for spending. The consumption Euler equation is given by:

$$\begin{cases} c_t = c_1 c_{t-1} + (1 - c_1) \mathbb{E}_t c_{t+1} + c_2 (l_t - \mathbb{E}_t l_{t+1}) - c_3 (r_t - \mathbb{E}_t \pi_{t+1}) + \epsilon_t^b \\ \epsilon_t^b = \rho_b \epsilon_{t-1}^b + \eta_t^b \end{cases} \quad (4.2)$$

with $c_1 = \frac{\lambda}{\gamma} / (1 + \frac{\lambda}{\gamma})$, $c_2 = (\sigma_c - 1)(w_{ss} l_{ss} / c_{ss}) / (\sigma_c (1 + \frac{\lambda}{\gamma}))$, $c_3 = (1 - \frac{\lambda}{\gamma}) / ((1 + \frac{\lambda}{\gamma}) \sigma_c)$, where λ, γ and σ_c denote the habit formation in consumption, steady state-growth rate and the elasticity of intertemporal substitution respectively, while x_{ss} corresponds to the steady-state level of a given variable x . The equation implies that current consumption is a weighted average of the past and expected future consumption, expected growth in hours worked and the ex-ante real interest rate. ϵ_t^b corresponds to the risk premium shock modeled as an AR(1) process, where η_t^b is an i.i.d-normal disturbance. Next, the investment Euler equation is defined as:

$$\begin{cases} i_t = i_1 i_{t-1} + (1 - i_1) \mathbb{E}_t i_{t+1} + i_2 q_t + \epsilon_t^i \\ \epsilon_t^i = \rho_i \epsilon_{t-1}^i + \eta_t^i \end{cases} \quad (4.3)$$

with $i_1 = \frac{1}{1 + \bar{\beta}\gamma}$, $i_2 = \frac{1}{(1 + \bar{\beta}\gamma)(\gamma^2 \phi)}$, where $\bar{\beta} = \beta \gamma^{-\sigma_c}$, ϕ is the steady-state elasticity of capital adjustment cost and β is the HH discount factor. q_t denotes the real value of existing capital

¹⁶ In particular, the benchmark model has more structure on the exogenous shocks, where the mark-up shocks each follow an ARMA(1,1) process, and the technology and government spending shocks follow a VAR(1) process. We refer the reader to SW (2003) and SW (2007) for more details about the microfoundations of the benchmark model.

stock. Similar to the consumption Euler, the equation implies that investment is a weighted average of past and expected future consumption, as well as the real value of existing capital stock. ϵ_t^i represents the AR(1) investment shock, where η_t^i is an i.i.d-normal disturbance. The value of capital-arbitrage equation is given by:

$$q_t = q_1 \mathbb{E}_t q_{t+1} + (1 - q_1) \mathbb{E}_t r_{t+1}^k - (r_t + \mathbb{E}_t \pi_{t+1}) + \frac{1}{c_3} \epsilon_t^b \quad (4.4)$$

with $q_1 = \bar{\beta}(1 - \delta)$, implying the real value of capital stock is a weighted average of its expected future value and expected real rental rate on capital, net of ex-ante real interest rate and the risk premium shock. The production function is characterized as:

$$\begin{cases} y_t = \phi_p(\alpha k_t^s + (1 - \alpha)l_t + \epsilon_t^a) \\ \epsilon_t^a = \rho_a \epsilon_{t-1}^a + \eta_t^a \end{cases} \quad (4.5)$$

Where k_t^s denotes the capital services used in production, α is the share of capital in production and ϕ_p is (one plus) the share of fixed costs in production. ϵ_t^a denotes the AR(1) total factor productivity shock. Capital is assumed to be the sum of the previous amount of capital services used and the degree of capital utilization, hence:

$$k_t^s = k_{t-1} + z_t \quad (4.6)$$

Moreover, the degree of capital utilization is a positive function of the degree of rental rate, $z_t = z_1 r_t^k$, with $z_1 = \frac{1-\psi}{\psi}$, ψ being the elasticity of the capital utilization adjustment cost. Next the equation for installed capital is given by:

$$k_t = k_1 k_{t-1} + (1 - k_1) i_t + k_2 \epsilon_t^i \quad (4.7)$$

with $k_1 = \frac{1-\delta}{\gamma}$, $k_2 = (1 - \frac{1-\delta}{\gamma})(1 + \bar{\beta}\gamma)\gamma^2\phi$. The price mark-up equation is given by:

$$\mu_t^p = \alpha(k_t^s - l_t) + \epsilon_t^a - w_t \quad (4.8)$$

Which means the price mark-up μ_t^p is the marginal product of labor net of the current wage. The NKPC is characterized as:

$$\begin{cases} \pi_t = \pi_1 \mathbb{E}_t \pi_{t+1} - \pi_2 \mu_t^p + \epsilon_t^p \\ \epsilon_t^p = \rho_p \epsilon_{t-1}^p + \eta_t^p \end{cases} \quad (4.9)$$

with $\pi_1 = \bar{\beta}\gamma$, $\pi_2 = (1 - \beta\gamma\xi_p)(1 - \xi_p)/[\xi_p((\phi_p - 1)\epsilon_p + 1)]$, where ξ_p corresponds to the degree of price stickiness, while ϵ_p denotes the Kimball goods market aggregator. The equation implies that current inflation is determined by the expected future inflation, the price mark-up and

the AR(1) price mark-up shock ϵ_t^p , where η_t^p is an i.i.d-normal disturbance. The rental rate of capital is given by:

$$r_t^k = -(k_t - l_t) + w_t \quad (4.10)$$

Which implies the rental rate of capital is decreasing in the capital-labor ratio and increasing in the real wages. The wage mark-up is given as the real wages net of marginal rate of substitution between working and consuming, hence:

$$\mu_t^w = w_t - (\sigma_l l_t + \frac{1}{1 - \lambda/\gamma}(c_t - \frac{\lambda}{\gamma}c_{t-1})) \quad (4.11)$$

Where σ_l denotes the elasticity of labor supply. The real wage equation is given by:

$$\begin{cases} w_t = w_1 w_{t-1} + (1 - w_1)(\mathbb{E}_t w_{t+1} + \mathbb{E}_t \pi_{t+1}) - w_2 \mu_t^w + \epsilon_t^w \\ \epsilon_t^w = \rho_w \epsilon_{t-1}^w + \eta_t^w \end{cases} \quad (4.12)$$

with $w_1 = 1/(1 + \bar{\beta}\gamma)$, and $w_2 = ((1 - \bar{\beta}\gamma\xi_w)(1 - \xi_w)/(\xi_w(\phi_w - 1)\epsilon_w + 1))$. Hence the real wage is a weighted average of the past and expected wage, expected inflation, the wage mark-up and the wage mark-up shock ϵ_t^w , where η_t^w is an i.i.d-normal disturbance. Finally, monetary policy is assumed to follow a standard generalized Taylor rule similar to the one used in Section 3:

$$\begin{cases} r_t = \rho r_{t-1} + (1 - \rho)(r_\pi \pi_t + r_y x_y) + r_{dy}(\Delta x_t) + \epsilon_t^r \\ \epsilon_t^r = \rho_r + \epsilon_{t-1}^r + \eta_t^r \end{cases} \quad (4.13)$$

Where x_t denotes the output gap, and ϵ_t^r is the AR(1) monetary policy shock, with η_t^r the i.i.d-normal disturbance. Hence the monetary policy responds output gap growth on top of inflation and the output gap. In this paper, following the approach in [Slobodyan & Wouters \(2012a\)](#), we deviate from [SW \(2007\)](#) and model the output gap as the deviation of output from the underlying productivity process, i.e. $x_t = y_t - \epsilon_t^a$ ¹⁷. For convenience, Table 3 provides a summary of all structural (deep) parameters of the system.

¹⁷In the benchmark model, the output gap is defined as the deviation of output from the potential output, which requires modeling the flexible economy. We adapt the definition considered in this paper particularly because it does not require the flexible economy. This substantially reduces the number of forward-looking variables, and accordingly the number of first-order autocorrelations that are numerically approximated.

Table 3: **Smets-Wouters (2007): Structural Parameters of the System.**

| |
|---|
| γ : Steady-state growth rate |
| g : Steady-state share of government spending |
| \bar{l} ($\bar{\pi}$) Steady-state level of labour (inflation) |
| δ : Depreciation rate of capital |
| ϵ_t^g : Exogenous spending shock |
| ϵ_t^b : Risk premium shock |
| ϵ_t^i : Investment-specific technology shock |
| ϵ_t^a : Productivity shock |
| ϵ_t^w (ϵ_t^p) : Wage (Price) mark-up shock |
| ϵ_t^r : Monetary policy shock |
| $\iota_p(\iota_w)$: Price (Wage) indexation |
| λ : Habit formation in consumption |
| ϕ : Capital adjustment cost |
| ϕ_p : (One plus) the share of fixed costs in production |
| ψ : Capital utilization adjustment cost |
| $\xi_p(\xi_w)$: Calvo price (wage) stickiness |
| σ_c : (Inverse of) the elasticity of intertemporal substitution for labor. |
| σ_l : Elasticity of labor supply with respect to the real wage |
| β : Household discount factor |
| α : Share of capital in production |
| $\epsilon_p(\epsilon_w)$: Kimball Goods (Labor) market aggregator |
| ϕ_w : (One plus) steady-state labor mark-up |
| ρ : Interest rate smoothing |
| $r_y(r_{dy})$: Policy reaction to output gap (output gap growth) |
| r_π : Policy reaction to inflation |

4.1 Prior Distributions and Measurement Equations

Similar to the small-scale model, we estimate the SW model for the U.S historical quarterly macroeconomic data. As noted in the previous section, most macroeconomic variables in the U.S are characterized by a volatility reduction in the mid-80s, often referred to as the Great Moderation. Particularly in order to focus on the post-Great Moderation era in the upcoming sections, here we restrict our sample period to 1985:I-2016:IV. The observable variables used in the estimation are the log difference of real GDP (y_t^{obs}), real consumption (c_t^{obs}), real investment (inv_t^{obs}), real wage (w_t^{obs}), log hours worked (l_t^{obs}), inflation (π_t^{obs}) and the federal funds rate (r_t^{obs}) for the U.S economy. Although the model does not endogenously feature a financial sector, the most recent period of post-2007 is still included in the estimation to see how the model responds to the sharp changes during the Global Financial Crisis under the REE and

BLE estimations. Accordingly, the measurement equations are given as:

$$\begin{cases} d(\log(y_t^{obs})) = \bar{\gamma} + (y_t - y_{t-1}) \\ d(\log(c_t^{obs})) = \bar{\gamma} + (c_t - c_{t-1}) \\ d(\log(inv_t^{obs})) = \bar{\gamma} + (inv_t - inv_{t-1}) \\ d(\log(w_t^{obs})) = \bar{\gamma} + (w_t - w_{t-1}) \\ \log(l_t^{obs}) = \bar{l} + l_t \\ (\log(\pi_t^{obs})) = \bar{\pi} + \pi_t \\ (\log(r_t^{obs})) = \bar{r} + r_t \end{cases} \quad (4.14)$$

This system corresponds to (2.23) in our general framework. Similar to the estimation of the small-scale model, we keep our prior distributions as close as possible to those typically used in the literature. Our results from the previous section show that, the introduction of learning into the system typically affects the estimates of shock persistence parameters, which in turn lead to differences in the estimated shock volatilities. Therefore we assume more diffuse priors for the shock standard deviations compared to our preceding section, increasing their mean and variance from 0.1 to 0.5, and from 2 to 4 respectively¹⁸. The remaining prior distributions are summarized in Table 4, along with the fixed parameters of the system.

4.2 Posterior Results

Before discussing the posterior estimation results, we briefly discuss the convergence diagnostics similar to the previous section. Given the larger number of forward-looking variables, the SW model takes longer to converge compared to the small-scale model with 24 iterations. Figure 5 shows the norm distance between consecutive learning parameters, and consecutive estimated structural parameters at each step, as well as the largest eigenvalue of the Jacobian matrix $DG(\beta^{(k)})$ at each step. It is readily seen that both norm distances monotonically converge towards zero, while the largest eigenvalue stabilizes after a few iterations¹⁹. The top panel of Figure 7 shows the histograms of the first-order autocorrelations for the seven forward-looking variables resulting from the MC simulations at the estimated posterior mode along with the Dip test of unimodality for each parameter. The bottom panel in the same figure shows the results of Algorithm I with randomized initial values. Similar to the small-scale NKPC model, all of the results indicate a unique iteratively E-stable equilibrium. However, it turns out that the uniqueness of this equilibrium is not robust to small changes in the estimated parameters,

¹⁸However, the estimates of shock standard deviations turn out fairly robust to changes in the prior distributions, since the data is typically very informative about these parameters.

¹⁹As can be seen from the figure, the number of iterations until convergence can be drastically reduced by using a slightly larger convergence criterion c . In this case we deliberately use a very small $c = 10^{-5}$ in order to make our approximation very accurate.

and we may observe a second, high-persistence equilibrium that co-exists with our estimated equilibrium over certain parameter regions. We discuss this in more detail in the monetary policy section.

Tables 5 and 6 summarize the posterior estimation results of the BLE and RE models over the period 1985:I-2016:IV. To start with the estimates of the structural parameters, our overall results are similar to those observed in the small-scale model. With the introduction of learning into the system, the expectations become backward-looking and the system becomes more inertial, while the contemporaneous links between the state variables become weaker. This leads to lower estimates for a number of parameters under learning: To start with the inverse intertemporal elasticity of substitution σ_c , it is much lower under BLE with a mode of 1.02, compared with 1.56 under RE. This parameter mainly affects the consumption dynamics in 4.2, where, other things being equal, σ_c determines the impact from the ex-ante risk premium on consumption. This impact is stronger under BLE, which is an intuitive result since there is no indirect effect through expectations. Another implication of the different estimates on σ_c relates to the relation between labor growth and consumption: Recall $\sigma_c > 1$ implies consumption and labor are complements, while the opposite implies they are substitutes. Although they are clearly complements given our estimate under RE, the same does not apply to the case under BLE: The confidence interval on σ_c covers values both smaller and larger than one, implying the impact of labor growth on consumption is not identified in this case. Similar results on σ_c are also observed in some specifications of Slobodyan & Wouters (2012b). The capital adjustment cost ϕ turns out much lower under BLE with a mode of 4.39, compared with 7.55 under RE. Looking at the investment Euler equation 4.3, this mainly affects the transmission from the real value of capital and the ex-ante risk premium on investment. As expected, this effect is stronger under BLE given our estimates. As a side effect, 4.7 implies that the lower ϕ under BLE dampens the impact of the investment shock on the capital stock. Another real friction parameter that becomes lower under BLE is the elasticity of capital utilization adjustment cost ψ , which implies the capital utilization is more sensitive to changes in the rental rate of capital. As a consequence, it is less costly to change the capital utilization under BLE. Next turning to the frictions on the nominal side, both price and wage stickiness parameters ξ_p and ξ_w are lower under BLE, with 0.74 and 0.67 respectively, while the corresponding values are 0.92 and 0.9 under RE. These estimates imply both nominal wages and prices adjust more frequently under BLE: The average length of price contracts under BLE is 3.84 quarters, while it increases to 12.5 under RE. Similarly, the average length of wage contracts under BLE is only 3 quarters, compared with 10 quarters under RE. While such high estimates for nominal price and wage stickiness are not uncommon for RE models, they are fairly unrealistic and usually at odds with evidence from microeconomic studies²⁰. Our estimates for the nominal rigidities under

²⁰Microeconomic evidence on price stickiness in general seems quite heterogeneous across different sectors

BLE are closer to those found in the empirical studies, and in line with the previous findings of [Milani \(2007\)](#). The elasticity of labor supply is estimated higher under BLE with 2.36 compared to 1.41 under RE. This implies the wage mark-ups are more sensitive to changes in the labor supply under BLE, and consequently the direct impact of changes in labor on real wages is larger. For the remaining two frictions, namely the habit formation λ and the share of fixed costs ϕ_p , there are no discernible differences in the estimates, which turn out 0.79 and 1.5 under BLE respectively, while they are 0.78 and 1.46 under RE²¹. Furthermore, no large differences arise in parameters that mainly affect the steady-state of the model, namely $\bar{\pi}, \bar{\beta}, \bar{l}, \bar{\gamma}$ and α , as well as the monetary policy parameters r_π, r_y, r_{dy} and ρ .

For the structural shock parameters, it is mostly those shocks that relate to the forward-looking endogenous variables that are affected with the introduction of learning into the system. Accordingly, the productivity, government spending and monetary policy shocks have fairly similar persistence and standard deviation (of the i.i.d component) estimates under both specifications: While the first two are highly persistent and close to unit root, the monetary policy shock is only weakly persistent at 0.35 and 0.27 under BLE and RE respectively. The remaining four shocks are all substantially more volatile under BLE: The risk premium, investment, price and wage mark-up shocks have standard deviations of 0.55, 1.27, 0.19 and 0.85 in their i.i.d. component under BLE, while the corresponding values are 0.19, 0.29, 0.11 and 0.42 under RE. Furthermore, the investment and price mark-up shocks are much less persistent under BLE at 0.54 and 0.16 respectively, while these persistence parameters are 0.81 and 0.47 under RE. While the risk-premium shock persistence is fairly similar under both specifications at 0.3 and 0.36, the confidence interval under RE is fairly wide, covering highly persistent values of up to 0.9. The only remaining shock, wage mark-up, is practically no different than white noise under both estimations. Our overall results suggest that, with the introduction of learning, the shocks typically become less persistent and more volatile. This is exactly the result one would expect: On the one hand, since the system becomes more inertial under BLE, a lower degree of exogenous persistence suffices to generate enough persistence in the state variables. On the other hand, since the exogenous shocks do not have a contemporaneous effect on the state variables through expectations, they become more volatile to produce enough contemporaneous reaction in the system. The resulting marginal posterior likelihood for the RE model is -572 , while the BLE model yields a likelihood of -546 , implying that, similar to the small-scale NKPC model, replacing RE with BLE in the system leads to a sizeable improvement in the

and countries. Nevertheless, there is a general consensus that prices change around once a year; see e.g. [Nakamura & Steinsson \(2013\)](#) and [Klenow & Malin \(2010\)](#). Similar to the price stickiness, the microeconomic evidence suggests the frequency of nominal wage changes is less than a year, see e.g. [Heckel et al. \(2008\)](#); this suggests that our estimate under BLE is more reasonable.

²¹The fact that λ does not turn out lower under BLE is surprising at first glance, since this parameter mainly introduces more inertia into consumption dynamics. Recall, however, that this parameter also affects the impact of the ex-ante risk premium on consumption. A closer examination reveals that it is in fact the risk premium, and not the past consumption that drives the high value of habit formation under BLE.

model fit. We complement our results with the impulse responses of consumption, investment, output, hours worked and inflation to the exogenous shocks in Figure 9. The overall patterns confirm our claim that the system becomes more inertial under BLE, since the shocks typically have a longer-lasting effect and their propagation through the system happens at a much slower rate. Further, the initial impact of the shocks are typically smaller under BLE as expected, especially for the productivity, spending and monetary policy shocks that have similar levels of estimated volatility. Overall, our results are in line with the conclusions of Milani (2007), Eusepi & Preston (2011) and Collard & Dellas (2004), where the introduction of learning leads to more persistence in the economy. On the contrary, our results differ from those obtained in Slobodyan & Wouters (2012a), where the introduction of learning leads to very little change in the parameter estimates and only improves the model fit. Figure 6 shows the plots of prior and posterior distributions of all estimated parameters under BLE and RE, which allows us to examine about which parameters the data is the most informative, and which parameters do not steer away from their priors. Further, it allows for a visual inspection of whether there are any discernible differences between the modes and means, which provides a robustness check for the results since the numerical computation of the learning parameters are based on the posterior mode. To start with the parameters under BLE, the data is very informative about the exogenous shock volatility parameters overall, which are characterized by very tight posterior distributions. The same also applies to the elasticity of intertemporal substitution σ_c , where the posterior distribution is substantially different than the prior, while the elasticity of labor supply σ_l remains close to the prior distribution. The nominal and real friction parameters also typically remain close to their prior distributions, with two notably exceptions of price and wage stickiness. Next turning to the policy parameters, the data is informative about the interest rate smoothing, and policy responses to output gap and output gap growth, while the policy response to inflation barely moves away from the prior distribution. The parameters relating to the steady state of the model also typically remain close to their prior distributions, with the exception of the share of capital α . Finally turning to the parameters that relate to the exogenous shock persistence, the data is typically very informative about these, similar to the shock volatility parameters. Next turning to the posterior distributions for the RE estimation, most of the results remain the same. The data is typically very informative about the parameters relating to the shock volatility and persistence parameters, while the discussion on the nominal and real frictions, as well as the policy and steady-state parameters, is virtually the same as in the BLE case. One notable difference arises in the distributions of risk premium persistence and habit formation, which are seemingly bimodal. While our results in Figure 6 suggest a high level of habit formation and a fairly weak autocorrelation in the risk-premium, the figure suggests another mode with a moderate level of habit formation and almost unit-root risk premium. Other than these two parameters, we conclude that, under both estimations, there are no major differences in terms of the informativeness of the data, and the estimated

means typically remain close to the modes.

Figure 5: Convergence of the norm distance for the learning parameters, estimated structural parameters and the largest eigenvalue of the system. We use a critical value of $c = 10^{-5}$ as our stopping criterion.

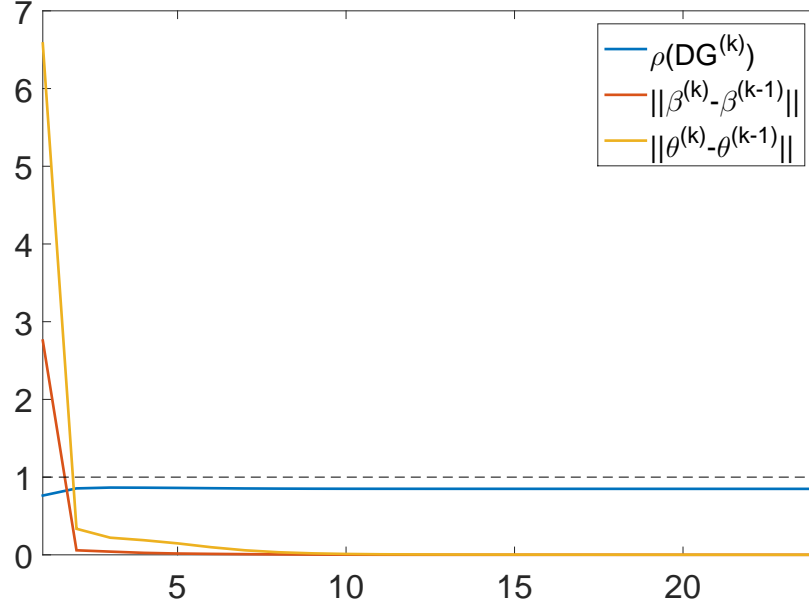
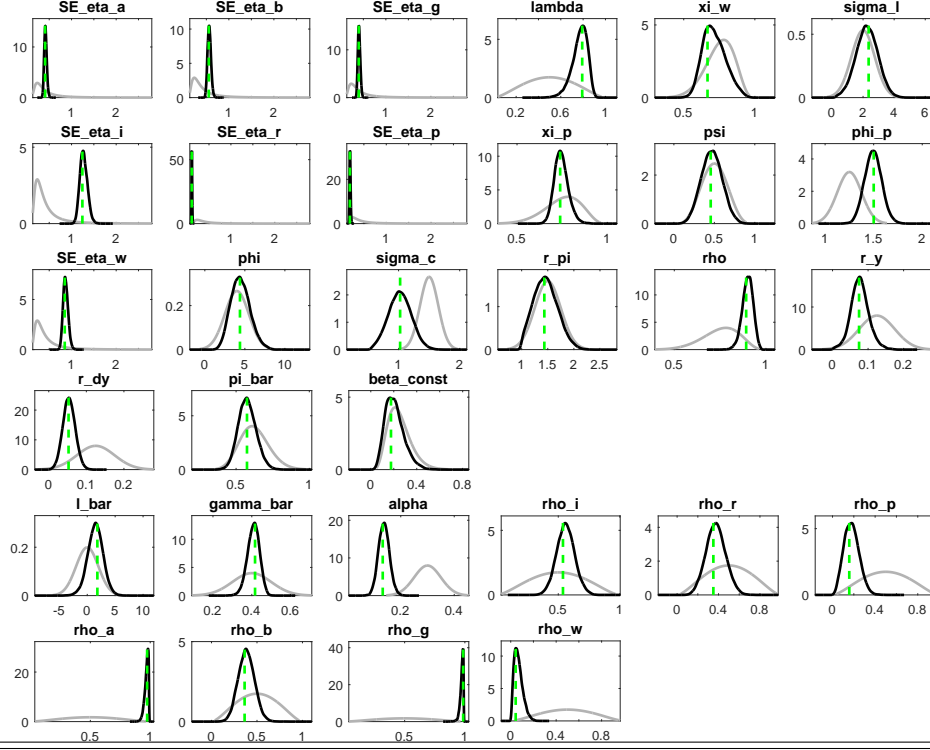


Table 4: Fixed parameters and the prior distributions of the estimated parameters for the Smets-Wouters (2007) model.

| Fixed Parameters | | | |
|--|--------------|-------|-------|
| δ | 0.025 | | |
| ϕ_w | 1.5 | | |
| g | 0.18 | | |
| ϵ_p | 10 | | |
| ϵ_w | 10 | | |
| Prior | Distribution | Mean | Var. |
| Parameters related to nominal and real frictions | | | |
| ϕ | Normal | 4 | 1.5 |
| σ_c | Normal | 1.5 | 0.15 |
| λ | Beta | 0.5 | 0.2 |
| ξ_w | Beta | 0.75 | 0.1 |
| σ_l | Normal | 2 | 0.75 |
| ξ_p | Beta | 0.75 | 0.1 |
| ψ | Beta | 0.5 | 0.15 |
| ϕ_p | Normal | 1.25 | 0.125 |
| Policy related parameters | | | |
| r_π | Normal | 1.5 | 0.25 |
| ρ | Beta | 0.75 | 0.1 |
| r_y | Normal | 0.125 | 0.05 |
| r_{dy} | Normal | 0.125 | 0.05 |
| Steady-state related parameters | | | |
| $\bar{\pi}$ | Gamma | 0.625 | 0.1 |
| $\bar{\beta}$ | Gamma | 0.25 | 0.1 |
| \bar{l} | Normal | 0 | 2 |
| $\bar{\gamma}$ | Normal | 0.4 | 0.1 |
| α | Normal | 0.3 | 0.05 |
| Parameters related to shock persistence | | | |
| ρ_a | Beta | 0.5 | 0.2 |
| ρ_b | Beta | 0.5 | 0.2 |
| ρ_g | Beta | 0.5 | 0.2 |
| ρ_i | Beta | 0.5 | 0.2 |
| ρ_r | Beta | 0.5 | 0.2 |
| ρ_p | Beta | 0.5 | 0.2 |
| ρ_w | Beta | 0.5 | 0.2 |
| Shock variance parameters | | | |
| η_a | Inv. Gamma | 0.5 | 4 |
| η_b | Inv. Gamma | 0.5 | 4 |
| η_g | Inv. Gamma | 0.5 | 4 |
| η_i | Inv. Gamma | 0.5 | 4 |
| η_r | Inv. Gamma | 0.5 | 4 |
| η_p | Inv. Gamma | 0.5 | 4 |
| η_w | Inv. Gamma | 0.5 | 4 |

Figure 6: Prior and Posterior Distributions under BLE and RE: The grey and bold curves correspond to the prior and posterior distributions respectively, while the dotted green lines mark the posterior mode.

BLE:



Rational Expectations:

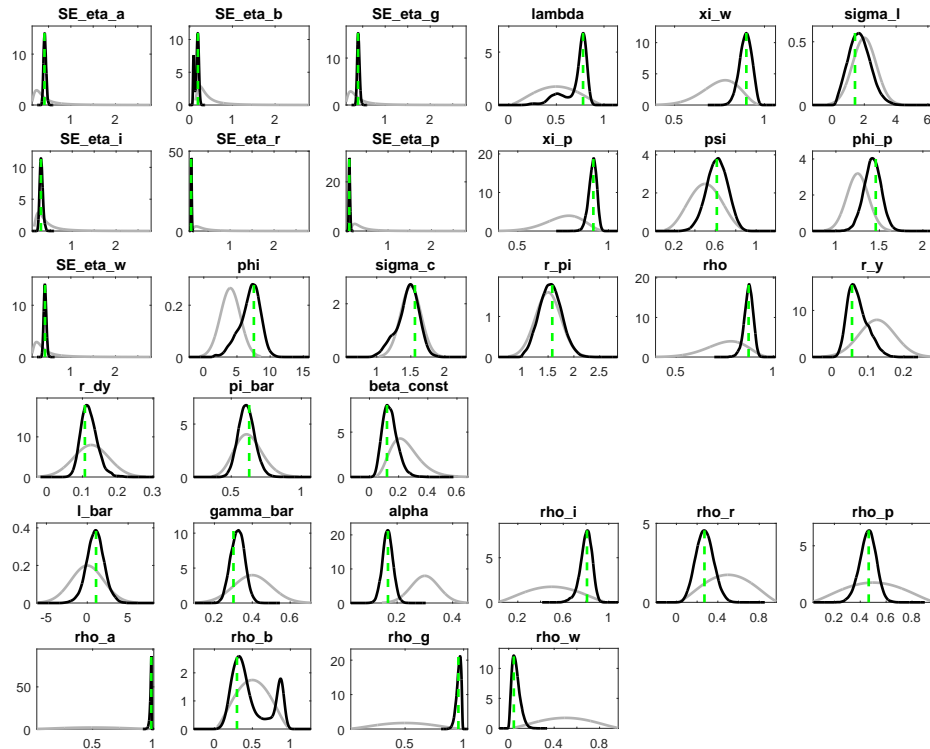


Table 5: **Full Sample Estimation Results, 1985:I-2016:IV.** Frictions, Policy and Steady-State Parameters. Lapl. refers to the Laplace likelihood approximation based on the posterior mode, while MHM refers to the Modified Harmonic Mean likelihood based on the posterior distribution.

| | BLE | REE | | | | | | |
|----------------|---------|---------|--------|----------|------|------|--------|----------|
| Laplace | -546.22 | -572.9 | | | | | | |
| MHM | -545.88 | -571.97 | | | | | | |
| Acc. Rate | 0.2944 | 0.2943 | | | | | | |
| Parameter | Mode | Mean | Hpd 5% | Hpd 95 % | Mode | Mean | Hpd 5% | Hpd 95 % |
| ϕ | 4.39 | 4.4 | 2.5 | 6.25 | 7.55 | 6.92 | 4.32 | 9.41 |
| σ_c | 1.02 | 1.02 | 0.71 | 1.31 | 1.56 | 1.45 | 1.17 | 1.71 |
| λ | 0.79 | 0.77 | 0.66 | 0.87 | 0.78 | 0.7 | 0.47 | 0.85 |
| ξ_w | 0.67 | 0.72 | 0.58 | 0.84 | 0.9 | 0.89 | 0.84 | 0.95 |
| σ_l | 2.36 | 2.23 | 1.08 | 3.38 | 1.41 | 1.7 | 0.53 | 2.73 |
| ξ_p | 0.74 | 0.74 | 0.68 | 0.81 | 0.92 | 0.91 | 0.88 | 0.95 |
| ψ | 0.46 | 0.47 | 0.26 | 0.68 | 0.61 | 0.62 | 0.45 | 0.78 |
| ϕ_p | 1.5 | 1.49 | 1.35 | 1.64 | 1.46 | 1.42 | 1.25 | 1.58 |
| r_π | 1.43 | 1.46 | 1.07 | 1.79 | 1.58 | 1.54 | 1.18 | 1.89 |
| ρ | 0.89 | 0.9 | 0.85 | 0.95 | 0.87 | 0.87 | 0.84 | 0.91 |
| r_y | 0.07 | 0.08 | 0.04 | 0.12 | 0.06 | 0.07 | 0.03 | 0.12 |
| $r_{\delta y}$ | 0.05 | 0.05 | 0.03 | 0.08 | 0.11 | 0.12 | 0.08 | 0.16 |
| $\bar{\pi}$ | 0.57 | 0.58 | 0.48 | 0.68 | 0.63 | 0.61 | 0.51 | 0.7 |
| $\bar{\beta}$ | 0.18 | 0.21 | 0.08 | 0.34 | 0.12 | 0.14 | 0.06 | 0.22 |
| \bar{l} | 1.81 | 1.46 | -0.75 | 3.67 | 1.07 | 0.98 | -0.8 | 2.7 |
| $\bar{\gamma}$ | 0.42 | 0.41 | 0.36 | 0.46 | 0.3 | 0.32 | 0.26 | 0.38 |
| α | 0.13 | 0.14 | 0.11 | 0.17 | 0.17 | 0.17 | 0.14 | 0.2 |

Table 6: **Full Sample Estimation Results, 1985:I-2016:IV**. Shock persistence and standard deviation parameters. The reported likelihoods are as defined in Table 7.

| | BLE | REE | | | | | | |
|-----------|---------|---------|--------|----------|------|------|--------|----------|
| Laplace | -546.22 | -572.9 | | | | | | |
| MHM | -545.88 | -571.97 | | | | | | |
| Acc. Rate | 0.2944 | 0.2943 | | | | | | |
| Parameter | Mode | Mean | Hpd 5% | Hpd 95 % | Mode | Mean | Hpd 5% | Hpd 95 % |
| ρ_a | 0.97 | 0.97 | 0.95 | 0.99 | 0.99 | 0.98 | 0.97 | 0.99 |
| ρ_b | 0.36 | 0.38 | 0.24 | 0.53 | 0.3 | 0.47 | 0.21 | 0.9 |
| ρ_g | 0.99 | 0.97 | 0.95 | 0.99 | 0.96 | 0.96 | 0.93 | 0.99 |
| ρ_i | 0.54 | 0.56 | 0.44 | 0.68 | 0.81 | 0.8 | 0.72 | 0.89 |
| ρ_r | 0.35 | 0.37 | 0.22 | 0.52 | 0.27 | 0.27 | 0.14 | 0.41 |
| ρ_p | 0.16 | 0.18 | 0.06 | 0.3 | 0.47 | 0.46 | 0.35 | 0.56 |
| ρ_w | 0.04 | 0.07 | 0.01 | 0.12 | 0.05 | 0.06 | 0.01 | 0.12 |
| η_a | 0.41 | 0.41 | 0.37 | 0.46 | 0.41 | 0.42 | 0.37 | 0.46 |
| η_b | 0.55 | 0.57 | 0.51 | 0.63 | 0.19 | 0.16 | 0.08 | 0.22 |
| η_g | 0.4 | 0.4 | 0.36 | 0.45 | 0.4 | 0.41 | 0.36 | 0.45 |
| η_i | 1.24 | 1.27 | 1.14 | 1.4 | 0.29 | 0.3 | 0.23 | 0.35 |
| η_r | 0.11 | 0.11 | 0.1 | 0.12 | 0.11 | 0.12 | 0.11 | 0.13 |
| η_p | 0.19 | 0.19 | 0.17 | 0.21 | 0.11 | 0.11 | 0.09 | 0.13 |
| η_w | 0.85 | 0.87 | 0.78 | 0.96 | 0.42 | 0.42 | 0.37 | 0.47 |

Figure 7: Top Panel: Histograms of the long-run learning parameters resulting from 1000 Monte Carlo simulations (each with 20000 periods) of the SW model at the posterior mode along with the corresponding tests of unimodality, where the BLE is given by $\beta^* = (0.99, 0.84, 0.99, 0.98, 0.51, 0.98)$. Bottom Panel: Results from 500 runs of Algorithm I with randomized initial values. Both results suggest a unique iteratively E-stable equilibrium at the estimated posterior mode.

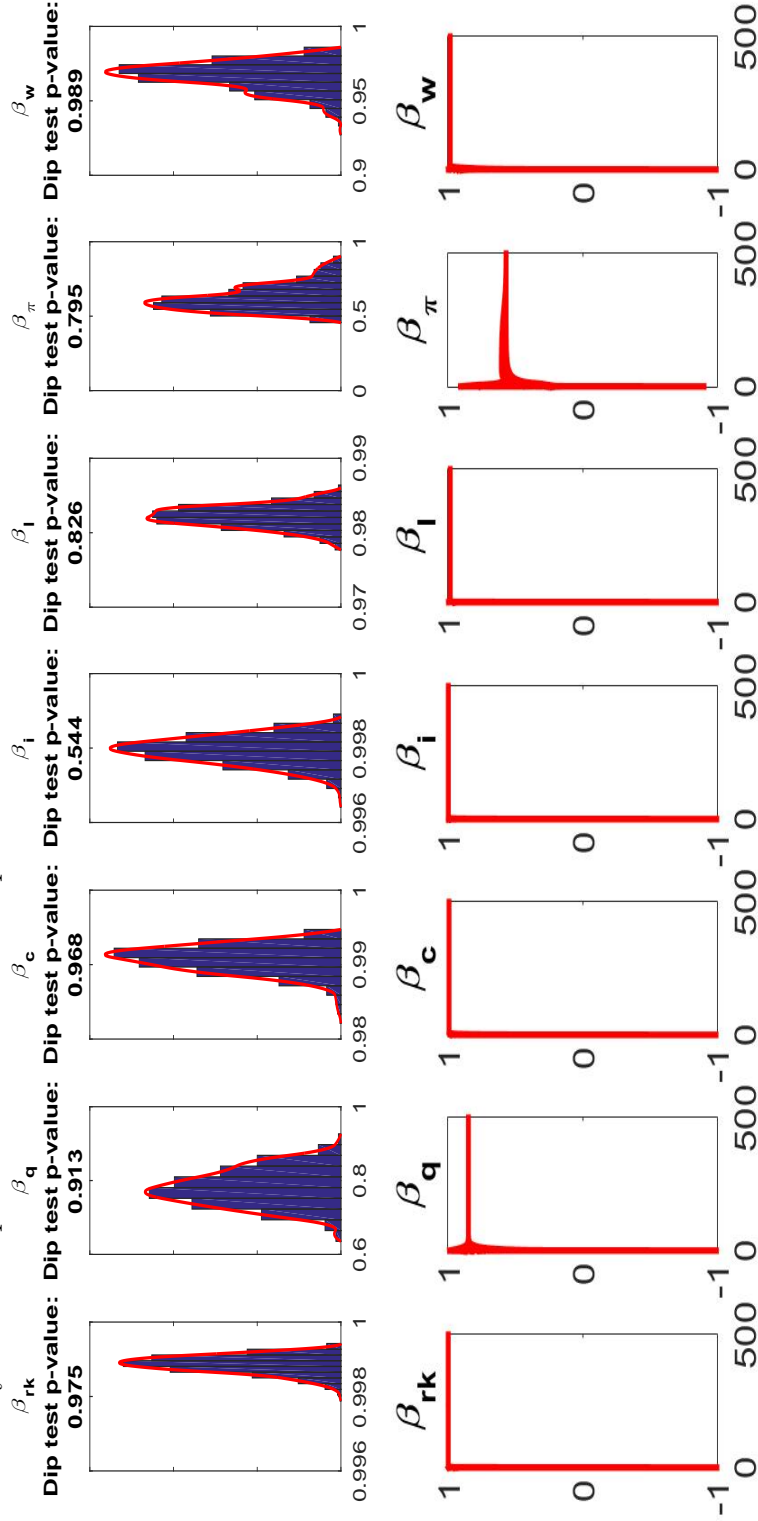
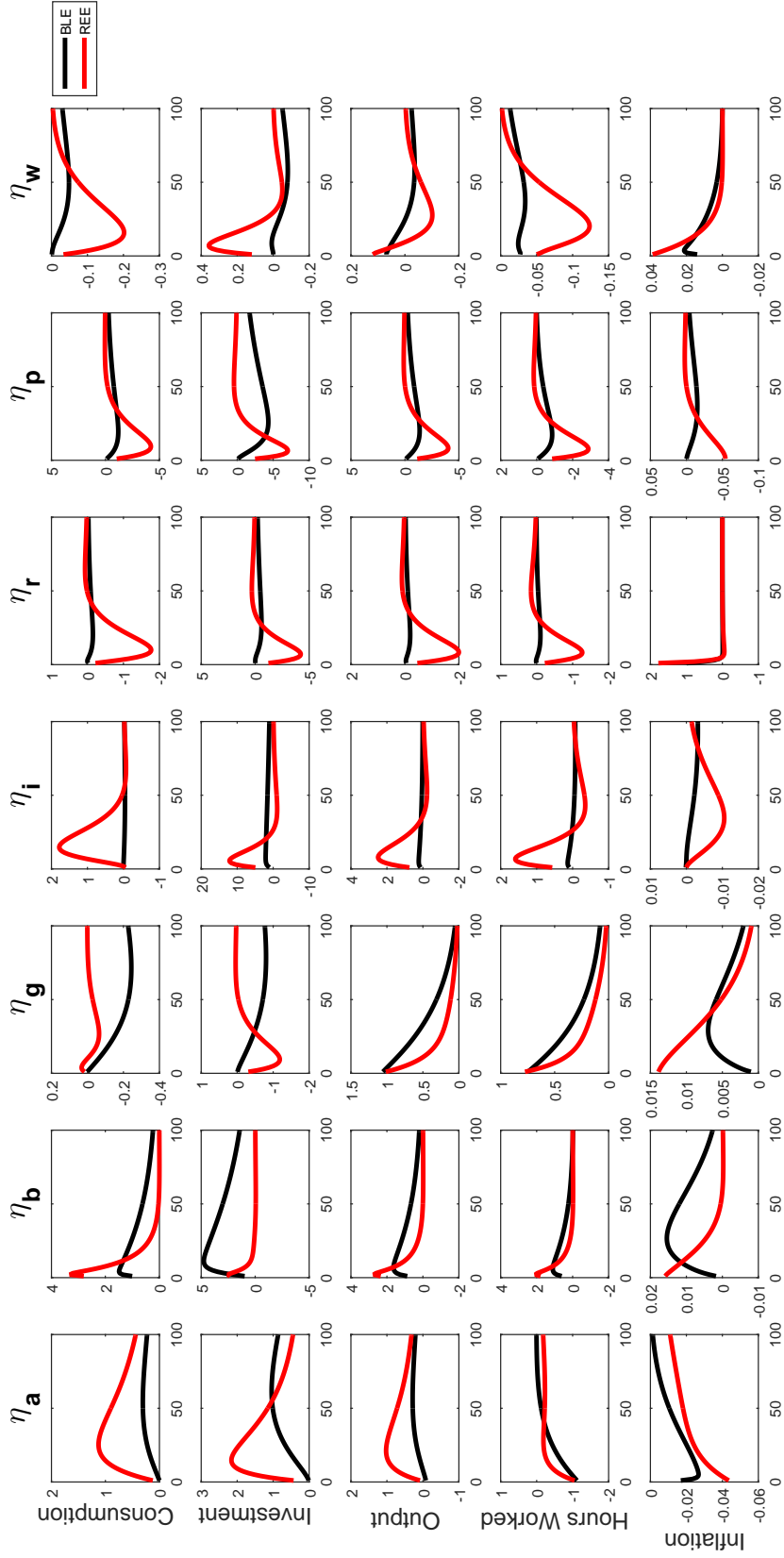


Figure 8: Impulse response functions for consumption, investment, output, inflation and labor (hours worked) based on the posterior mode estimations. The bold lines represent the impulse responses under BLE, while the dotted lines correspond to the RE counterparts. The shock sizes are the same for both BLE and RE models.



5 Applications

5.1 Forecasting

Table 7 shows the out-of-sample root-mean squared error (RMSE) results from forecasting the seven observable variables over the period 2000:I-2016:IV of both the rational expectations and BLE models at 1-, 2-, 4-, 8- and 12- step ahead horizons, where each time period corresponds to a quarter²². The last 5 rows of the same table contain the overall percentage gains or losses of the BLE model relative to RE in terms of the RMSE reduction.

A casual inspection of the comparison table reveals that, overall, the BLE model yields more accurate forecasts compared to its RE counterpart, leading to positive aggregate gains at all horizons. This improvement is particularly more emphasized over the short- and medium-term horizons, while the effect is somewhat dampened over longer horizons. For output growth, the BLE forecasts are better by 5 % over 1 and 2 quarters-ahead, while 1- and 2-years ahead forecasts deteriorate to 4 and 1 % respectively. At the 3-year horizon, the RE model performs better by 3 %. For inflation, the differences are 2 and 10 % at the 1 and 2 quarters ahead in favour of the BLE model, while they decline to 8 and 4 % at 1- and 2-years ahead respectively. Unlike output growth, the BLE model still performs better at the 3-year horizon with a difference of 6 %. For consumption growth, the results are mostly in favour of the RE model. While the BLE model performs better by 1 % at the 1-quarter horizon, the RE model is better at all subsequent horizons with up to a 10% difference. A similar story also holds for wage growth, where the difference remains close to zero at all horizons but in favour of the RE model. Investment growth shows a pattern similar to output growth and inflation, where the BLE model performs better by 9, 13 and 17 % at the 1-, 2- and 4-step ahead horizons, while the difference declines to 14 and 7 % at the longer horizons. Interest rate and labor are two exceptions to our story, where the RE forecasts are particularly bad over all horizons: For interest rate, the difference increases in favour of the BLE model as the forecast horizon grows, up to 57 % at the 3-year ahead. Similarly for labor, the BLE model always yields better forecasts, with the difference increasing up to 32 % at longer horizons. These results are also reflected in the overall measures²³: The forecasts under BLE are better by 3 and 11 % at the 1- and 2-step ahead horizons, while peaking at 21 % at the 1-year ahead horizon. The difference starts to decline at longer terms, with 19 and 15 % respectively. Further, if we were to neglect the particularly large difference between the interest rate and labor forecasts of the two models, this difference at longer horizons would be much closer to zero. Our overall results indicate that the improved likelihood of the BLE model over RE is clearly reflected in its forecasting performance. The general pattern in the differences

²²In practical terms, we re-estimate both the RE and BLE models at each period to produce our forecasts, which means we re-compute the underlying BLE at each step.

²³Following Smets & Wouters (2007), the overall measure is the log determinant of the uncentered forecast error covariance matrix.

suggests that the restrictions under learning dynamics are more useful particularly in capturing the short and medium-term momentum in economic fluctuations. These conclusions are in line with the results from the time-varying AR(2) beliefs of [Slobodyan & Wouters](#), where the BLE model performs better over short horizons but its performance deteriorates over longer horizons. The biggest difference in our paper and theirs, however, is the magnitude of the improvement over the RE model, which is much larger for our BLE specification compared to the time-varying AR(2) model.

Next we provide a more detailed comparison of the 1-step ahead forecasts to examine the time-varying performance of the forecasts of our models. To this end, we compute the cumulative RMSE for both the BLE and RE models at each period for the entire forecasting period. Subtracting the resulting cumulative MSE series for the BLE model from that of RE yields a time-varying performance measure of the BLE model relative to the RE²⁴. The *level* and *slope* of the resulting curve are both informative: Whenever the resulting series is above 0, the cumulative RMSE of the RE model is worse than BLE *up to that point*. Whenever the series is upward (downward) sloping over a given period, the performance of the BLE model improves (deteriorates) over that period relative to the RE model. Figure 9 plots the resulting series for all observable variables.

To start with the forecasts on output growth, both models yield fairly similar forecasts over early 2000s, while the performance of the BLE model notably increases over the latter period after the recent financial crisis. For inflation, the BLE model performs better in the earlier years, while its relative performance deteriorates and becomes similar to RE in the latter years. Interest rate forecasts are fairly stable in favour of the BLE model over the whole period, although the relative performance of the BLE model slightly increases in the latter period. Labor growth shows a similar pattern to that of output growth with similar performances over the early period, and the RE model's performance deteriorates afterwards. Real wage growth performance is fairly stable over the sample period in favour of the RE model, although the difference becomes smaller as we move towards the latter years. Similarly, the performances for consumption and investment growth are fairly stable over time, where the BLE model outperforms over a small period around 2005, leading to very similar results for consumption growth over the entire period, and a better performance of the BLE model for investment growth. Overall, these comparisons serve as a robustness check for the results in Table 7 and show that, the improvements of the BLE forecasts over RE are not limited to a small sub-sample only, but rather arise systematically over the entire forecasting period.

To close this section, we briefly discuss the relative performance of the DSGE model com-

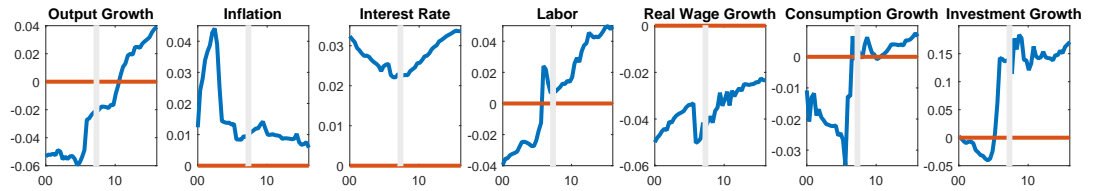
²⁴More precisely, denote the squared forecast error for variable i at period j as $fe_{i,j}$. Then, at each period, the cumulative mean squared error *up to that point* is given by : $CMSE_t = \frac{1}{t} \sum_{j=1}^t fe_{i,j}$. Then we subtract compute $CMSE_t^{BLE} - CMSE_t^{RE}$. While this is not common in the DSGE models, it is a commonly used approach to evaluate time-varying performance in the asset pricing literature; see e.g. [Campbell & Thompson \(2007\)](#).

pared to Bayesian VARs: It is well known that modern DSGE models are able to outperform unrestricted and Bayesian VARs, therefore we leave the results of a comparison of the model fit and forecasting performance between several BVARs and the DSGE model under BLE to Appendix F in Table 15, which show that, consistent with the previous results in the literature, the DSGE model under BLE outperforms the BVARs both in terms of the model fit and the forecasting performance.

Table 7: The RMSE resulting from the out-of-sample forecasting under RE and BLE models over the period 2000:I-2016:IV at long- and short-term horizons. The last part corresponds to the relative gains & losses of the BLE model over RE in terms of RMSE reduction in percentages, i.e. a positive (negative) number indicates the BLE forecasts are more (less) accurate.

| | | Output | Inf. | Cons. | Inv. | Wage | Int. | Labor | Overall |
|--------------|-----|--------|-------|-------|-------|-------|-------|-------|---------|
| RE | | | | | | | | | |
| | 1q | 0.73 | 0.22 | 0.62 | 1.82 | 1.06 | 0.15 | 0.64 | -10.35 |
| | 2q | 0.79 | 0.24 | 0.64 | 2.26 | 1.00 | 0.24 | 0.92 | -7.46 |
| | 4q | 0.80 | 0.24 | 0.63 | 2.65 | 1.00 | 0.42 | 1.61 | -3.22 |
| | 8q | 0.79 | 0.24 | 0.63 | 2.66 | 1.01 | 0.67 | 2.91 | 0.38 |
| | 12q | 0.75 | 0.24 | 0.65 | 2.46 | 1.04 | 0.82 | 3.99 | 1.81 |
| BLE | | | | | | | | | |
| | 1q | 0.69 | 0.22 | 0.62 | 1.65 | 1.08 | 0.12 | 0.59 | -10.84 |
| | 2q | 0.75 | 0.21 | 0.66 | 1.97 | 1.01 | 0.15 | 0.72 | -8.98 |
| | 4q | 0.76 | 0.22 | 0.69 | 2.19 | 1.00 | 0.22 | 1.12 | -6.11 |
| | 8q | 0.78 | 0.23 | 0.70 | 2.28 | 1.01 | 0.32 | 1.99 | -2.29 |
| | 12q | 0.77 | 0.23 | 0.7 | 2.28 | 1.05 | 0.36 | 2.77 | -0.38 |
| Gains/losses | | | | | | | | | |
| | 1q | 5.32 | 2.39 | 1.01 | 9.37 | -2.20 | 21.97 | 7.72 | 3.46 |
| | 2q | 5.28 | 10.08 | -3.13 | 12.87 | -0.91 | 37.68 | 21.10 | 10.87 |
| | 4q | 4.33 | 8.14 | -8.93 | 17.38 | -0.06 | 46.77 | 30.17 | 20.61 |
| | 8q | 1.19 | 4.17 | -9.99 | 14.30 | -0.42 | 52.12 | 31.55 | 19.05 |
| | 12q | -3.17 | 5.84 | -8.44 | 7.22 | -0.89 | 56.75 | 30.49 | 15.6 |

Figure 9: Cumulative RMSE of the BLE relative to the RE forecast over the 1-quarter-ahead horizon, 2000:I-2016:IV. Whenever the blue line is above (below) zero, the cumulative performance under BLE *up to that period* is better (worse) under BLE. The vertical line corresponds to the onset of the Global Financial Crisis.



5.2 Monetary Policy Implications

As shown in Section 4, the estimated approximate BLE is the unique iteratively E-stable BLE at the posterior mode, while the Monte Carlo simulations provide no evidence that other E-stable BLE exist. It turns out, however, the uniqueness of the equilibrium is sensitive to small changes in some of the structural parameters and another equilibrium with high persistence & high variance exists over some parameter regions. In this section, we illustrate this phenomenon in terms of the monetary policy parameters r_π and r_y ²⁵.

To start with the analysis, the top panel of Figure 10 shows the convergence of the learning parameters when we use the fixed-point iteration (2.17) with randomized initial values, where we increase the output gap reaction to 0.5 from its estimated value of 0.07. We observe that, unlike the previous Figure 7, the first-order autocorrelations of inflation and wage converge to two different values depending on the initial state, which shows the presence of two co-existing iteratively E-stable equilibria. The presence of another E-stable equilibrium is confirmed by the Monte Carlo simulations in the second panel of the same figure, where the dip test clearly rejects unimodality for β_π ²⁶. In this setting, the low-persistence equilibrium corresponds to the one resulting from our estimation, which is iteratively E-stable at the posterior mode when $r_y = 0.07$, as well as when r_y is increased to 0.5. The second, high-persistence equilibrium is not iteratively E-stable at the posterior mode, but becomes stable once the value of r_y is increased to 0.5²⁷. The bottom two panels show example simulations of inflation and wages to illustrate the co-existence of these two equilibria: Depending on the initial states, the system either converges to the low-persistence/low-variance equilibrium (blue line), or the high persistence/high variance equilibrium (orange line).

In order to see the monetary policy implications of this result, we use the most common approach in the literature and assume the central bank has an objective function in terms of minimizing the inflation and output gap volatilities (see e.g. Cooley & Hansen (1992), Woodford (2013), Schmitt-Grohé & Uribe (2005)). Accordingly, the top panel of Figure 5.2 shows the variances of these two variables over the empirically plausible range of policy reactions to inflation and output gap²⁸. Each point in the figure corresponds to the equilibrium value(s) at

²⁵Although we limit our multiple equilibrium analysis to these two policy parameters in particular, similar results are likely to hold for structural parameters of the model that affect the persistence of inflation.

²⁶Note that the unimodality of β_w is not rejected in the Monte Carlo simulations. This is not surprising since the two equilibrium values are fairly close, therefore the difference turns out statistically insignificant in a finite sample of simulations

²⁷We consider several intermediate cases for values of r_y between 0.07 and 0.5 in Appendix D. Our numerical simulations show that the largest eigenvalue of the Jacobian matrix at the high-persistence equilibrium lies outside the unit circle at the posterior mode, but it is pushed inside the unit circle as r_y is increased, thus making the high-persistence equilibrium iteratively E-stable.

²⁸In practical terms, in order to obtain these two figures, we use Algorithm I with randomized initial values at each parameter combination of r_y and r_π .

the given parameter combination. A casual inspection reveals that the high-persistence/high-variance equilibrium is only stable over the region where the reaction to output gap is too strong relative to inflation. Whenever the output gap reaction is fairly strong, the second equilibrium disappears as long as the inflation reaction is also strong enough. Furthermore, the high-variance equilibrium never appears for values of $r_\pi > 2$, i.e. when the inflation reaction is sufficiently strong, regardless of the values of output gap reaction. Despite the existence of the high-variance equilibrium over certain parameter combinations, the top panel of Figure 5.2 reveals that this equilibrium has a very small basin of attraction with respect the initial values of $\beta^{(0)}$. The same argument also extends to numerical simulations of the system, where we observe convergence to the high-variance equilibrium only for very large initial values. Furthermore, even when the two equilibria co-exist, it takes implausibly large shocks to cause an endogenous switch from the low-persistence equilibrium to the high-persistence one²⁹. An implication of these results is that, once the system converges to the low-persistence equilibrium, a switch to the high-persistence equilibrium due to an exogenous shock becomes unlikely. Therefore, in the bottom panel of Figure 5.2, we provide a comparison of the monetary policy impact under the REE and the low-persistence equilibrium under BLE. The first result that stands out is, inflation is unresponsive to changes in the monetary policy under both REE and BLE for a wide range of policy parameters. However, we observe an important difference in terms of the variance of output gap, which is substantially higher under BLE over the entire parameter space. To interpret this, recall that the estimated shock variances of i.i.d shocks under BLE are substantially higher in order to generate enough contemporaneous reaction in system. As a side effect, these shock variances drive the variances of endogenous latent variables in the system. Therefore the output gap process turns out more volatile under BLE, along with other endogenous variables on the real side of the economy, such as investment, capital accumulation and the real value of capital. In terms of the central-bank's stabilization policy, this implies a larger trade-off between the variance of output gap and inflation under BLE, since achieving a given amount of reduction in terms of inflation variance requires a larger increase in terms of the output gap variance.

²⁹We omit these numerical simulations here for brevity.

Figure 10: Multiplicity of BLE in the SW model, with the low-persistence equilibrium $\beta_1^* = (0.99, 0.93, 0.98, 0.99, 0.97, 0.29, 0.93)$ and high-persistence equilibrium $\beta_2^* = (0.99, 0.93, 0.98, 0.99, 0.97, 0.98)$. Top panel: Results from 500 runs of Algorithm I with randomized initial values when we set the parameter $r_y = 0.5$ and leave the remaining parameters at the estimated posterior mode. Second panel: The corresponding Monte Carlo simulations and tests of unimodality. Bottom two panels: Simulated time series of inflation and real wages, where the simulations only differ in terms of the initial values of the system in order to illustrate path dependence.

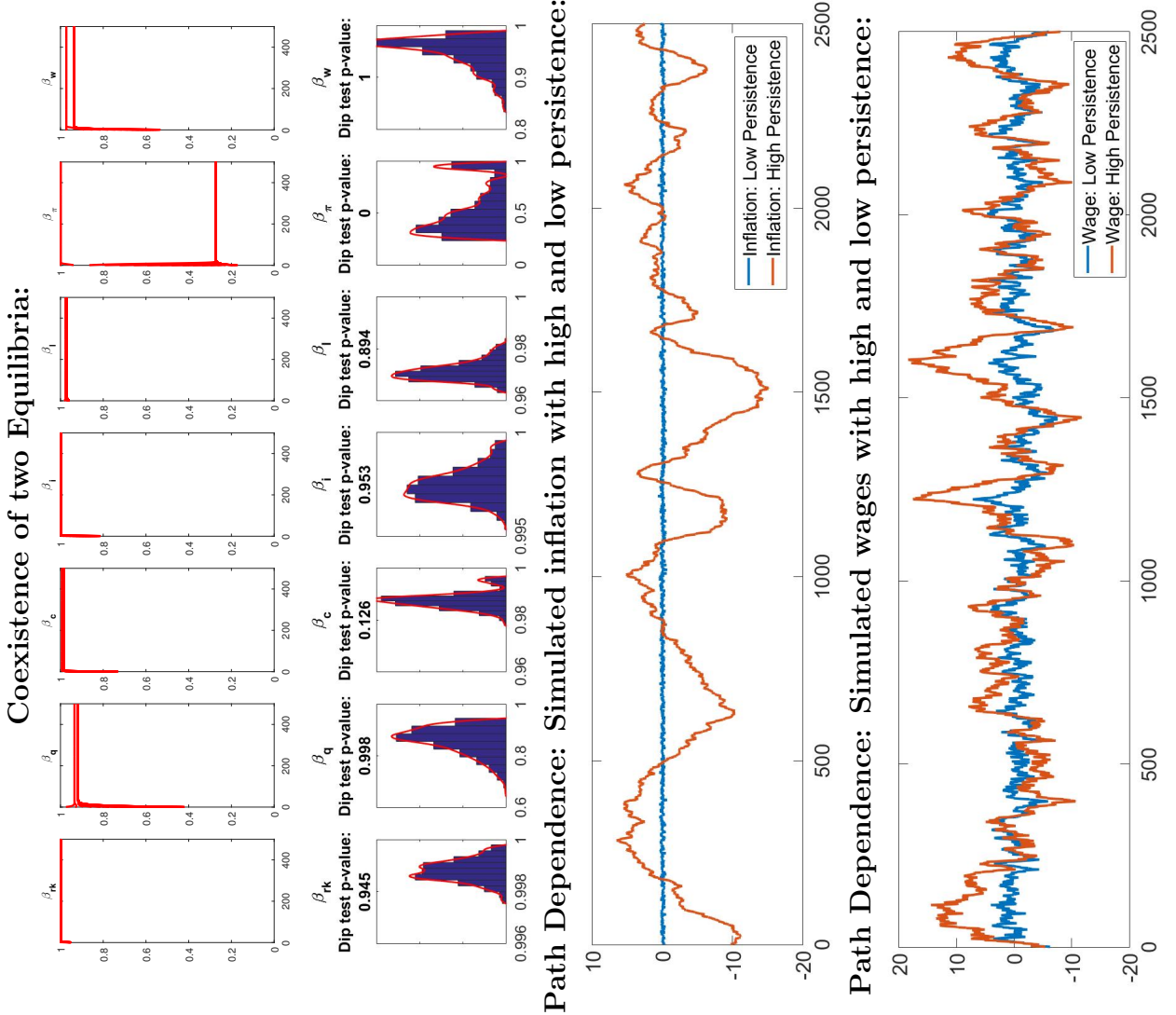
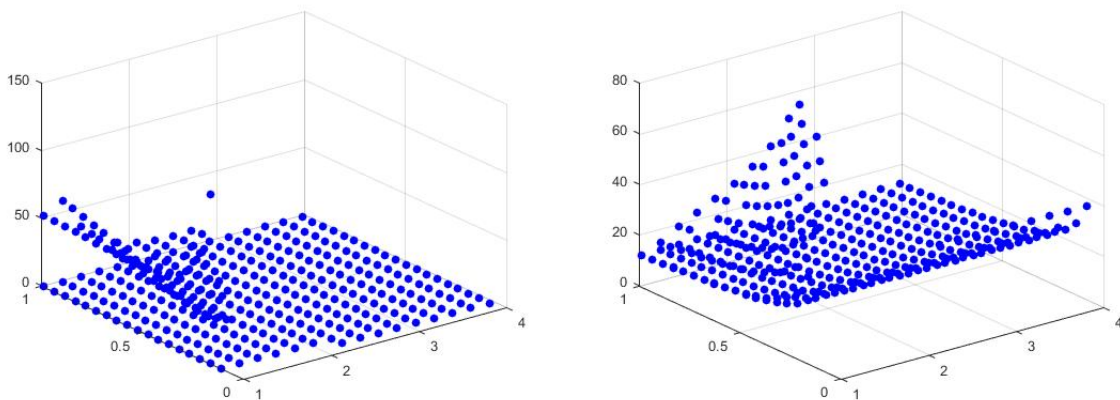
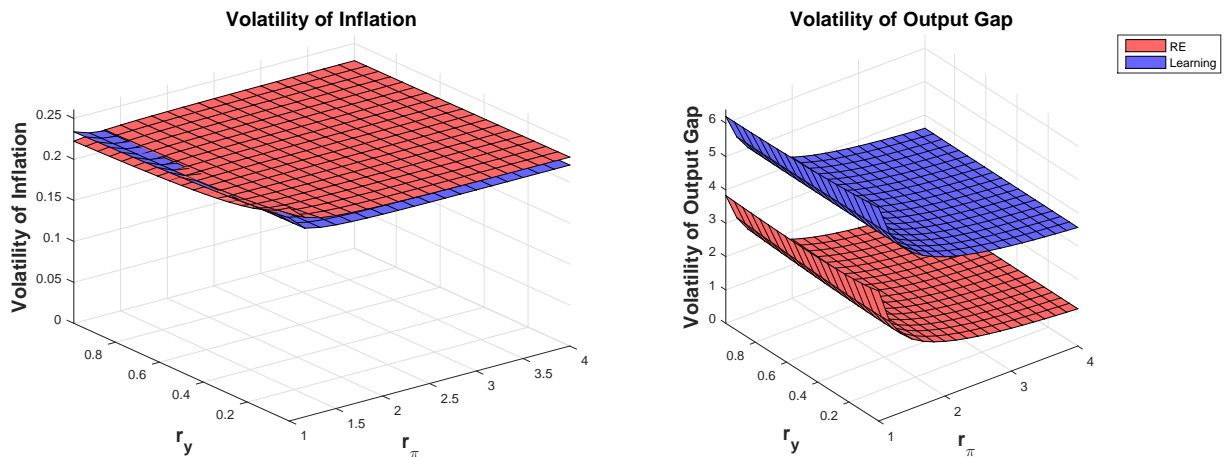


Figure 11: The top panel shows the multiplicity under BLE, with the variance of inflation on the left and the variance of output gap on the bottom when r_y and r_π are varied. We observe two co-existing iteratively E-stable equilibria over a small range of parameter combinations. The bottom panel compares the changes in these two variances at the estimated posterior mode under REE and the low-persistence equilibrium under BLE.

Multiple Equilibria in BLE:



Comparison of REE and low-persistence equilibrium in BLE:



6 Model Sensitivity

Our results in the preceding sections show that, when we replace the assumption of Rational Expectations with the simple AR(1) learning rule, both the empirical fit and forecasting performance of the model improve, while important differences arise in terms of the parameter estimates. A natural question that follows is how robust these results are to the estimation

samples and small changes in the model specification. Accordingly, in this section we present the estimation results at the posterior mode first across two different subsamples, then for small changes in the model specification under both BLE and REE assumptions.

6.1 Subsample Estimations

We re-estimate the SW model for the period before and after the recent Global Financial Crisis (GFC) of 2007. Using these two sample periods also allows us to investigate whether the presence of a potentially binding ZLB has an impact on our estimations. The results are presented in Tables 8 and 9 under both REE and BLE specifications. It is readily seen that the improved likelihood of the learning model over RE is robust across these two subsamples: While the resulting likelihoods are -339 and -213 before and after the GFC under BLE respectively, they turn out to be -351 and -216 under REE. Moreover, most of the differences in parameter estimates that were observed over the entire sample period also arise across these subsamples: The price and wage stickiness parameters turn out lower under BLE, implying stronger feedback from price and wage mark-ups to inflation and real wages respectively. Furthermore, the shocks typically turn out less persistent, but more volatile under BLE. There are, however, some notable differences across the subsamples: The main difference arises in the steady-state related parameters, particularly the steady-state level of labor, the common growth rate and the share of capital in production. This is an expected result since these parameters have only a marginal impact on the endogenous propagation mechanism, and mostly relate to the averages of the observable variables, which are clearly different across these two subsamples. Under the REE specification, the capital adjustment cost and habit formation both turn out substantially lower in the latter period, while the risk-premium shock becomes highly persistent. Under BLE, the risk-premium shock turns out to be a near white-noise in the early subsample, while the government spending shock is lower in the latter. With the exception of these differences, the parameter estimates are qualitatively similar to those obtained in the previous section, which confirms our main conclusion that the system becomes more inertial under BLE by making the contemporaneous links in the system weaker, and this trade-off leads to an improvement in the empirical fit of the model.

Table 8: Subsample Estimations of the Structural Parameters under Rational Expectations and BLE. The two sub-samples correspond to 1985:I-2006:IV (before the Global Financial Crisis (GFC)) and 2007:I-2016:IV (after GFC).

| | Before GFC | | After GFC | |
|----------------------|-----------------|-----------------|-----------------|-----------------|
| | BLE | REE | BLE | REE |
| Laplace Parameter | -339.31 Mode | -350.67 Mode | -212.91 Mode | -215.56 Mode |
| ϕ | 3.34 | 6.57 | 4.43 | 2.53 |
| σ_c | 1.19 | 1.47 | 1.45 | 1.35 |
| λ | 0.61 | 0.73 | 0.77 | 0.3 |
| ξ_w | 0.77 | 0.92 | 0.72 | 0.77 |
| σ_l | 2.1 | 1.95 | 2.03 | 1.84 |
| ξ_p | 0.76 | 0.88 | 0.78 | 0.88 |
| ψ | 0.56 | 0.59 | 0.48 | 0.48 |
| ϕ_p | 1.53 | 1.52 | 1.29 | 1.2 |
| r_π | 1.59 | 1.63 | 1.41 | 1.38 |
| ρ | 0.88 | 0.85 | 0.88 | 0.82 |
| r_y | 0.13 | 0.12 | 0.1 | 0.16 |
| $r_{\delta y}$ | 0.07 | 0.13 | 0.05 | 0.13 |
| $\bar{\pi}$ | 0.61 | 0.6 | 0.6 | 0.6 |
| $\bar{\beta}$ | 0.19 | 0.13 | 0.23 | 0.19 |
| \bar{l} | 2.74 | 3 | -1.54 | -2.39 |
| $\bar{\gamma}$ | 0.49 | 0.46 | 0.23 | 0.26 |
| α | 0.18 | 0.22 | 0.08 | 0.15 |

Table 9: Subsample Estimations of the Shock persistence and standard deviations under Rational Expectations and BLE. The two subsamples correspond to 1985:I-2006:IV (before the Global Financial Crisis (GFC)) and 2007:I-2016:IV (after GFC).

| | Before GFC | | After GFC | |
|-----------|------------|---------|-----------|---------|
| | BLE | REE | BLE | REE |
| Laplace | -339.31 | -350.67 | -212.91 | -215.56 |
| Parameter | Mode | Mode | Mode | Mode |
| ρ_a | 0.91 | 0.9 | 0.92 | 0.89 |
| ρ_b | 0.14 | 0.15 | 0.49 | 0.9 |
| ρ_g | 0.98 | 0.97 | 0.56 | 0.92 |
| ρ_i | 0.35 | 0.63 | 0.78 | 0.71 |
| ρ_r | 0.27 | 0.14 | 0.46 | 0.5 |
| ρ_p | 0.24 | 0.49 | 0.12 | 0.31 |
| ρ_w | 0.2 | 0.2 | 0.06 | 0.07 |
| η_a | 0.37 | 0.36 | 0.47 | 0.46 |
| η_b | 0.48 | 0.2 | 0.59 | 0.13 |
| η_g | 0.41 | 0.41 | 0.32 | 0.38 |
| η_i | 1.22 | 0.38 | 1.33 | 0.32 |
| η_r | 0.11 | 0.12 | 0.11 | 0.13 |
| η_p | 0.16 | 0.1 | 0.22 | 0.15 |
| η_w | 0.7 | 0.29 | 1.12 | 0.57 |

6.2 Empirical Importance of Frictions & Shocks

In this section, we turn to an examination of the model stability when there are small changes in the model parameters. A common method in the literature is to fix the model parameters one at a time and re-estimate the model with the remaining parameters, see e.g. Smets-Wouters (2007). Accordingly, we fix each nominal & real friction and shock persistence parameter at a low value one at a time, and re-estimate the remaining parameters under both BLE and RE³⁰. This approach allows us to obtain an intuitive measure of the marginal importance of each parameter by looking at the likelihood loss resulting from fixing the parameter. Further, it allows us to check for the stability of the remaining parameter estimates, i.e. to observe the extent to which the overall results vary when we make small changes to our model specification.

Tables 10 and 11 show the resulting estimations at the posterior mode under both specifications, along with the likelihood losses that arise from shutting off a given parameter. Taking this as our measure of the empirical importance of the given parameter, in general we observe that, typically, if the parameter that is shut off is more important, it also leads to more changes in the estimates of the remaining parameters. To start with the results under BLE, the Calvo probabilities appear to be the most important parameters in the friction group. Shutting off the wage stickiness results in a loss of 46 in terms of likelihood, where the habit formation and elasticity of labor supply turn out lower and the wage mark-up shock becomes much more persistent and volatile. Lowering the price stickiness has more direct consequences where the system dynamics become explosive under BLE. Varying the initial values $\beta^{(0)}$ for Algorithm II, as well as simulating the system with $\xi_p = 0.1$ confirms this result, implying the price stickiness is essential for the existence of an iteratively E-stable BLE. Habit formation and the capital adjustment cost also appear important for the empirical fit under BLE, as shutting them off comes at a cost of 20 and 16 respectively, leading to more persistent & volatile risk-premium and investment shocks. The remaining two frictions, the capital utilization adjustment cost and fixed cost in production, do not appear important, as shutting them off comes at almost no cost in terms of the likelihood, and the estimates of remaining parameters are fairly similar compared to the baseline. Next turning the shock persistence parameters, the most important ones are government spending, productivity and risk premium shocks, since shutting them off comes at a cost of 85, 157 and 63 respectively. In each case, the relevant friction and remaining shock parameters typically increase to make up for the loss. The price mark-up and investment shocks also lead to sizable losses of 14 and 25 respectively, although we do not observe any important changes in the estimates of the remaining parameters. Finally the persistence of monetary policy and wage mark-up shocks appear unimportant, since shutting off the first one results in only a small loss in likelihood, while the shutting off the first one actually improves

³⁰Similar to the previous section, the reported likelihoods are based on the Laplace Approximation, which is assumed to be an accurate approximation of the marginal posterior likelihood.

the likelihood. Next turning to the REE specification, we observe mostly similar results: The Calvo probabilities are the most important parameters in the friction group, as shutting off the price and wage stickiness parameters comes at a cost of 133 and 24 respectively. The same argument also applies to habit formation, which results in a loss of 15 in likelihood. Unlike the case under BLE, the capital adjustment cost appears unimportant in this case, but the capital utilization adjustment cost results in a loss of 10. Finally, the fixed cost in production appears unimportant similar to before. In each case, the changes in the estimates of remaining parameters are similar to the discussion under BLE, where the relevant frictions and shocks adjust to make up for the loss of shutting off a given parameter. Next turning to the shock persistence parameters, the most important ones are the productivity and government spending shocks just like before: Shutting these off results in a likelihood loss of 142 and 69 respectively. Similarly, the price mark-up and investment persistence result in sizable losses of 18 and 34 respectively, although no important changes arise in the estimates of remaining parameters. While the results from fixing the wage mark-up and monetary policy persistence are similar to the case of BLE, an important difference arises for the risk-premium shock persistence since it appears unimportant under REE.

Finally we turn to a comparison of the results under BLE and REE, which provides the differences in likelihood after each re-estimation. We observe the difference remains positive in favour of the BLE specification in a vast majority of the cases: The REE model provides a better model fit only in the case where the risk premium persistence is shut-off, which substantially worsens the likelihood under BLE but does not affect that of the REE model. While this exercise shows the robustness of the improved model fit under BLE, it also reveals another important difference under these two specifications: Shutting off the friction and shock persistence parameters leads to a larger loss of likelihood under BLE in most cases. This difference again naturally arises due to the difference between the expectation formation rules: Since the expectations take into account all contemporaneous shocks under REE, the feedback between the exogenous shocks and the endogenous variables is more dispersed on average. On the contrary, since expectations are completely backward-looking under BLE, the dependence of the forward-looking variables on individual shocks is more emphasized, and the feedback between the exogenous shocks and endogenous variables is more concentrated. Consequently, shutting off individual parameters typically has more dire consequences under the BLE specification. As a case in point to show how these interdependencies affect the system, we provide the variance decompositions for three key variables in Table 13, namely for output, consumption and investment growth rates. It becomes evident that for the growth rates of consumption and output, the fluctuations are mainly driven by the risk premium shock, where the share of this shock on the respective variance decompositions increases from 37.5% to 57.7% and from 75.3% to 99.3% under BLE relative to REE. Given this result, it is not surprising that shutting off the risk-premium shock persistence leads to a larger loss in likelihood. On the contrary, the

investment shock plays a larger role in the variance decomposition of the investment growth with a share of 87.5%, compared with 65.9% under BLE. This leads to a larger loss under REE when the investment shock persistence is shut off. Accordingly, based on the likelihood losses of Table 12, our results imply the variance decompositions are more concentrated in general under BLE, leading to larger likelihood losses on average when individual parameters are shut off. Overall, our estimation results have the following implication: On the one hand, the shock persistence and friction parameters turn out to be lower on average under BLE, because the system becomes more inertial with the introduction of learning. On the other hand, the contribution of each shock persistence and friction parameter also increases on average under BLE, because the introduction of BLE leads to more concentrated interdependencies between the endogenous variables and exogenous shocks.

Table 10: Empirical Importance of Shock Persistence and Friction Parameters under BLE. The Bayes Factor row shows the difference in likelihood between the baseline model and the respective model in each column.

| | Baseline | $\xi_p = 0.5$ | $\xi_w = 0.5$ | $\psi = 0.1$ | $\lambda = 0.1$ | $\phi = 2$ | $\phi_p = 1.1$ | $\rho_p = 0$ | $\rho_w = 0$ | $\rho_g = 0$ | $\rho_a = 0$ | $\rho_b = 0$ | $\rho_i = 0$ | $\rho_r = 0$ |
|----------------|----------|---------------|---------------|--------------|-----------------|------------|----------------|--------------|--------------|--------------|--------------|--------------|--------------|--------------|
| Likl | -546,2 | Explosive | -591,9 | -549,02 | -566,22 | -561,79 | -553,45 | -559,77 | -540,46 | -630,97 | -703,06 | -609,59 | -571,68 | -551,07 |
| Difference | - | - | 45,7 | 2,82 | 20,02 | 15,59 | 7,25 | 13,57 | -5,74 | 84,77 | 156,86 | 63,39 | 25,48 | exp(4,87) |
| ϕ | 4.39 | | 4,36 | 4,73 | 4,25 | | 4,96 | 4,42 | 4,4 | 4,58 | 3,19 | 5,45 | 4,78 | 4,24 |
| σ_c | 1.02 | | 1,13 | 1,07 | 0,67 | 0,96 | 1,08 | 1,03 | 1,03 | 0,58 | 1,39 | 0,88 | 1,01 | 1,01 |
| λ | 0.79 | | 0,47 | 0,77 | | 0,5 | 0,67 | 0,79 | 0,79 | 0,36 | 0,44 | 0,83 | 0,78 | 0,79 |
| ξ_w | 0.67 | | | 0,67 | 0,67 | 0,67 | 0,66 | 0,66 | 0,67 | 0,6 | 0,64 | 0,63 | 0,65 | 0,67 |
| σ_l | 2.36 | | 0,26 | 2,36 | 2,27 | 2,18 | 2,37 | 2,41 | 2,39 | 1,52 | 2,48 | 2,55 | 2,39 | 2,36 |
| ξ_p | 0.74 | | 0,75 | 0,74 | 0,75 | 0,73 | 0,73 | 0,7 | 0,74 | 0,77 | 0,77 | 0,74 | 0,74 | 0,74 |
| ψ | 0.46 | | 0,39 | | 0,34 | 0,32 | 0,42 | 0,46 | 0,45 | 0,37 | 0,7 | 0,39 | 0,46 | 0,46 |
| ϕ_p | 1.5 | | 1,51 | 1,49 | 1,33 | 1,48 | | 1,5 | 1,5 | 1,34 | 1,47 | 1,46 | 1,5 | 1,49 |
| r_π | 1.43 | | 1,46 | 1,42 | 1,46 | 1,52 | 1,45 | 1,43 | 1,44 | 1,52 | 1,46 | 1,47 | 1,4 | 1,52 |
| ρ | 0.89 | | 0,9 | 0,89 | 0,89 | 0,91 | 0,9 | 0,89 | 0,89 | 0,91 | 0,9 | 0,9 | 0,89 | 0,92 |
| r_y | 0.07 | | 0,08 | 0,08 | 0,08 | 0,07 | 0,08 | 0,07 | 0,08 | 0,07 | 0,09 | 0,08 | 0,08 | 0,07 |
| r_{dy} | 0.05 | | 0,06 | 0,05 | 0,08 | 0,06 | 0,05 | 0,05 | 0,05 | 0,07 | 0,06 | 0,05 | 0,05 | 0,07 |
| $\bar{\pi}$ | 0.57 | | 0,59 | 0,57 | 0,57 | 0,61 | 0,59 | 0,56 | 0,58 | 0,66 | 0,58 | 0,58 | 0,57 | 0,58 |
| $\bar{\beta}$ | 0.18 | | 0,16 | 0,17 | 0,17 | 0,18 | 0,17 | 0,17 | 0,18 | 0,29 | 0,17 | 0,18 | 0,18 | 0,17 |
| \bar{l} | 1.81 | | 1,75 | 1,83 | 0,87 | 1,14 | 1,78 | 1,79 | 1,82 | -0,19 | 2,92 | 1,5 | 2,04 | 2,01 |
| $\bar{\gamma}$ | 0.42 | | 0,4 | 0,41 | 0,38 | 0,35 | 0,4 | 0,42 | 0,41 | 0,14 | 0,49 | 0,42 | 0,44 | 0,42 |
| α | 0.13 | | 0,14 | 0,12 | 0,13 | 0,13 | 0,13 | 0,13 | 0,13 | 0,08 | 0,22 | 0,13 | 0,13 | 0,13 |
| ρ_a | 0.97 | | 0,98 | 0,97 | 0,98 | 0,99 | 0,98 | 0,97 | 0,98 | 0,99 | | 0,97 | 0,97 | 0,97 |
| ρ_b | 0.36 | | 0,44 | 0,36 | 0,81 | 0,47 | 0,38 | 0,36 | 0,36 | 0,7 | 0,4 | | 0,38 | 0,37 |
| ρ_g | 0.99 | | 0,98 | 0,99 | 0,96 | 0,93 | 0,98 | 0,99 | 0,99 | | 0,99 | 0,98 | 0,99 | 0,99 |
| ρ_i | 0.54 | | 0,69 | 0,58 | 0,67 | 0,84 | 0,69 | 0,54 | 0,55 | 0,71 | 0,71 | 0,6 | | 0,53 |
| ρ_r | 0.35 | | 0,35 | 0,35 | 0,32 | 0,35 | 0,35 | 0,35 | 0,35 | 0,34 | 0,35 | 0,35 | 0,34 | |
| ρ_p | 0.16 | | 0,11 | 0,17 | 0,18 | 0,14 | 0,17 | | 0,16 | 0,11 | 0,1 | 0,14 | 0,17 | 0,16 |
| ρ_w | 0.04 | | 0,85 | 0,04 | 0,04 | 0,04 | 0,04 | 0,04 | | 0,05 | 0,04 | 0,05 | 0,04 | 0,04 |
| η_a | 0.41 | | 0,41 | 0,42 | 0,43 | 0,42 | 0,41 | 0,41 | 0,41 | 0,5 | 1,09 | 0,41 | 0,41 | 0,41 |
| η_b | 0.55 | | 0,57 | 0,55 | 0,72 | 0,58 | 0,56 | 0,55 | 0,55 | 0,68 | 0,56 | 0,85 | 0,56 | 0,55 |
| η_g | 0.4 | | 0,39 | 0,4 | 0,39 | 0,39 | 0,4 | 0,4 | 0,4 | 0,53 | 0,42 | 0,4 | 0,4 | 0,4 |
| η_i | 1.24 | | 1,35 | 1,27 | 1,37 | 1,39 | 1,33 | 1,24 | 1,25 | 1,38 | 1,35 | 1,34 | 1,52 | 1,24 |
| η_r | 0.11 | | 0,11 | 0,11 | 0,11 | 0,11 | 0,11 | 0,11 | 0,11 | 0,11 | 0,11 | 0,11 | 0,11 | 0,11 |
| η_p | 0.19 | | 0,19 | 0,19 | 0,19 | 0,19 | 0,19 | 0,21 | 0,19 | 0,19 | 0,19 | 0,19 | 0,19 | 0,19 |
| η_w | 0.85 | | 1,79 | 0,85 | 0,84 | 0,84 | 0,85 | 0,84 | 0,84 | 0,86 | 0,86 | 0,85 | 0,85 | 0,85 |

Table 11: Empirical Importance of Shock Persistence and Friction Parameters under REE. The Bayes Factor row shows the difference in likelihood between the baseline model and the respective model in each column.

| | Baseline | $\xi_p = 0.1$ | $\xi_w = 0.1$ | $\psi = 0.1$ | $\lambda = 0$ | $\phi = 2$ | $\phi_p = 1.1$ | $\rho_p = 0$ | $\rho_w = 0$ | $\rho_g = 0$ | $\rho_a = 0$ | $\rho_b = 0$ | $\rho_i = 0$ | $\rho_r = 0$ |
|----------------|----------|---------------|---------------|--------------|---------------|------------|----------------|--------------|--------------|--------------|--------------|--------------|--------------|--------------|
| Likl | -572,9 | -705,47 | -597,37 | -583 | -587,62 | -575,12 | -575,93 | -591,35 | -566,71 | -642,34 | -714,45 | -575,87 | -606,47 | -573,62 |
| Difference | | 132,57 | 24,47 | 10,1 | 14,72 | 2,22 | 3,03 | 18,45 | -6,19 | 69,44 | 141,55 | 2,97 | 33,57 | 0,72 |
| ϕ | 7,55 | 7,25 | 2,88 | 8,06 | 0,68 | | 3,55 | 7,55 | 7,54 | 8,18 | 5,23 | 7,57 | 7,33 | 3,98 |
| σ_c | 1,56 | 1,59 | 1,27 | 1,53 | 1,4 | 1,3 | 1,25 | 1,56 | 1,56 | 1,56 | 1,01 | 1,59 | 1,01 | 1,29 |
| λ | 0,78 | 0,77 | 0,29 | 0,81 | | 0,33 | 0,37 | 0,78 | 0,78 | 0,8 | 0,57 | 0,81 | 0,86 | 0,42 |
| ξ_w | 0,9 | 0,87 | | 0,89 | 0,86 | 0,87 | 0,88 | 0,9 | 0,9 | 0,87 | 0,86 | 0,9 | 0,85 | 0,88 |
| σ_l | 1,41 | 1,44 | 0,25 | 1,73 | 1,93 | 1,95 | 2,02 | 1,34 | 1,46 | 1,27 | 2,25 | 1,3 | 2,23 | 2 |
| ξ_p | 0,92 | | 0,93 | 0,92 | 0,94 | 0,93 | 0,95 | 0,93 | 0,92 | 0,88 | 0,89 | 0,91 | 0,89 | 0,93 |
| ψ | 0,61 | 0,85 | 0,56 | | 0,56 | 0,56 | 0,55 | 0,6 | 0,62 | 0,7 | 0,81 | 0,65 | 0,59 | 0,59 |
| ϕ_p | 1,46 | 1,81 | 1,25 | 1,4 | 1,18 | 1,25 | | 1,46 | 1,46 | 1,46 | 1,39 | 1,51 | 1,46 | 1,29 |
| r_π | 1,58 | 1,83 | 1,57 | 1,46 | 1,48 | 1,47 | 1,48 | 1,54 | 1,57 | 1,65 | 1,36 | 1,57 | 1,41 | 1,5 |
| ρ | 0,87 | 0,87 | 0,86 | 0,87 | 0,87 | 0,87 | 0,86 | 0,87 | 0,87 | 0,88 | 0,86 | 0,86 | 0,84 | 0,89 |
| r_y | 0,06 | 0 | 0,1 | 0,06 | 0,11 | 0,11 | 0,12 | 0,06 | 0,06 | 0,05 | 0,1 | 0,05 | 0,08 | 0,1 |
| r_{dy} | 0,11 | 0,08 | 0,17 | 0,09 | 0,21 | 0,17 | 0,17 | 0,11 | 0,11 | 0,09 | 0,12 | 0,1 | 0,07 | 0,15 |
| $\bar{\pi}$ | 0,63 | 0,62 | 0,59 | 0,62 | 0,6 | 0,59 | 0,6 | 0,62 | 0,63 | 0,59 | 0,56 | 0,64 | 0,62 | 0,6 |
| $\bar{\beta}$ | 0,12 | 0,14 | 0,13 | 0,12 | 0,12 | 0,13 | 0,14 | 0,12 | 0,12 | 0,23 | 0,16 | 0,12 | 0,15 | 0,13 |
| \bar{l} | 1,07 | -0,29 | 1,64 | 1,52 | 1,24 | 1,07 | 1,07 | 1,19 | 1,06 | -0,05 | 0,95 | 1,17 | 0,53 | 1,07 |
| $\bar{\gamma}$ | 0,3 | 0,24 | 0,4 | 0,32 | 0,38 | 0,35 | 0,35 | 0,31 | 0,3 | 0,12 | 0,45 | 0,29 | 0,33 | 0,35 |
| α | 0,17 | 0,18 | 0,18 | 0,14 | 0,18 | 0,17 | 0,15 | 0,17 | 0,17 | 0,08 | 0,25 | 0,17 | 0,13 | 0,16 |
| ρ_a | 0,99 | 0,99 | 0,98 | 0,99 | 0,97 | 0,98 | 0,99 | 0,99 | 0,99 | 0,99 | | 0,99 | 0,99 | 0,98 |
| ρ_b | 0,3 | 0,23 | 0,92 | 0,36 | 0,92 | 0,9 | 0,9 | 0,3 | 0,3 | 0,29 | 0,89 | | 0,75 | 0,88 |
| ρ_g | 0,96 | 0,93 | 0,97 | 0,97 | 0,97 | 0,98 | 0,98 | 0,96 | 0,96 | | 0,96 | 0,94 | 0,96 | 0,98 |
| ρ_i | 0,81 | 0,78 | 0,76 | 0,85 | 0,92 | 0,86 | 0,78 | 0,81 | 0,81 | 0,83 | 0,7 | 0,79 | | 0,8 |
| ρ_r | 0,27 | 0,28 | 0,19 | 0,29 | 0,13 | 0,18 | 0,2 | 0,28 | 0,27 | 0,28 | 0,25 | 0,29 | 0,37 | |
| ρ_p | 0,47 | 0,96 | 0,43 | 0,46 | 0,43 | 0,44 | 0,44 | | 0,46 | 0,49 | 0,42 | 0,47 | 0,43 | 0,45 |
| ρ_w | 0,05 | 0,02 | 0,94 | 0,05 | 0,04 | 0,04 | 0,04 | 0,04 | | 0,05 | 0,07 | 0,04 | 0,06 | 0,04 |
| η_a | 0,41 | 0,38 | 0,42 | 0,43 | 0,43 | 0,42 | 0,46 | 0,41 | 0,41 | 0,48 | 0,93 | 0,41 | 0,43 | 0,42 |
| η_b | 0,19 | 0,21 | 0,08 | 0,18 | 0,12 | 0,09 | 0,08 | 0,19 | 0,19 | 0,2 | 0,09 | 0,26 | 0,1 | 0,08 |
| η_g | 0,4 | 0,4 | 0,4 | 0,39 | 0,41 | 0,4 | 0,4 | 0,4 | 0,4 | 0,54 | 0,45 | 0,4 | 0,39 | 0,4 |
| η_i | 0,29 | 0,3 | 0,32 | 0,23 | 0,59 | 0,34 | 0,3 | 0,29 | 0,29 | 0,25 | 0,32 | 0,3 | 0,88 | 0,29 |
| η_r | 0,11 | 0,12 | 0,13 | 0,11 | 0,13 | 0,12 | 0,12 | 0,11 | 0,11 | 0,11 | 0,12 | 0,11 | 0,11 | 0,12 |
| η_p | 0,11 | 0,76 | 0,11 | 0,11 | 0,11 | 0,11 | 0,11 | 0,23 | 0,11 | 0,11 | 0,12 | 0,11 | 0,11 | 0,11 |
| η_w | 0,42 | 0,44 | 1,06 | 0,42 | 0,43 | 0,43 | 0,42 | 0,42 | 0,43 | 0,42 | 0,44 | 0,42 | 0,43 | 0,42 |

Table 12: Comparison of the results under BLE and REE. The bottom panel corresponds to the difference in the log likelihood under BLE and REE for a given column.

| | Baseline | $\xi_p = 0.1$ | $\xi_w = 0.1$ | $\psi = 0.1$ | $\lambda = 0$ | $\phi = 2$ | $\phi_p = 1.1$ | $\rho_p = 0$ | $\rho_w = 0$ | $\rho_g = 0$ | $\rho_a = 0$ | $\rho_b = 0$ | $\rho_i = 0$ | $\rho_r = 0$ |
|------------|----------|---------------|---------------|--------------|---------------|------------|----------------|--------------|--------------|--------------|--------------|--------------|--------------|--------------|
| BLE Logl. | -546,2 | Explosive | -591,9 | -549,02 | -566,22 | -561,79 | -553,45 | -559,77 | -540,46 | -630,97 | -703,06 | -609,59 | -571,68 | -551,07 |
| REE Logl. | -572,9 | -705,47 | -597,37 | -583 | -587,62 | -575,12 | -575,93 | -591,35 | -566,71 | -642,34 | -714,45 | -575,87 | -606,47 | -573,62 |
| Difference | 26,7 | - | 5,47 | 33,98 | 21,4 | 13,33 | 22,48 | 31,58 | 26,25 | 11,37 | 11,39 | -33,72 | 34,79 | 22,55 |

Table 13: Variance Decompositions of output, consumption and investment growth under BLE and REE over the period 1985:I-2016:IV.

| | BLE | | | REE | | |
|--------------|--------------|--------------|----------------|--------------|--------------|----------------|
| | Δy_t | Δc_t | Δinv_t | Δy_t | Δc_t | Δinv_t |
| Productivity | 0.36% | 0.15% | 0.16% | 2.59% | 3.66% | 2.15% |
| Risk Premium | 57.7% | 99.3% | 33.4% | 37.5% | 75.3% | 4.65% |
| Spending | 34.2% | 0.07% | 0.07% | 28.8% | 0.04% | 0.93% |
| Investment | 6.69% | 0.03% | 65.9% | 21% | 8.49% | 87.2% |
| Policy | 0.35% | 0.42% | 0.42% | 8% | 10.8% | 3.87% |
| Price | 0.03% | 0.03% | 0.02% | 1.67% | 1.51% | 1.11% |
| Wage | 0.67% | 0.02% | 0.01% | 0.51% | 0.21% | 0.13% |

7 Conclusions

There is an increasing consensus in the literature that the Rational Expectations Hypothesis is too flawed and unrealistic to be used in macroeconomic modeling. But abandoning the norm immediately brings a new question: What do we replace it with? Imposing more realistic assumptions clearly lead to better and more realistic models, but they also make it substantially harder to empirically validate the models at hand. The real challenge lies in coming up with more plausible and parsimonious models that allow us to make use of the state-of-the-art econometric tools at hand. In this paper, we imposed a simple univariate AR(1) learning rule as an alternative to the rational expectations approach, and introduced a simple numerical framework to estimate linearized DSGE models under BLE. Subsequently applying it to the baseline NKPC model and the workhorse model of Smets-Wouters shows that, a simple deviation as such leads to substantial improvements in the empirical fit of the model and its ability to capture the short-term momentum in the macroeconomic variables. More importantly, our results show that the stochastic structure and the monetary policy implications of the economy substantially change. These results imply at least several promising venues of future research: The first one that naturally comes to mind is, how far can we take the idea of modeling our agents as econometricians? The advantage of the univariate AR(1) rule that we used in this paper lies in its parsimony and intuitiveness. Our results indicate that slightly more complicated sample autocorrelation rules might lead to further improvements in the model fit, such as an AR(2) rule where the agent takes into account *the persistence in the growth rate of variables*, on top of the mean and the persistence in levels; or a simple VAR(1) rule where the agent is also able to interpret the *cross-correlations* in the variables. Such extensions are fairly easy to implement in our current econometric methodology, since we do not rely on analytical expressions to obtain our results. Another important extension relates to a more rigorous monetary policy analysis: In this paper, we only provided a preliminary analysis by examining how the economy responds

to changes in the monetary policy, but the extent to which the optimal monetary policy differs under rational expectations and BLE remains an open question. Finally, the important role of the risk-premium shock under learning in the SW model is interesting, since it indicates the unmodeled financial sector plays an important role in our estimations. Therefore applying our methodology in a setup where we explicitly model the financial sector might yield better results and more accurately capture the feedback between the macroeconomic and financial variables.

References

- Adjemian, S., Bastani, H., Juillard, M., Mihoubi, F., Perendia, G., Ratto, M., & Villemot, S. (2011). Dynare: Reference manual, version 4.
- Branch, W. A. (2004). Restricted perceptions equilibria and learning in macroeconomics. *Post Walrasian Macroeconomics: Beyond the Dynamic Stochastic General Equilibrium Model*, (pp. 135–160).
- Bullard, J. & Duffy, J. (2001). Learning and excess volatility. *Macroeconomic Dynamics*, 5(02), 272–302.
- Bullard, J. & Mitra, K. (2002). Learning about monetary policy rules. *Journal of Monetary Economics*, 49(6), 1105–1129.
- Campbell, J. Y. & Thompson, S. B. (2007). Predicting excess stock returns out of sample: Can anything beat the historical average? *The Review of Financial Studies*, 21(4), 1509–1531.
- Christiano, L. J., Eichenbaum, M., & Evans, C. L. (2005). Nominal rigidities and the dynamic effects of a shock to monetary policy. *Journal of political Economy*, 113(1), 1–45.
- Collard, F. & Dellas, H. (2004). The new keynesian model with imperfect information and learning. *IDEI Working Paper*, 273.
- Cooley, T. F. & Hansen, G. D. (1992). Tax distortions in a neoclassical monetary economy. *Journal of Economic Theory*, 58(2), 290–316.
- Estrella, A. & Fuhrer, J. C. (2002). Dynamic inconsistencies: Counterfactual implications of a class of rational-expectations models. *The American Economic Review*, 92(4), 1013–1028.
- Eusepi, S. & Preston, B. (2011). Expectations, learning, and business cycle fluctuations. *The American Economic Review*, 101(6), 2844–2872.

- Evans, G. W. & Honkapohja, S. (2012). *Learning and Expectations in Macroeconomics*. Princeton University Press.
- Fuster, A., Hebert, B., & Laibson, D. (2012). Natural expectations, macroeconomic dynamics, and asset pricing. *NBER Macroeconomics Annual*, 26(1), 1–48.
- Fuster, A., Laibson, D., & Mendel, B. (2010). Natural expectations and macroeconomic fluctuations. *The Journal of Economic Perspectives*, 24(4), 67–84.
- Gaspar, V., Smets, F., & Vestin, D. (2006). Adaptive learning, persistence, and optimal monetary policy. *Journal of the European Economic Association*, 4(2-3), 376–385.
- Greenberg, E. (2012). *Introduction to Bayesian Econometrics*. Cambridge University Press.
- Hartigan, J. A. & Hartigan, P. (1985). The dip test of unimodality. *The Annals of Statistics*, (pp. 70–84).
- Heckel, T., Le Bihan, H., & Montornès, J. (2008). Sticky wages: evidence from quarterly microeconomic data.
- Herbst, E. P. & Schorfheide, F. (2015). *Bayesian Estimation of DSGE Models*. Princeton University Press.
- Hirose, Y. & Inoue, A. (2016). The zero lower bound and parameter bias in an estimated dsge model. *Journal of Applied Econometrics*, 31(4), 630–651.
- Hirose, Y. & Sunakawa, T. (2016). Parameter bias in an estimated dsge model.
- Hommes, C. & Sorger, G. (1998). Consistent expectations equilibria. *Macroeconomic Dynamics*, 2(3), 287–321.
- Hommes, C. & Zhu, M. (2014). Behavioral learning equilibria. *Journal of Economic Theory*, 150, 778–814.
- Hommes, C. & Zhu, M. (2016). Behavioral learning equilibria, persistence amplification & monetary policy.
- Klenow, P. J. & Malin, B. A. (2010). *Microeconomic Evidence on Price-Setting*. Technical report, National Bureau of Economic Research.
- Lansing, K. J. (2009). Time-varying us inflation dynamics and the new keynesian phillips curve. *Review of Economic Dynamics*, 12(2), 304–326.
- Marcet, A. & Nicolini, J. P. (2003). Recurrent hyperinflations and learning. *The American Economic Review*, 93(5), 1476–1498.

- Milani, F. (2005). Adaptive learning and inflation persistence. *University of California, Irvine-Department of Economics*.
- Milani, F. (2007). Expectations, learning and macroeconomic persistence. *Journal of monetary Economics*, 54(7), 2065–2082.
- Mitra, K., Evans, G. W., & Honkapohja, S. (2017). Fiscal policy multipliers in an rbc model with learning. *Macroeconomic Dynamics*, (pp. 1–44).
- Muth, J. F. (1961). Rational expectations and the theory of price movements. *Econometrica: Journal of the Econometric Society*, (pp. 315–335).
- Nakamura, E. & Steinsson, J. (2013). Price rigidity: Microeconomic evidence and macroeconomic implications. *Annu. Rev. Econ.*, 5(1), 133–163.
- Office, C. B. & Congress, U. (2001). Cbo’s method for estimating potential output: An update. *August (Washington, DC: Congressional Budget Office)*.
- Orphanides, A. & Williams, J. (2004). Imperfect knowledge, inflation expectations, and monetary policy. In *The inflation-targeting debate* (pp. 201–246). University of Chicago Press.
- Preston, B. J. (2003). Learning about monetary policy rules when long-horizon expectations matter.
- Sargent, T. J. (1991). Equilibrium with signal extraction from endogenous variables. *Journal of Economic Dynamics and Control*, 15(2), 245–273.
- Schmitt-Grohé, S. & Uribe, M. (2005). Optimal fiscal and monetary policy in a medium-scale macroeconomic model. *NBER Macroeconomics Annual*, 20, 383–425.
- Slobodyan, S. & Wouters, R. (2012a). Learning in a medium-scale dsge model with expectations based on small forecasting models. *American Economic Journal: Macroeconomics*, 4(2), 65–101.
- Slobodyan, S. & Wouters, R. (2012b). Learning in an estimated medium-scale dsge model. *Journal of Economic Dynamics and control*, 36(1), 26–46.
- Smets, F. & Wouters, R. (2003). An estimated dynamic stochastic general equilibrium model of the euro area. *Journal of the European Economic Association*, 1(5), 1123–1175.
- Smets, F. & Wouters, R. (2007). Shocks and frictions in us business cycles: A bayesian dsge approach. *The American Economic Review*, 97(3), 586–606.
- Williams, N. (2003). *Adaptive Learning and Business Cycles*. Technical report, Princeton University mimeo.

Woodford, M. (2003). Interest and prices. Princeton University Press.

Woodford, M. (2013). Macroeconomic analysis without the rational expectations hypothesis. *Annu. Rev. Econ.*, 5(1), 303–346.

A Data Appendix

The observable variables used in systems (3.2) and (4.14) are defined as:

$$\begin{cases} y_t^{obs} = 100\log(GDPC09_t/LNS_{index_t}) \\ \pi_t^{obs} = 100\log(\frac{GDPDEF09_t}{GDPDEF09_{t-1}}) \\ i_t^{obs} = 100\log((\frac{FPI_t}{GDPDEF09_t})/LNS_{index_t}) \\ c_t^{obs} = 100\log((\frac{PCEC}{GDPDEF09_t})/LNS_{index_t}) \\ l_t^{obs} = 100\log(\frac{PRS85006103_t}{GDPDEF09_t}) \\ w_t^{obs} = 100\log((\frac{PRS85006103_t}{GDPDEF09_t})/LNS_{index_t}) \\ r_t^{obs} = 100\log(\frac{Funds_t}{4}) \end{cases} \quad (A.1)$$

where the time series are given as:

GDPC09: Real GDP, Billions of Chained 2009 Dollars, Seasonally Adjusted Annual Rate. Source: Federal Reserve Economic Data (FRED).

GDPDEF09: GDP-Implicit Price Deflator, 2009=100, Seasonally Adjusted. Source: FRED.

PCEC: Personal Consumption Expenditures, Billions of Dollars, Seasonally Adjusted. Source: FRED.

FPI: Fixed Private Investment, Billions of Dollars. Seasonally Adjusted. Source: FRED.

CE16OV: Civilian Employment Level, Thousands of Persons, Seasonally Adjusted, Source: FRED.

$$CE16OV_{index} = \frac{CE16OV}{CE16OV(1992:03)}$$

Funds: Federal Funds Rate, Daily Figure Averages in Percentages. Source: FRED.

LNU00000000: Unadjusted civilian noninstitutional population, Thousands, 16 years over. Source: U.S. Bureau of Labor Statistics (BLS)

LNS10000000: Civilian noninstitutional populations, Thousands, 16 years & over, Seasonally Adjusted.

Source: BLS.

$$LNS_{index} = \frac{LNS10000000}{LNS10000000(1992:03)}$$

PRS85006023: Nonfarm Business Sector, Average Weekly Hours, Index 2009=100, Seasonally Adjusted. Source: FRED

PRS85006103: Nonfarm Business Sector, Hourly Compensation, Index 2009=100, Seasonally Adjusted. Source: FRED.

The observable variable x_t^{obs} for the output gap used in the alternative estimations of the small-scale model is defined as:

$$x_t = 100 \frac{GDPC09 - GDPOT}{GDPOT}$$

with **GDPOT**³¹: CBO's Estimate of the Potential Output, Billions of Chained 2009 Dollars, Not Seasonally Adjusted Quarterly Rate. Source: FRED.

B Theoretical Moments for BLE

In order to compute the law of motion under BLE, recall we relax the assumption that shocks are observed. Accordingly re-writing the law of motion as in Section 2 and plugging in the AR(1) expectation formation rule yields the following implied ALM:

$$S_t = \bar{\gamma} + \gamma_1 S_{t-1} + \gamma_2 (\alpha_{t-1} + \beta_{t-1}^2 (S_{t-1} - \alpha_{t-1})) + \gamma_3 \eta_t \quad (\text{B.1})$$

Taking expectations on both sides yields:

$$\mathbb{E}[S_t] = \bar{\gamma} + \gamma_1 \mathbb{E}[S_{t-1}] + \gamma_2 \alpha_{t-1} + \gamma_2 \beta_{t-1}^2 \mathbb{E}[S_{t-1}] - \gamma_2 \beta_{t-1}^2 \alpha_{t-1} + \gamma_3 \mathbb{E}[\eta_t] \quad (\text{B.2})$$

The i.i.d assumption on the shocks implies that the last two terms are zero. Through stationarity, we have $\mathbb{E}[S_t] = \mathbb{E}[S_{t-1}] = \bar{S}$, and the first consistency requirement of a **BLE** imposes $\bar{S} = \alpha_{t-1} = \alpha$. Then:

$$\bar{S} = \bar{\gamma} + \gamma_1 \bar{S} + \gamma_2 \bar{S} + \gamma_2 \beta_{t-1}^2 \bar{S} - \gamma_2 \beta_{t-1}^2 \bar{S} \quad (\text{B.3})$$

which reduces to :

$$\bar{S} = (I - \gamma_1 - \gamma_2)^{-1} \bar{\gamma} \quad (\text{B.4})$$

For the remainder, we assume $\alpha_{t-1} = \alpha = \bar{\gamma} = \bar{S} = 0$, which is the case for both models considered in this paper, which reduces the law of motion to:

$$S_t = (\gamma_1 + \gamma_2 \beta_{t-1}^2) S_{t-1} + \gamma_3 \eta_t \quad (\text{B.5})$$

The first-order autocovariance matrix is given by:

$$\mathbb{E}[S_t S_{t-1}] = (\gamma_1 + \gamma_2 \beta_{t-1}^2) \mathbb{E}[S_{t-1} S_{t-1}] + \gamma_3 \mathbb{E}[\eta_t S_{t-1}] \quad (\text{B.6})$$

³¹In order to calculate the potential output, CBO uses the theoretical framework in a standard Solow growth model setup, see [Office & Congress \(2001\)](#) for more details.

We have $\mathbb{E}[\eta_t S_{t-1}] = 0$, while $\mathbb{E}[\eta_{t-1} S_{t-1}] = \mathbb{E}[\eta_{t-1}((\gamma_1 + \gamma_2 \boldsymbol{\beta}_{t-1}^2) S_{t-1} + \gamma_3 \eta_t)] = \gamma_3 \Sigma_\eta$. Further denoting $(\gamma_1 + \gamma_2 \boldsymbol{\beta}_{t-1}^2) = M(\boldsymbol{\beta}_{t-1})$, the first-order autocovariance matrix $\mathbb{E}[S_t S_{t-1}] = \Gamma_1$ and the variance-covariance matrix $\mathbb{E}[S_t S_t] = \Gamma_0$, the expression in (B.8) reduces to:

$$\Gamma_1 = M(\boldsymbol{\beta}_{t-1})\Gamma_0 + \gamma_3 \Sigma_\eta \quad (\text{B.7})$$

which implies we need an expression for Γ_0 in order to compute Γ_1 . Taking the variance on both sides of (B.7) yields:

$$\Gamma_0 = M(\boldsymbol{\beta}_{t-1})\Gamma_0 M(\boldsymbol{\beta}_{t-1})' + \gamma_3 \Sigma_\eta \gamma_3' \quad (\text{B.8})$$

Vectorizing both sides implies:

$$\text{Vec}(\Gamma_0) = \text{Vec}(M(\boldsymbol{\beta})\Gamma_0 M(\boldsymbol{\beta}_{t-1})' + \gamma_3 \Sigma_\eta \gamma_3') \quad (\text{B.9})$$

Using $\text{Vec}(ABC) = (C' \otimes A)\text{Vec}(B)$, and $\text{Vec}(A+B) = \text{Vec}(A) + \text{Vec}(B)$, the above expression reduces to:

$$\text{Vec}(\Gamma_0) = (M(\boldsymbol{\beta}_{t-1}) \otimes M(\boldsymbol{\beta}_{t-1}))\text{Vec}(\Gamma_0) + (\gamma_3 \otimes \gamma_3)\text{Vec}(\Sigma_\eta) \quad (\text{B.10})$$

Hence:

$$\text{Vec}(\Gamma_0) = [I - M(\boldsymbol{\beta}_{t-1}) \otimes M(\boldsymbol{\beta}_{t-1})]^{-1}(\gamma_3 \otimes \gamma_3)\text{Vec}(\Sigma_\eta) \quad (\text{B.11})$$

Putting everything together yields the system of equations in Proposition 2.1.

Local Stability under SAC Learning

The E-stability principle applies under SAC-learning, see [Hommes & Zhu \(2016\)](#) Appendix C for a detailed treatment. Accordingly, a BLE corresponds to the fixed point of the ODE:

$$\begin{cases} \frac{d\alpha}{d\tau} = \bar{S}(\alpha, \beta) - \alpha \\ \frac{d\beta}{d\tau} = G - \beta \end{cases}$$

And the eigenvalues of its Jacobian are the solution to:

$$(I - \gamma_1 - \gamma_2 \boldsymbol{\beta}^{*2})^{-1}(\gamma_1 + \gamma_2 - I)(DG_\beta(\boldsymbol{\beta}^*) - I) = 0$$

Therefore, if all eigenvalues of $(I - \gamma_1 - \gamma_2 \boldsymbol{\beta}^{*2})^{-1}(\gamma_1 + \gamma_2 - I)$ have negative real parts, and all eigenvalues of $(DG_\beta(\boldsymbol{\beta}^*) - I)$ have real parts less than one, then the BLE $(\boldsymbol{\alpha}^*, \boldsymbol{\beta}^*)$ is locally stable.

C Proof of Propositions 2.3 and 2.4

Proposition 2.3: Assume $\rho(DG(\beta^*)) < 1$ and $\xi(DG(\beta^*)) < 0$ hold. Given $\rho(DG(\beta^*)) < 1$, $\exists \|\cdot\| \in \mathbb{R}^n$ s.t. $\|DG(\beta^*)\| < 1$. Assuming $G(\beta) : [-1, 1]^N \rightarrow [-1, 1]^N$ is continuously differentiable, $\exists c, d \in \mathbb{R}$ s.t:

$$\|DG(\beta)\| \leq c, \forall \beta \in \beta_d(\beta^*) := \{\bar{\beta} \in [-1, 1] : \|\bar{\beta} - \beta^*\| < d\}.$$

Let $\beta_1, \beta_2 \in \beta_d(\beta^*)$. Then:

$$G(\beta_2) - G(\beta_1) = \int_0^1 DG(\beta_1 + t(\beta_2 - \beta_1))(\beta_2 - \beta_1) dt$$

Hence

$$\begin{aligned} \|G(\beta_2) - G(\beta_1)\| &= \int_0^1 \|DG(\beta_1 + t(\beta_2 - \beta_1))(\beta_2 - \beta_1)\| dt \leq \\ &\leq \int_0^1 \|DG(\beta_1 + t(\beta_2 - \beta_1))\| \|\beta_2 - \beta_1\| dt \leq c \|\beta_2 - \beta_1\|. \end{aligned}$$

This shows $\|G(\beta_2) - G(\beta_1)\| \leq c \|\beta_2 - \beta_1\|$, which implies $G(\beta) : [-1, 1]^N \rightarrow [-1, 1]^N$ is a local contraction on \hat{I} by definition. Accordingly, Banach's fixed point theorem implies that $G(\beta^{(k)}) = \beta^{(k+1)}$ converges to $\beta^*, \forall \beta^{(0)} \in \hat{I}$.

Proof of the Corollary: To see first why the simple iteration scheme does not converge to locally unstable BLE, consider the case with only one forward-looking variable. Denoting by $G(\beta)$ the first-order autocorrelation function, the local stability in the 1-dimensional case is governed by the condition $\frac{\partial G(\beta)}{\partial \beta}|_{(\beta=\beta^*)} < 1$. Now assume the simple fixed-point iteration 2.17 has converged for some $\beta^{(0)}, k \in \mathbb{N}$ and $c \in \mathbb{R}$. This implies: $|\beta^{(k)} - \beta^{(k-1)}| < c$ and $|\beta^{(k-1)} - \beta^{(k-2)}| > c$. Under the assumption $\frac{\partial G(\beta)}{\partial \beta} > 0$, this simplifies to: $\beta^{(k)} - \beta^{(k-1)} < c$ and $\beta^{(k-1)} - \beta^{(k-2)} > c$. Further, by definition of the iteration 2.17, we have: $\beta^{(k)} = G(\beta^{(k-1)})$, implying:

$$\beta^{(k)} = G(\beta^{(k-1)}) = G(G(\beta^{(k-2)})) = G^2(\beta^{(k-2)}) = \dots = G^k(\beta^{(0)}) \quad (\text{C.1})$$

Now suppose $\beta^{(k)} \approx \beta^{(k-1)} = \beta^*$ is a locally unstable BLE, such that $\frac{\partial G(\beta)}{\partial \beta}|_{(\beta=\beta^*)} > 1$. This implies $\frac{G(\beta^*) - G(\bar{\beta})}{\beta^* - \bar{\beta}}$ for some $\bar{\beta}$ in the neighbourhood of β^* . Taking $\bar{\beta} = \beta^{k-1}$ and using $\beta^* = \beta^k$ then yields:

$$\frac{G(\beta^{(k-1)}) - G(\beta^{(k-2)})}{\beta^{(k-1)} - \beta^{(k-2)}} > 1 \Rightarrow \beta^{(k)} - \beta^{(k-1)} > \beta^{(k-1)} - \beta^{(k-2)} \quad (\text{C.2})$$

which contradicts the assumption that the iteration converged. Hence the iteration cannot converge to an unstable BLE, which establishes our result in the 1-dimensional case.

Next we show this result does not apply to the Quasi-Newton iteration from 2.18, which is given by :

$\beta^{(k+1)} = \beta^{(k)} + f'(\beta^{(k)})^{-1}f(\beta^{(k)})$, where $f(\beta^{(k)}) = G(\beta^{(k)}) - \beta^{(k)}$. Re-arranging the expression yields:

$$\beta^{(k+1)} = \beta^{(k)} + (DG(\beta^{(k)}) - I)^{-1}(G(\beta^{(k)}) - \beta^{(k)}).$$

Denoting $(DG(\beta^{(k)}) - I)^{-1}(G(\beta^{(k)}) - \beta^{(k)}) = \phi(\beta^{(k)})$, the iteration is a local contraction on a closed neighbourhood $\hat{I} = [\underline{I}, \bar{I}]$ whenever $\rho(I - \phi'(\beta^*)) < 1$. Note that we have:

$$\begin{aligned}\phi'(\beta) &= (G'(\beta) - I)^{-2}G''(\beta)(G(\beta) - \beta) + (G'(\beta) - I)^{-1}(G'(\beta) - I) = \\ &= (G'(\beta) - I)^{-1}((G'(\beta) - I)^{-1}G''(\beta)(G(\beta) - \beta) + G'(\beta) - I)\end{aligned}$$

Evaluating the last expression above at any stable or unstable BLE with $G(\beta^*) = \beta^*$, we get:

$$\phi'(\beta^*) = (G'(\beta^*) - I)^{-1}(G'(\beta^*) - I) = I.$$

Accordingly, $\rho(\phi'(\beta^*)) < 1$ holds trivially at any BLE. Under the assumption that $\phi(\beta)$ is continuously differentiable, one can use the exact same steps as before to show that the iteration is a contraction on the closed interval $\hat{I} = [\underline{I}, \bar{I}]$ for any $\beta^* = G(\beta^*)$.

Proof of Proposition 2.4: The first part of the proposition again trivially follows from Definition 2.1: The first consistency requirement is satisfied by construction, and the second consistency requirement is satisfied as long as $\theta^{(k)} = \theta^{(k-1)}$. In this case we have $G(\beta^{(k-1)}, \theta^{(k-1)}) = \beta^{(k)} \approx \beta^{(k-1)}$, hence the second consistency requirement in the definition is also approximately satisfied and we have an approximate BLE. Next we lay out our assumptions for local contraction of the mapping and convergence of $\{\theta^{(k)}\}_{k=1}^{\infty}$. Note that, the solution to our maximization problem can be written as:

$$(\theta^*, \beta^*) = \operatorname{argmax}_{\theta} p(\theta|Y_{1:T}), \text{ with } p(\theta|Y_{1:T}) = \frac{p(Y_{1:T}|\theta)p(\theta)}{p(Y_{1:T})} \text{ and } \beta^* = G(\beta^*, \theta^*).$$

At each step of the iteration, we have $\hat{\theta}^{(0)} = \operatorname{argmax}_{\theta} p(\theta|Y_{1:T}, \beta^{(k)})$. We assume this relation can be denoted as $\hat{\theta}^{(k)} = \eta(Y_{1:T}, \beta^{(k)})$ for some function $\eta(\cdot)$. Since the observables $Y_{1:T}$ are fixed throughout the iteration, we can further re-write this as $\hat{\theta}^{(k)} = \hat{\eta}(\beta^{(k)})$ for some $\hat{\eta}$. This last relation follows from the fact that, each $\beta^{(k)}$ during the iteration simply corresponds to a non-linear scaling of the parameter set θ . Accordingly, the $\hat{\eta}$ can be interpreted as a non-linear function that captures this scaling effect³². Given this, we can write the iteration as :

$$\beta^{(k)} = G(\beta^{(k)}, \hat{\theta}^{(k)}) = G(\beta^{(k-1)}, \hat{\eta}(\beta^{(k-1)}))$$

³² This further implies $\frac{\hat{\eta}(\beta^*)}{\theta^*} = \frac{\hat{\eta}(\beta^{(k)})}{\theta^{(k)}} = \frac{\hat{\eta}(\beta^{(l)})}{\theta^{(l)}}, \forall k, l$.

which has the same functional form as the iteration in Proposition 2.3. Accordingly, we can use the exact same steps of the previous proof to show that, $\exists ||.|| \in \mathbb{R}^n$ s.t:

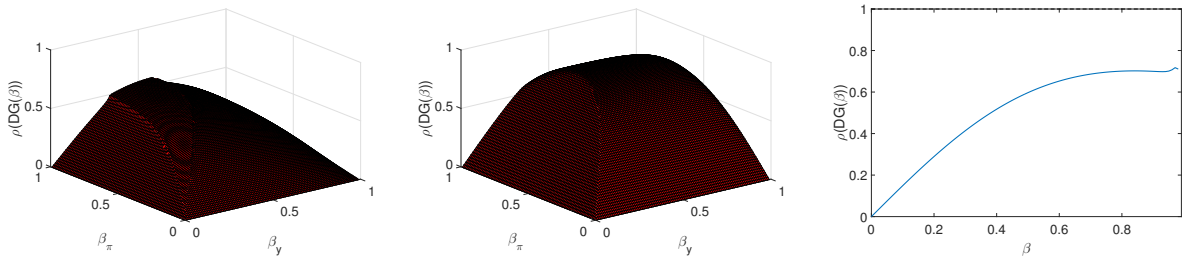
$$||G(\beta_2, \hat{\eta}(\beta_2)) - G(\beta_1, \hat{\eta}(\beta_1))|| < c||\beta_2 - \beta_1||$$

for some $0 \leq c < 1$ and $\beta_1, \beta_2 \in \beta_d(\beta^*)$. This shows that, indeed, $G(\cdot)$ is a local contraction on some closed interval \hat{I} , and applying the Banach Fixed Theorem yields:

$(\beta^*, \theta^*) = \lim_{k \rightarrow \infty} G^k(\beta^{(0)}, \theta^{(0)}) = \lim_{k \rightarrow \infty} G^k(\beta^{(0)}, \hat{\eta}(\beta^{(0)}))$ Further, recall that we only check for the convergence of the first-order autocorrelation matrix $\beta^{(k)}$ in our applications. Given our assumption $\hat{\theta}^{(k)} = \hat{\eta}(\beta^{(k)})$, this implies $\hat{\theta}^{(k)}$ must converge along with the learning parameters.

Starting Values for the Iterations in Algorithms I and II: Note that, in practical terms, we do not establish the basin of attraction (i.e. the neighbourhood \hat{I}) for the local contractions in Algorithm I or Algorithm II. Recall, however, local stability is a necessary condition for local contraction. Accordingly, we use the numerically approximated Jacobian matrix to observe the absolute value of the largest eigenvalue over the parameter space, which are provided in Figure 12 for the NKPC-model with fixed parameters, and the NKPC and SW models at the prior mean. Note that, due to the large parameter space in the Smets-Wouters model, we only consider the cases with $\beta_i = \beta_j, \forall i, j \in \{1, \dots, N\}$. The plots show that, for all cases considered, the largest eigenvalue of the Jacobian is inside the unit circle. While this still does not guarantee local contraction for any set of initial values $\beta^{(0)}$, it shows that the necessary condition for local contraction is satisfied.

Figure 12: Largest eigenvalue of the Jacobian $\rho(DG(\beta))$ as a function of β : The first figure shows $\rho(DG(\beta))$ for the small-scale model with fixed parameters, while the second figure corresponds to $\rho(DG(\beta))$ for the estimated small-scale system at the prior mean. The last figure shows $\rho(DG(\beta))$ for the SW-model at the prior mean. Due to the 7-dimensional parameter space, we only consider the case with $\beta_i = \beta_j, \forall i, j \in \{1, \dots, N\}$.



D Multiple BLE in the Smets-Wouters Model

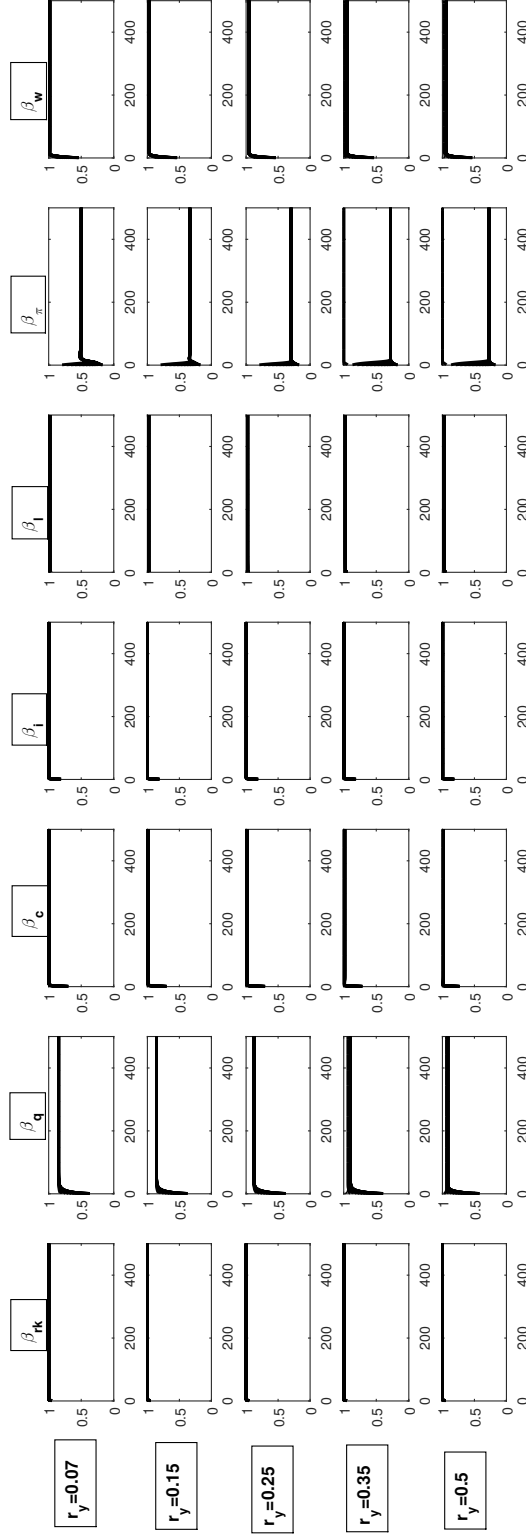
This subsection provides a more detailed look into the high-persistence equilibrium in the Smets-Wouters model. Figure 13 shows the results from 100 runs of Algorithm I for different values of r_y : the first panel corresponds to the results at the posterior mode from Section 4, while the last panel is the case from Section 5 for $r_y = 0.5$. The middle panels correspond to three intermediate cases: We observe that the high-persistence equilibrium becomes iteratively E-stable when r_y exceeds 0.25. Furthermore, our numerical simulations of the model show that the largest eigenvalue of the Jacobian matrix $DG(\beta)$ is outside the unit interval at the posterior mode and becomes smaller as we increase r_y . These results suggest that the high-persistence equilibrium is not iteratively E-stable, but possibly E-stable at the posterior mode. Recalling that we do not observe convergence to this equilibrium in our Monte Carlo simulations in Section 4, this would further imply the equilibrium has a negligible basin of attraction.

E Additional Estimations of the small-scale NKPC

Alternative Specifications of Output Gap

Our results in Section 3 are based on the HP-filtered measure of output gap. While this is a commonly used definition of output gap in empirical studies, there are also alternative definitions in the literature. The aim of this subsection is to check whether our results are sensitive to the specification of output gap. Accordingly, we provide the estimation results under BLE and REE with two alternatives: Output gap based on the quadratically de-trended output, and based on CBO's measure of potential output. Using these two alternative measures, re-estimating the small-scale model under BLE and REE yields the results in Table 14, which shows that the majority of our main conclusions holds with these specifications as well: In both cases, estimating the model under BLE results in a sizable likelihood gain. The persistence parameters of the inflation and output gap shocks, as well as the relative risk aversion coefficient turn out substantially lower, while their standard deviations shoot up. Furthermore, under the CBO-based measure of output gap, the NKPC slope is larger under BLE and there is no discernible difference in the monetary policy parameters. All of these results are qualitatively same as in Section 3. One difference we observe under the first specification resulting from quadratic de-trending is, the NKPC slope and the policy reaction to output gap both turn out lower under BLE, which are at odds with the other specifications. It is however well known that the NKPC slope is very sensitive to the specification of output gap, and our estimations here confirm this result. Furthermore, the very low estimate of output gap reaction under this specification implies the output gap process is most likely too noisy with this definition, and the model under BLE is more sensitive to this change in the structure of the time series.

Figure 13: Results from 100 runs of Algorithm I with randomized initial values $\beta^{(0)}$. The x-axis denotes the number of iterations, while the y-axis corresponds to the first-order autocorrelation of each forward-looking variable. We increase the value of r_y in each row from 0.07 and 0.5.



Alternative Specifications of the Learning Rule: A Sketch of the General Case and Illustration with AR(2) Rule

While our focus in this paper has been the parsimonious univariate AR(1) learning rule, our framework can be easily extended to incorporate any AR(p) rule with $p \geq 1$. In this section, we briefly sketch out this more general case of the PLM and provide a small example. Accordingly, suppose the representative agent's PLM is a univariate AR(p) rule, which corresponds to the following for each forward-looking variable x_t :

$$x_t = \alpha^x + \beta_1^x x_{t-1} + \dots \beta_p^x x_{t-p} + v_t = \alpha + \sum_{i=1}^N \beta_i^x x_{t-i} + v_t$$

where $v_t \sim NID$ with $\mathbb{E}_t[v_{t+1}] = 0$. The corresponding 1-step ahead forecast is then:

$$\mathbb{E}_t x_{t+1} = \mathbb{E}_t(\alpha^x + \beta_1^x x_{t-1} + \dots \beta_p^x x_{t-p+1} + v_t) = \alpha^x + \beta_2^x x_{t-1} + \dots + \beta_p^x x_{t-p+1} + \beta_1^x \mathbb{E}_t[x_t]$$

where x_t is not yet realized at the time of expectation formation. Accordingly, plugging in X_t into the above expression yields:

$$\alpha^x + \beta_1^x(\alpha^x + \beta_1^x x_{t-1} + \dots + \beta_p^x x_{t-p}) + \beta_2^x x_{t-1} + \dots + \beta_n^x x_{t-p+1}$$

which, after some re-writing, yields:

$$\mathbb{E}_t[x_{t+1}] = \alpha^x(1 + \beta_1^x) + \beta_1^x \sum_{i=1}^p \beta_i^x \beta_{t-i}^x + \sum_{i=1}^{p-1} x_{t-i}$$

Generalizing the above expression to the N-dimensional vector X_t then yields:

$$\mathbb{E}_t[X_{t+1}] = (I + \beta_1)\alpha + \beta_1 \sum_{i=1}^p \beta_i X_{t-i} + \sum_{i=1}^{p-1} \beta_{i+1} X_{t-i}$$

where $\alpha = (\alpha^1 \dots \alpha^N)$ and $\beta_i = \text{diag}(\beta_i^1, \dots, \beta_i^N)$ for all $i \in \{1 \dots p\}$. Recall the AR(1) corresponds to an inference rule based on the unconditional mean and first-order autocorrelation, or in other words, the observed sample mean and persistence. Along the same lines, and AR(2) rule corresponds to inference rule based on the unconditional mean, first-order autocorrelation and the first-order autocorrelation of the first-difference. In other words, this coincides with the observed sample mean, persistence and the persistence in the rate of change. Adding higher order AR terms simply corresponds to observing the persistence of the higher-order differences of a given series, hence it is easy to see that the autoregressive rules rapidly lose their intuitive appeal as we continue adding higher order terms into the PLM. Nevertheless, one can still use

the framework outlined in this paper to estimate an approximate equilibrium arising from any given AR(p) PLM. While the estimation of a system with N forward-looking variables under the AR(1) rules involves the approximation of N variables, this number increases Np for a given AR(p) rule.

As an example, we provide the estimation of the small-scale NKPC model of Section 3 under an AR(2) learning rule in the last column of . We estimate this model with the CBO-based specification of the output gap, accordingly the results are comparable to the neighboring columns. We observe that the parameter estimates are almost identical compared to the AR(1) case: The only noticeable difference arises in the resulting log-likelihood, where the AR(2) leads to a slight improvement over the AR(1). Since the AR(2) model imposes more restrictions on the model compared to AR(1), an immediate question that follows is whether the improved likelihood of the AR(2) model also extends to an improved forecasting performance, which we leave to future work.

Table 14: Alternative estimations of the small-scale NKPC model: We compare the results under BLE and REE with two alternative specifications of output gap. In the first case output gap is defined as the deviation of output from a quadratic trend, while in the latter we take the output gap based on CBO’s measure of potential output. The last column corresponds to the estimation of the same model with the CBO-implied output gap, when we replace the AR(1) learning rule with that of AR(2).

| | | | Laplace | BLE det. | REE det. | BLE CBO. | REE CBO. | BLE AR(2) |
|-------------|------------|------|-----------|----------|----------|----------|----------|-----------|
| | | | | -374.67 | -396.46 | -350.75 | -374.73 | -344.73 |
| | Prior | | Posterior | | | | | |
| | Dist | Var | | Mode | Mode | Mode | Mode | Mode |
| η_y | Inv. Gamma | 2 | | 0.79 | 0.06 | 0.75 | 0.09 | 0.74 |
| η_π | Inv. Gamma | 2 | | 0.3 | 0.07 | 0.29 | 0.03 | 0.29 |
| η_r | Inv. Gamma | 2 | | 0.3 | 0.32 | 0.29 | 0.3 | 0.29 |
| \bar{y} | Normal | 0.25 | | 0.39 | 0.43 | 0.03 | 0.2 | 0.36 |
| $\bar{\pi}$ | Gamma | 0.25 | | 0.8 | 0.5 | 0.82 | 0.57 | 0.78 |
| \bar{r} | Gamma | 0.25 | | 1.07 | 0.68 | 1.19 | 1.13 | 1.37 |
| κ | Beta | 0.15 | | 0.007 | 0.081 | 0.019 | 0.005 | 0.02 |
| τ | Gamma | 0.5 | | 3.01 | 4.64 | 2.59 | 4.57 | 2.51 |
| ϕ_π | Gamma | 0.25 | | 1.5 | 1.71 | 1.43 | 1.43 | 1.41 |
| ϕ_y | Gamma | 0.25 | | 0.12 | 0.05 | 0.31 | 0.24 | 0.28 |
| ρ_y | Beta | 0.2 | | 0.38 | 0.94 | 0.42 | 0.94 | 0.51 |
| ρ_π | Beta | 0.2 | | 0.33 | 0.99 | 0.31 | 0.89 | 0.3 |
| ρ_r | Beta | 0.2 | | 0.89 | 0.77 | 0.89 | 0.79 | 0.87 |

F Forecasting Performance: Comparisons with Bayesian VARs

An established result in the literature is that, the structural Bayesian VARs (SBVAR) resulting from the linearized DSGE models typically lead to a better empirical performance over their purely statistical Bayesian VAR (BVAR) counterparts. In this subsection we provide a short comparison of the Smets-Wouters model with the corresponding BVAR, which is reported in Table 15. The first row of Table 15 shows the estimation results over the period 1985:I-2016:IV. Since the data is heteroskedastic over the pre- and post-80s period, we provide two alternatives of the BVARs with a fairly short training sample of 2 years, and a long one with 28.5 years (all available data). While the more parsimonious BVAR(1) specification yields the best fit in both cases, it is readily seen that the resulting fit is substantially worse compared to the DSGE model under learning. We also provide a comparison of the 1-step ahead forecasts of the BVARs with the DSGE model under learning. The inflation and interest rate forecasts of the BVARs are substantially better with the short training sample, while the remaining parameters yield lower RMSEs when we use the longer training sample. In either case, the forecast difference generally remains larger than zero in favour of the DSGE model.

Table 15: Likelihood and 1-step ahead RMSE Comparisons of the Bayesian VARs and the DSGE model under learning.

| | Training Sample: 8 quarters | | | | | Training Sample: 114 quarters | | | | |
|--|--------------------------------|---------|---------|---------|---------|----------------------------------|---------|---------|---------|---------|
| | BVAR(1) | BVAR(2) | BVAR(3) | BVAR(4) | BVAR(5) | BVAR(1) | BVAR(2) | BVAR(3) | BVAR(4) | BVAR(5) |
| Likelihood | -637 | -647 | -648 | -652 | -652 | -659 | -662 | -658 | -662 | -669 |
| | | | | | | | | | | -546 |
| Forecasts | Output | | | | | Inflation | | | | |
| | Inv | | | | | Interest | | | | |
| Training Sample : 8 quarters | Wage | | | | | Labor | | | | |
| | | | | | | | | | | |
| | | | | | | | | | | |
| | | | | | | | | | | |
| | | | | | | | | | | |
| | | | | | | | | | | |
| | BVAR(1) | 0,9 | 0,69 | 2,69 | 1,02 | 0,31 | 0,54 | 9,91 | | |
| | BVAR(2) | 0,86 | 0,79 | 2,78 | 1,05 | 0,33 | 0,4 | 10,19 | | |
| | BVAR(3) | 0,95 | 0,77 | 2,69 | 1,06 | 0,31 | 0,4 | 9,93 | | |
| | BVAR(4) | 0,94 | 0,85 | 2,52 | 1,02 | 0,32 | 0,39 | 9,79 | | |
| | BVAR(5) | 0,91 | 0,86 | 2,5 | 1,04 | 0,34 | 0,38 | 9,93 | | |
| Training Sample: 114 quarters | | | | | | | | | | |
| | | | | | | | | | | |
| | | | | | | | | | | |
| | | | | | | | | | | |
| | | | | | | | | | | |
| | | | | | | | | | | |
| | BVAR(1) | 0,64 | 0,58 | 2,09 | 1,06 | 0,44 | 0,99 | 6,52 | | |
| | BVAR(2) | 0,65 | 0,59 | 2,11 | 1,04 | 0,41 | 0,94 | 6,72 | | |
| | BVAR(3) | 0,68 | 0,6 | 2,16 | 1,02 | 0,4 | 0,94 | 6,68 | | |
| | BVAR(4) | 0,7 | 0,62 | 2,2 | 1,03 | 0,38 | 0,94 | 6,6 | | |
| | BVAR(5) | 0,74 | 0,65 | 2,22 | 1,02 | 0,37 | 0,91 | 6,57 | | |
| Gains/ Losses of BLE Forecasts (in percentage) | | | | | | | | | | |
| | | | | | | | | | | |
| Training Sample: 8 quarters | | | | | | | | | | |
| | | | | | | | | | | |
| | | | | | | | | | | |
| | | | | | | | | | | |
| | | | | | | | | | | |
| | | | | | | | | | | |
| | BVAR(1) | 0,38 | 0,09 | 0,44 | 0,37 | 0,26 | 0,89 | 0,95 | | |
| | BVAR(2) | 0,31 | 0,15 | 0,41 | 0,39 | 0,27 | 0,68 | 0,96 | | |
| | BVAR(3) | 0,34 | 0,09 | 0,32 | 0,39 | 0,16 | 0,53 | 0,95 | | |
| | BVAR(4) | 0,34 | 0,20 | 0,27 | 0,35 | 0,09 | 0,15 | 0,92 | | |
| | BVAR(5) | 0,31 | 0,23 | 0,25 | 0,37 | 0,15 | -0,11 | 0,89 | | |
| Training Sample: 114 quarters | | | | | | | | | | |
| | | | | | | | | | | |
| | | | | | | | | | | |
| | | | | | | | | | | |
| | | | | | | | | | | |
| | | | | | | | | | | |
| | BVAR(1) | 0,13 | -0,09 | 0,44 | 0,37 | 0,26 | 0,89 | 0,93 | | |
| | BVAR(2) | 0,09 | -0,14 | 0,22 | 0,38 | 0,41 | 0,86 | 0,93 | | |
| | BVAR(3) | 0,07 | -0,17 | 0,15 | 0,36 | 0,35 | 0,8 | 0,93 | | |
| | BVAR(4) | 0,11 | -0,1 | 0,16 | 0,36 | -0,24 | 0,65 | 0,88 | | |
| | BVAR(5) | 0,15 | -0,02 | 0,15 | 0,35 | 0,22 | 0,54 | 0,83 | | |